Investigating transcriptional control of *MECP2-BDNF-miR-132* homeostasis network; implicating the role of MeCP2E1/E2 overexpression and metabolic drugs

by

Marjorie Buist

A Thesis submitted to the Faculty of Graduate Studies of
The University of Manitoba
in partial fulfilment of the requirements of the degree of

MASTER OF SCIENCE

Department of Biochemistry and Medical Genetics
University of Manitoba
Winnipeg

Abstract

Rett Syndrome (RTT) and *MECP2* Duplication Syndrome (MDS) are caused by mutations in the *MECP2* gene encoding "methyl CpG binding protein 2" (MeCP2), a critical epigenetic regulator in the brain. There is no cure available for these diseases, but symptoms have been reversed in mouse models. The two isoforms of the protein, MeCP2E1 and E2 are differentially expressed in the brain and there is increasing evidence that they have unique functions, which is important to consider in developing therapeutic strategies for MeCP2-related disorders. MeCP2 has been shown to function as a transcriptional activator and repressor but the role of each isoform in transcriptional regulation has not been extensively studied. In this study, a new gain-of-function model of MeCP2 isoform-specific overexpression was generated in human brain cells through stable lentiviral transduction. Nascent RNA analysis was performed to test the transcriptional effects of the two isoforms on selected target genes, *BDNF* and *miR-132*, which form a homeostasis network with MeCP2, as well as *Nucleolin* and *ribosomal RNAs.* Both isoforms were shown to increase nascent *BDNF* transcripts. The results of the human brain cell line correspond with previous observations in human RTT brain tissues, indicating the model established here could be used in the future for additional screening studies. Small molecule drug screening for RTT therapies has recently focused on metabolic drugs which have the potential to correct metabolic defects in RTT patients as well as cognitive defects. The impact of these drugs on MeCP2 regulation is an important aspect of these studies, since MeCP2 levels are tightly controlled. In this study, the effect of simvastatin and metformin on *MECP2* and *BDNF* transcription was assessed in human brain cells. The results suggested that metformin controls *MECP2E1* and *BDNF* post-transcriptionally, but the effect on *MECP2E2* is transcriptional and is a promising drug for RTT. This study highlights the importance of isoform-specific analysis in studies of MeCP2 function and analysis of potential RTT therapies.

Acknowledgments

I would like to thank my supervisor, Dr. Mojgan Rastegar, for giving me the opportunity to be a part of her lab and for supporting and guiding me in the various research projects I have participated in, starting as a summer student and throughout my Master's degree. I have learned so much from her and I'm very grateful to have had the opportunity to work with her. I would also like to thank my committee members Dr. David Merz and Dr. Jean-Eric Ghia for their advice and encouragement.

My Master's program was made possible through funding provided by CIHR and NSERC agencies.

I would like to thank members of the Rastegar lab who taught me techniques or worked with me on various projects: Carl, Robby, Vichithra, Shervin, Shayan, David, Annan, Sandhini, Nada, Sari, Matthew, and Khatereh. I would also like to thank Monroe Chan who helped me with Flow Cytometry analyses. It's been a wonderful experience to be part of the Biochemistry and Medical Genetics Department and Regenerative Medicine Program communities which provided excellent opportunities for learning about research, allowing me to expand my knowledge on numerous fields. I would like to thank the organizers and members of the BMG mentorship groups which were an excellent source of support. Thanks to fellow students and friends Vasu, Alen, Camila, Stefan, Chris, Dino, Leo, Victor, as well as my labmates, for organizing "coffee group" breaks to recharge the batteries and have many good discussions!

Thanks and much love to my parents, Richard and Liz Buist. Thank you Dad for inspiring my love of science and medical research. I will cherish the memories of attending the Manitoba Neuroscience Network conference with you during my Master's. Thank you Mom for your steadfast encouragement. Thank you also to the rest of my family and friends who are each so important to me. Special thanks to my wonderful fiancé Jason. We met during my Master's program and your love, encouragement and understanding have made such a difference in improving my confidence and mindset.

In all this I thank my God and Savior Jesus Christ who has guided me and been my strength. Every day is an opportunity to marvel at the Lord's work in creation down to the finest details that we research and seek to learn more about.

Dedication

To my parents, Richard and Liz Buist

Table of Contents

List of Tables

List of Figures

List of abbreviations

5mC	5-methylcytosine
5hmC	5-hydroxymethylcytosine
AAV	Adeno-associated virus
AMPK	AMP-activated protein kinase
ASD	Autism Spectrum Disorder
BDNF	Brain-derived neurotrophic factor
CBP	CREB binding protein
ChIP	Chromatin immunoprecipitation
CTCF	CCCTC-binding factor (protein transcription factor)
	Corrected total cell fluorescence (methodology)
CTD	C-terminal Domain
CNS	Central Nervous System
CREB	cAMP response element binding
DNMT	DNA methyltransferase
ESC	Embryonic stem cell
EU	Ethynyl-uridine
GABA	Gamma-aminobutyric acid
IGF-1	Insulin-like growth factor 1

iPSC	Induced pluripotent stem cell
ID	Inter-Domain
LDL	Low-density lipoprotein
MBD	Methyl Binding Domain
MDD	Major Depressive Disorder
MDS	*MECP2* Duplication Syndrome
MeCP2	Methyl CpG binding protein 2
mTOR	Mammalian target of rapamycin
NID	NCoR Interaction Domain
NTD	N-terminal Domain
NLS	Nuclear localization signal
PTM	Post-translational modification
RTT	Rett Syndrome
PIC	Pre-initiation complex
Pol	Polymerase
TF	Transcription factor
TRD	Transcription Repression Domain
TSS	Transcription start site
qRT-PCR	Qualitative real-time polymerase chain reaction
UTR	Untranslated region
VEGF	Vascular endothelial growth factor

Chapter I: Introduction

Rett Syndrome (RTT) and *MECP2* Duplication Syndrome (MDS) are two neurodevelopmental disorders resulting from loss- and gain-of-function mutations in the *MECP2* gene encoding "methyl-CpG binding protein 2" (MeCP2).[1,2] These disorders have no available cure, and their mechanism of disease is still not fully clear. MeCP2 is an important epigenetic factor with key roles in neurodevelopment and maintenance of mature neurons in the brain throughout life.[3] The discovery that loss-of-function mutations in *MECP2* cause RTT was made in 1999 and gain-of-function mutations were linked to MDS in 2004-2005. In the 15-20 years that have passed, research has shown that MeCP2 dysregulation has broad effects in neurons impacting genomic organization and chromatin structure leading to deregulation in the processes of gene transcription, protein translation, activity of fundamental signaling pathways and growth factors, including mammalian target of rapamycin (mTOR), and abnormalities in metabolism.[4] The background of this body of relevant research will first be reviewed, followed by an outline of how this thesis will investigate selected targets involved in these cellular processes with a focus on the role of MeCP2 in transcriptional control of these genes.

I.i. Control of gene transcription in eukaryotes

I.i.a. Epigenetics and chromatin structure

The field of epigenetics was recently defined as "the study of molecules and mechanisms that can perpetuate alternative gene activity states in the context of the same DNA sequence."[5] Dysregulation of these processes is implicated in various neuropsychiatric diseases such as Major Depressive Disorder (MDD), Autism Spectrum Disorders (ASDs), Fragile X Syndrome, Rett Syndrome and schizophrenia.[6] Epigenetic regulation has critical structural and signaling roles by compacting DNA molecules within the nucleus and producing unique and dynamic gene expression states within the cells.[5,7] DNA is compacted through packaging with DNA-bound proteins to form the "chromatin" structure.[8,9] The most basic level of chromatin organization is the 11 nm fiber consisting of nucleosomes connected by linker DNA which appear like 'beads on a string'. A nucleosome is composed of 147 bp of DNA wrapped almost twice around a histone octamer.[10] The histone octamer consists of a $(H_3\text{-}H_4)_2$ tetramer and two H2A-H2B dimers.[11,12]

Linker histones H1, or the avian H5, bind to DNA where it enters and exits the nucleosome and play a role in the formation of higher order chromatin structures. Nucleosomes are negative regulators of gene expression since they limit the access of transcription machinery to DNA.[6,7] The genome is organized into topologically associated domains and is compacted and organized through higher order 3D chromosome folding.[13]

Heterochromatin and euchromatin refer to chromatin in repressive and active states, respectively. Heterochromatin is more highly condensed than euchromatin and is further divided into facultative and constitutive heterochromatin.[7] The inactivated X chromosome is an example of constitutive heterochromatin, which remains in the repressed state while facultative heterochromatin can dynamically move between repressive and active states. Unique and dynamic chromatin states can be distinguished by different chromatin modifications found there including DNA methylation, histone variants and post-translational modifications (PTMs), and RNA modifications.[14] The epigenetic factors which deposit, interpret and remove these modifications are called writers, readers, and erasers, respectively.[5,6]

Histone PTMs occur mostly on the N-terminal tails which extend out from the globular histone core, and include lysine acetylation, lysine and arginine methylation, serine and threonine phosphorylation, and lysine ubiquitination and sumoylation.[7] Histone Binding Proteins are readers of histone modifications, Histone Acetyltransferases are writers, and Histone Deacetylases are erasers.

DNA is epigenetically modified by methylation of cytosine bases. Methylation status affects gene expression, genomic stability, alternative splicing, X chromosome inactivation and expression of highly repetitive regions such as retrotransposons and satellite DNA.[6,7] The writers of DNA methylation, DNA methyltransferases (DNMTs) transfer the methyl from a donor to produce 5-methylcytosine (5mC), referred to as the fifth base of the genome. DNMT1 maintains methylation patterns during DNA replication while DNMT3A and 3B are *de novo* DNMTs. Ten-Eleven Translocation (TET) enzymes demethylate DNA through a series of oxidation reactions. The oxidized forms also have significant biological functions.[6] 5mC is oxidized to 5-hydroxymethylcytosine (5hmC), referred to as the sixth base of genome. Further oxidation reactions by TET proteins generate 5fC and 5caC.[14] Methyl Binding Proteins are the readers of

methylation marks, including MeCP2, other Methyl Binding Domain (MBD) proteins as well as proteins without a MBD. Various combinations of DNA and histone modifications can have unique effects on the chromatin environment.[6,7]

The DNA methylation mark 5mC is predominantly associated with repression of transcription when localized to promoter elements of genes while 5hmC is found in transcriptionally active chromatin regions and enhancers.[14] There are also studies showing 5hmC can be enriched at promoters of repressed genes. MeCP2 binds both 5mC and 5hmC.[15,16] The effects of 5mC and 5hmC are also genomic context-dependent and cell-type specific. The 5mC modification can occur in the context of CpG methylation and CpH methylation (H=C, A, or T). CpH methylation is prevalent in embryonic stem cells (ESCs), induced pluripotent stem cells (iPSCs), the adult brain, and mature neurons. The major regulatory proteins which recognize and bind CpH include MeCP2 and DNMT3A.[7]

I.i.b. Regulation check points, transcription machinery, and roles of RNA Polymerases I, II, III

RNA polymerases are responsible for catalyzing the synthesis of RNA using DNA molecules as template. There are three RNA polymerases in eukaryotes which transcribe different classes of RNA. Polymerase (Pol) I synthesizes ribosomal RNAs, Pol II synthesizes messenger RNAs, non-coding RNA, primary microRNAs, and enhancer RNAs, while Pol III produces transfer RNAs and small ribosomal RNA.[17,18]

The three stages of transcription are initiation, elongation, and termination.[17] Transcription initiates at the core promoter, which is about 100-200 bp in length and surrounds the transcription start sites (TSSs) at the 5’ ends of genes. Characteristic core promoter motifs in the DNA sequence include TATA box and downstream promoter elements.[19] Promoters will often contain conserved DNA sequence elements which may differ for Pol I, Pol II and Pol III. Access to the promoter sequence could be inhibited by the chromatin structure, with nucleosomes to be removed or shifted (chromatin remodeling) before transcription can begin. Such regulatory mechanisms have been experimentally shown for members of the *Hox* genes *in vitro* and *in vivo.*[11,20–22] Active promoters may contain nucleosome-depleted regions, flanked by +1

downstream and -1 upstream nucleosomes. CpG islands and their methylation status regulate the activity of some promoters.[17]

Core promoters on their own may only support low basal transcriptional activities. Additional regulation is provided by proximal promoters upstream of the core promoter as well as enhancers and silencers. These latter sequences could be more distant DNA regulatory elements, which can be even 1 million base pairs or more away from their target promoters.[17,19] Transcription factors (TFs) activate gene transcription through binding specifically to sequence elements in the promoters, enhancers, and silencers and can be studied by DNase I footprinting, electromobility shift assays, chromatin immunoprecipitation (ChIP), and other DNA-protein binding assays.[20,23,24] There are about 1,600 known human TFs.[17,18] Communications between enhancers, silencers and the core promoters are mediated by *trans*-acting factors which bind to motifs within the sequences. Transcription factor complexes can act to bridge enhancers, silencers, and promoters, requiring dynamic chromatin architecture. Topologically associated domains are defined regions of the genome where enhancers usually operate. TFs recruit additional proteins that regulate promoter accessibility and transcription initiation, recruiting RNA polymerase.[17,19]

In eukaryotes the assembly of polymerases with their associated initiation factors on the core promoter is called the "pre-initiation complex (PIC)".[17,18] The initiation factors bind to the DNA upstream of the transcription start site of a gene, forming a bridge between the polymerase and the gene to be transcribed. The PIC opens DNA, which occurs spontaneously for Pol I and Pol III but for Pol II requires the DNA translocase XPB, which uses ATP to unwind double-stranded DNA molecules to propel them into the polymerase active center.[17] After Pol II transcribes 20-60 nucleotides it undergoes promoter-proximal pausing, which in mammals is a major regulatory checkpoint. Additional factors are required for transcription to continue. Promoter-proximal pausing can regulate a gene by limiting the frequency of transcription initiation. Some transcription factors encourage release of polymerases from pausing. The 5' end of the nascent RNA is capped *via* reverse linkage in the 5' to 5' direction of N7-methylguanosine. This occurs during initiation and promoter-proximal pausing.[18] Phosphorylation of serine residues in the C-terminal domain (CTD) of RNA Pol II recruits capping enzymes. The CTD of Pol II is further

phosphorylated which recruits elongation factors allowing transcription to proceed.[17] Phosphorylation of the Pol II CTD also functions in recruiting factors involved in histone modification and chromatin remodeling, such as histone methyltransferases, which can occur during transcription. Elongation can be paused leading to polymerase backtracking, arrest, and termination. The presence of nucleosomes in a gene can result in RNA polymerases "arresting" and continuation of transcription can be rescued by TFIIS, an elongation factor, and a similar factor performs the same function for Pol I and Pol III.[17] Introns are removed from the pre-mRNA transcript during productive elongation through action of the spliceosome, a large dynamic complex consisting of small nuclear ribonucleoproteins and many other proteins.[25] Alternative splicing of exons in eukaryotes contributes to the diversification of proteins observed, and this process is mediated by heterogeneous ribonucleoproteins (hnRNPs).[26] The final step, termination, at the 3' end of gene is when the transcript is cleaved and the pre-mRNA becomes polyadenylated.[17,18]

I.i.c Effective ways to study gene transcription

Different modes of transcriptional regulation discussed above would determine which transcripts are synthesized within a cell. At any given time, a cell contains a total pool of various RNA transcripts including those which are stable (with a high half-life), unstable (with a low half-life), and newly synthesized transcripts. Commonly used total RNA analysis does not distinguish between the states of these transcripts but rather provides an overall view of the transcripts present at any given moment in time, referred to as the "steady state". In order to investigate the mechanisms behind altered transcript levels by specific drug treatments, developmental time points or other conditions, there are certain methods to analyze promoter activity, RNA synthesis and RNA stability. Promoter activity can be tested by reporter assays such as luciferase experiments[27] or beta-galactosidase reporter assays.[28] ChIP can be used to measure binding of RNA polymerase to promoter regions[29,20]. RNA stability can be assessed by actinomycin D treatment which inhibits RNA polymerase so that the stability of the existing pool of RNA transcripts can be analyzed. RNA synthesis and stability can be assessed through nascent RNA

analysis methods which label and isolate newly synthesized RNA during a certain time window and allow them to be distinguished from total transcripts.[18]

To date, there are a limited number of MeCP2 studies employing these methods, which makes it challenging to identify which genes are transcriptionally controlled by MeCP2. My thesis has focused on transcriptional gene regulation *via* measuring nascent RNA synthesis. Nascent RNAs can be detected either by biochemical enrichment or chemical induction of point mutations. Biochemical enrichment methods would include isolation of chromatin-associated RNA, Pol II-associated RNA, small-capped RNA, metabolically labelled RNAs, and RNA from elongation-competent Pol II complexes.[18] Global changes in transcription or transcript stability can be analyzed by global sequencing of nascent RNAs through a variety of methods. Imaging-based techniques are also available which quantify global transcript production in real time in the 3D space of the nucleus, tissue, or organism.[18,30,31] Targeted gene analysis of nascent RNA can also be performed using gene-specific primers and qualitative real-time polymerase chain reaction (qRT-PCR).[29,32–34] The goal of my thesis is to elucidate the role of MeCP2 in transcriptional control through nascent RNA analysis to gain a more comprehensive understanding of the mechanism of disease of Rett Syndrome and *MECP2* Duplication Syndrome caused by mutations in this fundamental protein.

I.ii. MeCP2 is a critical epigenetic reader in the brain

MeCP2 is one of five core members of the family of MBD proteins involved in epigenetic regulation of the genome through binding to methylated DNA. Mutations in all MBD proteins have been linked to Autism Spectrum Disorders and a variety of cancers.[35] *MECP2* mutations cause Rett Syndrome and *MECP2* Duplication Syndrome, neither of which have any cure.[1,2] The unique methylation landscape of the brain and the changes it undergoes during development contributes to the challenge of understanding and developing therapies for diseases caused by defects in the epigenetic machinery. In the brain, CpG methylation accounts for 75% of cytosine methylation and CpH the remaining 25%, significantly more than other tissues. In addition, 5hmC, a mark associated with active genes, is ten times higher in the mature brain compared to ESCs.[6] Recent reports from our lab indicate that not only MeCP2, but also other components of the DNA

methylation machinery (readers, writers and erasers) are regulated by sex and mouse strain in brain cells.[36–38] In this section the structure and function of the *MECP2* gene and the two protein isoforms, MeCP2E1 and MeCP2E2, will be discussed.

I.ii.a. *MECP2* gene and MeCP2 protein structure

MeCP2 was discovered as part of a study to screen for proteins that could bind to methylated DNA. Initially, MeCP2 was purified from rat brain tissue, where it was observed to be highly abundant compared to other tissues. In this study, MeCP2 was shown to be capable of binding a single symmetrically methylated CpG site without requiring further surrounding sequence specificity.[15,39] The *MECP2* gene is located on the X chromosome and is approximately 76 kb in size.[40] In females one copy of the gene is silenced through X chromosome inactivation.[41] The *Mecp2/MECP2* gene is comprised of four exons and three introns[42–44] (Figure 1). The 5' untranslated region (5' UTR) contains partial promoter activity and includes some *cis*-regulatory elements. The 3'UTR is about 8.5 kb long and contains a number of polyadenylation sites.[42,45–48] Alternative splicing of the gene produces two protein isoforms referred to as E1 and E2. Exons 1, 3, and 4 encode the E1 isoform while exons 2, 3 and 4 encode the E2 isoform.[43,44] The two isoforms differ only at their extreme N-terminal region of the N-terminal Domain (NTD) with E1 having 21 unique amino acids there while there are 9 amino acids that only exist in E2. The E1 isoform is 498 amino acids long while the E2 isoform contains 486 amino acids[43] (Figure 1). The remaining amino acid sequence of the NTD and protein domains are the same. Following the NTD are the Methyl Binding Domain (MBD)[49], Inter-Domain (ID), Transcription Repression Domain (TRD)[50] and C-terminal Domain (CTD). Apart from the main domains of the protein, MeCP2 also contains AT-hooks, which are short motifs which bind AT-rich DNA.[49,51] MeCP2 contains a nuclear localization signal (NLS) within the TRD responsible for import of the protein into nucleus. However, MeCP2 is also capable of diffusing into the nucleus independent of the NLS and remaining there due to its affinity for DNA.[52]

The predicted molecular weight of MeCP2 is approximately 53 kD but it has been observed to run at approximately 75-80 kD by SDS-PAGE in mouse, rat, and human contexts.[15,53–56] MeCP2 is a largely unstructured protein estimated to consist of approximately 4% alpha-helix, 21% beta-

sheet, 13% beta-turn, and 59% unstructured regions. The MBD is the only domain observed to adopt definite secondary structure.[57–59] The MBD is estimated to be 38% unstructured while the TRD 85% unstructured. As an intrinsically disordered protein MeCP2 can adopt a variety of structures to interact with a variety of protein partners.[59]

Figure 1. Schematics of the structure of the *MECP2* gene and transcripts and MeCP2 protein isoforms. Top: *MECP2* gene structure is shown with transcription start site (TSS) indicated, the four exons and three introns. The presence of multiple polyadenylation signals is indicated by arrows. Middle: Alternative splicing of the *MECP2* transcript produces the two *E1* and *E2* isoform transcripts. The translation start site ATG is shown for each isoform. Bottom: Structure of MeCP2 protein showing the domains: N-terminal Domain (NTD), Methyl Binding Domain (MBD), Inter-Domain (ID), Transcription Repression Domain (TRD) and C-terminal Domain (CTD). Schematics adapted from Liyanage et. al. 2014 and Kyle et. al. 2018.[4,48]

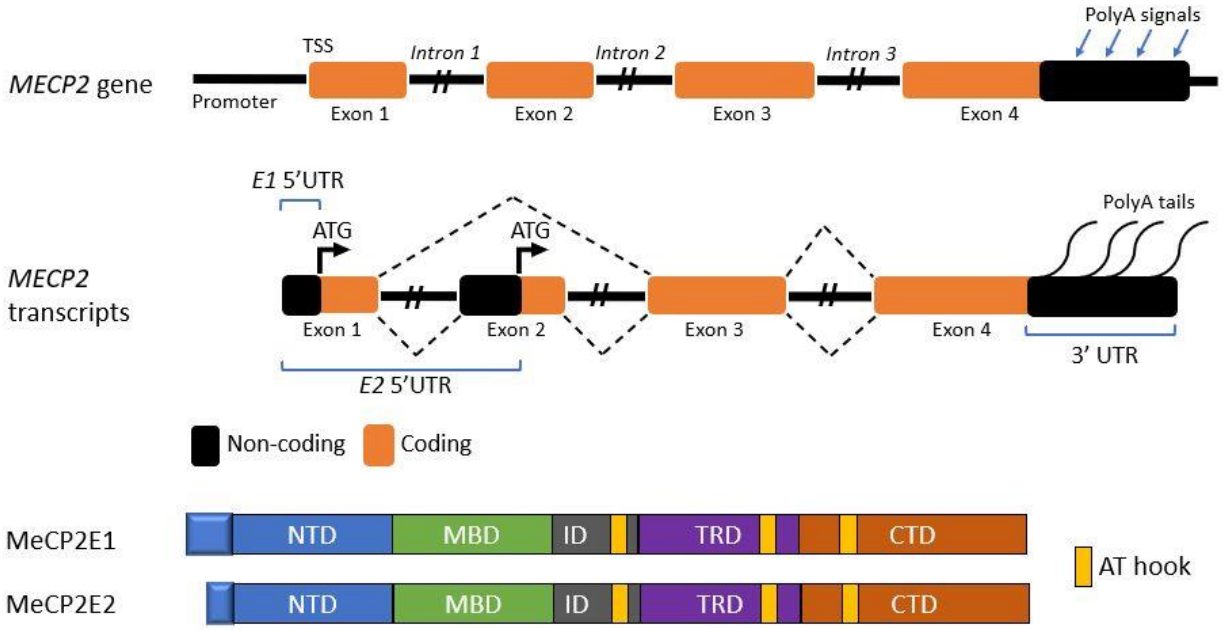

I.ii.b. Regulation of MeCP2 expression patterns

There are a number of regulatory mechanisms governing *Mecp2*/*MECP2*/MeCP2 expression in various cell types and tissues and during development at the transcriptional, post-transcriptional and post-translational levels. MeCP2 is highly expressed in the adult rat brain.[15] In adult mice the highest levels of MeCP2 protein have been detected in brain, lung and spleen tissues with

comparatively lower levels of MeCP2 in kidney and heart tissues and still lower levels in liver, stomach and small intestine.[46] In mouse neuronal nuclei, MeCP2 is expressed at an abundance equal to approximately half the number of nucleosomes. There are an estimated 16 x 10^6 molecules of MeCP2 in a neuronal nucleus, 2 x 10^6 molecules per glial nucleus, and 0.5 x 10^6 molecules per liver nucleus.[60]

Within the brain, expression of human and mouse MeCP2 protein increases in correlation with maturation of the central nervous system (CNS) and levels are maintained throughout adulthood.[3] MeCP2 expression is low in mouse embryonic stem cells, increases during embryonic and postnatal development and remains at high levels in adult mouse and rat brain.[39,54] In the human brain, MeCP2 protein levels increase dramatically throughout gestation. The percentage of neurons expressing MeCP2 continues to increase from birth until 10 years of age[46] and expression of MeCP2 in the brain continues into adulthood.[61] *Mecp2*/MeCP2 is expressed throughout different regions of the mouse brain. The E1 isoform is expressed uniformly in the olfactory bulb, striatum, cortex, hippocampus, thalamus, brain stem and cerebellum of adult mice, while E2 displays a more variable expression pattern. E2 expression is highest in the olfactory bulb and cerebellum, with moderate expression in striatum, cortex, hippocampus, and thalamus and lowest expression in the brain stem.[54] *Mecp2e1* transcripts are also uniformly expressed among these same brain regions while *Mecp2e2* transcripts show some variability, with levels in the brain stem and thalamus significantly lower than the cortex.[54] The time and region-specific expression of *Mecp2* is determined by a region of the promoter which initiates strong expression in mature neurons[62,63] as well as regulatory elements within the promoter and gene body.[55,64,65] Unique methylation patterns within the regulatory elements have been found within brain regions indicating this contributes to expression patterns of *Mecp2.*[54,55,65]

MeCP2 expression is also regulated post-transcriptionally. The 3'UTR of the *Mecp2/MECP2* gene plays a significant role in regulating the timing of onset of increase in protein expression through post-transcriptional mechanisms. The 3'UTR of the *Mecp2/MECP2* gene is one of the longest observed at 8.5 kb long and contains multiple polyadenylation signals resulting in different transcript sizes of approximately 1.8, 5.4, 7.5 and 10.2 kb.[33,42,45–47] The 3'UTR has 52 miRNA predicted binding sites.[66] A number of microRNAs that repress MeCP2 in the fetal brain and

primary cortical neurons are known[46,47,67,68] Though both short and long *MECP2* transcripts are expressed in pluripotent stem cells and neurons, MeCP2 protein is highly expressed in neurons, with lower expression in astrocytes and glial cells.[33,38,53,63] The levels of the short isoform remain consistent during neuronal maturation, but the steady state levels of the long isoform progressively increase. The post-transcriptional regulation of the long isoform regulates the increase in MeCP2 protein levels during maturation.[33]

At the protein level MeCP2 is regulated by a large number of post-translational modifications which play a role in regulating binding to various protein partners. These include acetylation, phosphorylation, ubiquitination and SUMOylation.[4] Recent evidence suggests the differences in the N-termini of the two protein isoforms influence the biophysical stability of MeCP2, interaction with DNA, stability, and interaction with protein partners.[69]

I.ii.c Functions of MeCP2

MeCP2 functions as a critical epigenetic regulator in processes of neurodevelopment. MeCP2 is a chromatin associated protein, which binds both heterochromatic and euchromatic regions of rat and mouse genomes.[15,39] Mouse nuclei contain DAPI-rich regions of heterochromatin called "chromocenters" where MeCP2 binding is enriched.[54] The binding of genes by MeCP2 corresponds with the level of DNA methylation in the mature mouse neuron genome.[60] MeCP2 also binds active regions of the genome by binding 5hmC, which is enriched in active genes of neurons.[16] MeCP2 was shown to be capable of displacing Histone H1 from preassembled chromatin containing methylated CpGs[50] and was shown to associate with nucleosomal DNA[70] and more specifically the linker DNA of nucleosomes.[71] In neurons, Histone H1 is present at one molecule for every two nucleosomes while in most other cell types it is present at one molecule per nucleosome.[60] In neurons MeCP2 is also present at one molecule per two nucleosomes. *Mecp2* null mice exhibit elevated Histone H1 by approximately 2-fold, indicating that neurons attempt to compensate for the lack of MeCP2 at nucleosomes.[60]

The MBD of MeCP2 is required for binding to methylated CpGs and localization of MeCP2 to heterochromatin.[49,72] MeCP2 exists as a monomer in solution but binds to DNA as a dimer.[57] MeCP2 molecules have been observed to interact with each other through the TRD/ID/CTD

regions of the protein, which has been suggested to function in chromatin compaction and chromatin architecture.[73–75] As a reader of DNA methylation, MeCP2 recruits other protein partners and has been shown to influence gene transcription and the process of silencing lentiviral vectors.[76] MeCP2 forms repressive complexes with Sin3A and histone deacetylases HDAC1 and HDAC2 through its TRD.[77,78] The TRD is capable of facilitating long range repression of gene expression.[50] The protein Brahma has also been demonstrated to link MeCP2 with the SWI/SNF chromatin remodeling complex associated with transcriptional repression.[79] MeCP2 has also been shown to interact with the transcriptional activator cAMP response element binding protein (CREB).[80] The regulatory role of MeCP2 is complex in that it can function both as transcriptional repressor and transcriptional activator.[78,80] It not only binds to gene promoters but also within gene bodies.[81]

Early in MeCP2 research, it was shown that *Mecp2*-null male mouse embryonic stem cells grew similarly to controls, but chimeric embryos derived from mutant cells exhibited severe developmental defects indicating that MeCP2 is crucial for embryonic differentiation.[82] *Mecp2*-null precursors from mice differentiate into morphologically mature neurons and glia but they display defects in dendritic arborization, thinner neocortical projection layers and smaller, less complex pyramidal neurons in layer II/III with increases in cell density, indicating MeCP2 role is in maturation and maintenance rather than cell fate decisions.[3] MeCP2 is critical for maturation of neurons in the dentate gyrus of the hippocampus in mice and regulation of gene expression in those neurons.[83] Similarly, in human cells MeCP2 protein is expressed in human wild-type embryonic stem cells and neural precursors but significantly more in neurons.[33,84] *MECP2*-null human neural precursors can also differentiate to neurons, but mutant neurons have reduced soma and nuclei size, reduced neurite complexity and action potential rates.[84] The loss of MeCP2 results in decreased synapse formation. Mice with increased MeCP2 initially have enhanced synaptic response,[85,86] however dendritic arborization becomes reduced as the mice age (Figure 2).[87]

Figure 2. Relationship between altered MeCP2 levels and neuronal morphology. Reductions in dendritic complexity result from reductions in MeCP2 levels as seen in ASD, MeCP2 mutations causing Rett Syndrome and increased MeCP2 levels due to duplication of the gene as observed in *MECP2* Duplication Syndrome. Reduced soma size is also observed in autism and Rett Syndrome, while soma size is increased in *MECP2* Duplication Syndrome.[88]

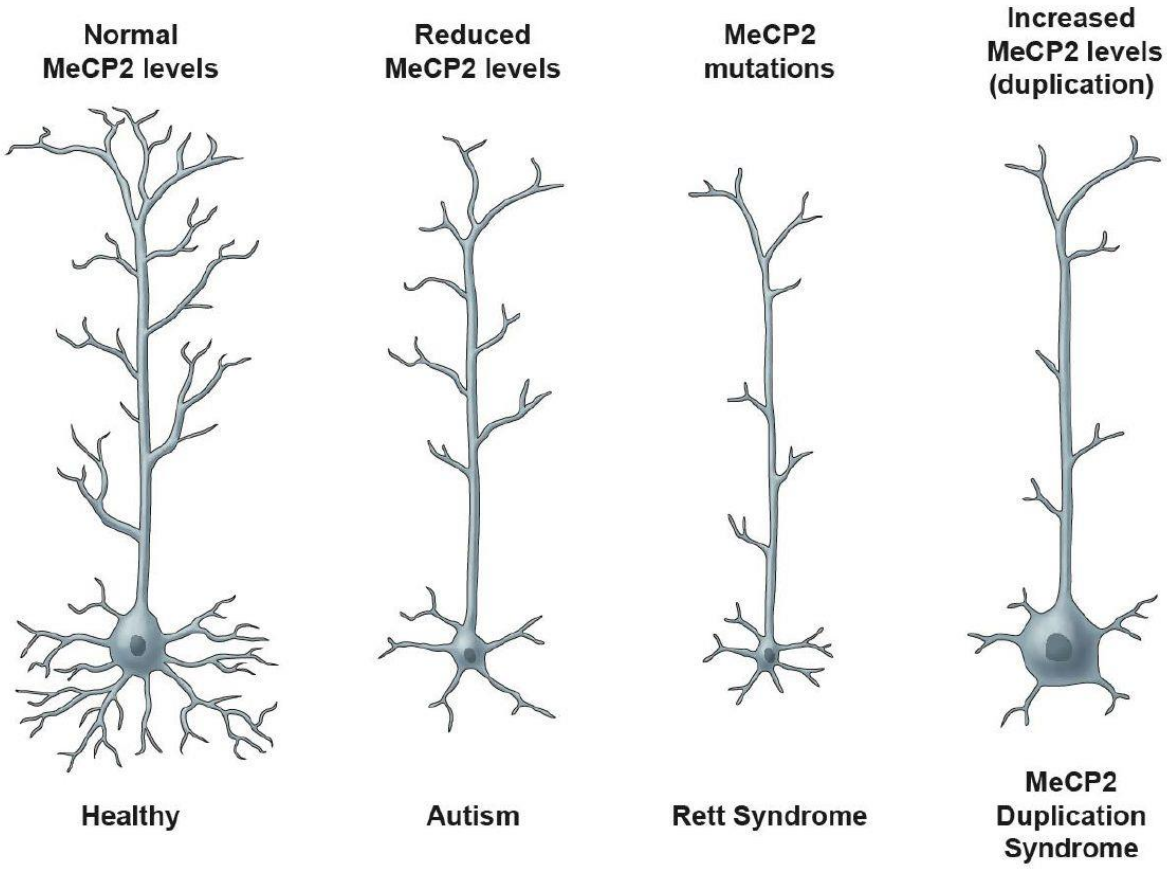

I.iii. Neurodevelopmental disorders and MECP2

I.iii.a. Rett Syndrome

Regulation of MeCP2 expression must be kept within a certain range in the brain, as it is evident that both its lack and excessive levels have devastating effects. Gain- and loss-of-function mutations in the *MECP2* gene result in *MECP2* Duplication Syndrome and Rett Syndrome, respectively. Rett Syndrome was first described by Dr. Andreas Rett[89] and is a severe progressive neurodevelopmental disorder affecting approximately 1 in 10,000-15,000 live female births.[90] RTT is caused by loss-of-function mutations of the *MECP2* gene encoding MeCP2.[1] 95% of typical RTT cases are caused by *MECP2* mutations.[1] Mutations are typically *de novo* with rare cases of familial inheritance, which aided in identifying *MECP2* mutations as the cause of RTT. Types of

mutations that have been observed in RTT patients include missense, frameshift, and nonsense. The mosaic pattern of X chromosome inactivation in females influences the severity of RTT in females.[1] Boys with loss-of-function mutations in *MECP2* do not typically survive, since they possess only one X chromosome. The majority of atypical cases of RTT are due to mutations in cyclin-dependent kinase-like 5 (CDKL5), which causes the early-onset seizure variant,[91] and mutations in Forkhead box G1 (FOXG1), which causes the congenital variant in which infants display hypotonia and severe developmental delays early in the first few months of life.[92]

Typical cases of RTT are characterized by normal development until 6-18 months of age, followed by developmental stagnation and regression involving loss of speech and purposeful hand use and development of microcephaly, seizures, ataxia and stereotypic hand movements.[90,93] Patients may also develop gastrointestinal problems, early-onset osteoporosis, bruxism and screaming spells.[94] The development of RTT features occurs over four stages (Figure 3). The first is a period of stagnation at about 6-18 months of age, in which developmental progress is delayed and patients present with microcephaly and muscle hypotonia. This is followed by a stage of rapid regression in years 1-4 where motor and communication skills are lost and there is the appearance of stereotypic hand movements, breathing irregularities, seizures and worsening of microcephaly. The pseudo-stationary stage begins at approximately 2 years of age and some patients remain in this stage for the remainder of life. There is potential for recovery of some skills in this stage, but seizures remain common, and patients may develop scoliosis (lateral curvature of the spine). Some patients progress to a fourth stage, that of late motor deterioration occurring from age 10 and lasting the remainder of life. Patients may become dependent on a wheelchair and/or a gastrostomy-tube.[4,95–97]

Figure 3. A timeline of the onset of Rett Syndrome. The progression of RTT is divided into four stages based on symptom progression and the approximate age of development of these symptoms. After an initial period of normal development patients display development stagnation, microcephaly and hypotonia between 6 to 18 months of age. A stage of rapid regression occurs between 1 and 4 years during which patients lose motor and communication skills they had previously acquired. Patients display stereotypic hand movements of hand wringing or washing motions, develop breathing abnormalities, seizures, and autistic features. Some patients remain in the third stage, the pseudo-stationary phase the remainder of their lives during which some cognitive improvements may be observed yet seizures continue, and scoliosis may develop. Some patients progress to a fourth severe stage involving significant decreases or total loss of mobility. The duration of these final stages will be affected by the severity of the case. While some patients succumb to the disease in their teenage years, others survive into middle age or beyond.[4,96]

Stage of RTT	Approximate age of occurrence	Symptoms
Stage I: Stagnation	6-18 months of age	➢ Microcephaly ➢ Muscle hypotonia ➢ Delayed development
Stage II: Rapid regression	1-4 years of age	➢ Loss of motor and communication skills ➢ Stereotypic hand movements ➢ Breathing irregularities ➢ Seizures ➢ Worsening microcephaly ➢ Autistic features
Stage III: Pseudo-stationary	2 years of age, may last years or duration of life	➢ Potential cognitive and social improvements ➢ Scoliosis ➢ Seizures ➢ Autonomic dysfunction
Stage IV: Late motor regression	10 years of age, lasting duration of life	➢ Decrease or loss of mobility ➢ Severe physical disability, dystonia ➢ Wheelchair dependency ➢ Parkinsonian features

The life expectancy of RTT patients is affected by the severity of the mutation. A study based in Australia found that 70% of patients were alive at 25 years of age, and patients may survive into middle age and beyond.[96,98,99] Causes of death include respiratory infection, aspiration/asphyxiation, respiratory failure, and seizure related illness.[99] RTT patients have an increased risk of unexpected death estimated at 26%, much higher than healthy individuals.[100]

RTT is a complex disorder with no known cure, and therapies are currently limited to symptom management. There is a large number of symptoms to address, and these can vary in severity from patient to patient. The loss of MeCP2 in neurons is considered to be the main driver of RTT, resulting in behavioral, sensorimotor and autonomic defects.[101] The brain of RTT Syndrome patients is typically of smaller gross volume due to decreased neuronal size with reduced dendritic complexity and synaptic density.[102] MeCP2 is expressed throughout the brain and reductions in neuronal size are observed in the cerebral cortex, thalamus, substantia nigra, basal ganglia, amygdala, cerebellum and hippocampus.[102] *MECP2* mutations also impact a number of regulatory processes in the peripheral system as well. In RTT patients, fatty liver and metabolic disease, lung lesions, cardiac effects, and bone defects have been observed.[4,101]

Hundreds of *MECP2* mutations have been identified.[103] 99.5% of mutations are *de novo* and approximately 70% are C > T transitions.[104] *MECP2* mutations most often originate from the paternal X chromosome[105] thought to be due to hypermethylation of the paternal X chromosome and increased chance of deamination of methylated cytosines at CpG sites.[106] Eight mutations are responsible for approximately 70% of all RTT cases and are either missense or nonsense mutations, R106W, R133C, T158M, R168X, R255X, R270X, R294X and R306C (Figure 4). R106W, R133C and T158M missense mutations occur in the methyl-binding domain of MeCP2. R168X occurs in the Inter-Domain and eliminates the entire transcriptional repression domain and remainder of protein. R255X, R270X and R294X occur within the TRD. R306C occurs in the NCoR interaction domain (NID).[4,107,108] C-terminal deletions make up approximately 8% of cases and large deletions 5% of cases.[108] The truncating mutations R168X, R255X and R270X and large INDELs result in the most severe cases as a significant portion of protein is lost.[108,109] Phenotypic variation can also occur between patients with the same mutation due to variable X chromosome inactivation patterns which are sometimes skewed to favor silencing of the mutant gene.[110,111]

Figure 4. The 8 most common mutations causing Rett Syndrome. The approximate location of each mutation is shown within the domain of MeCP2 where it is found. These 8 mutations are found in the Methyl Binding Domain, Inter-Domain (intervening) and Transcriptional Repression Domain.[88]

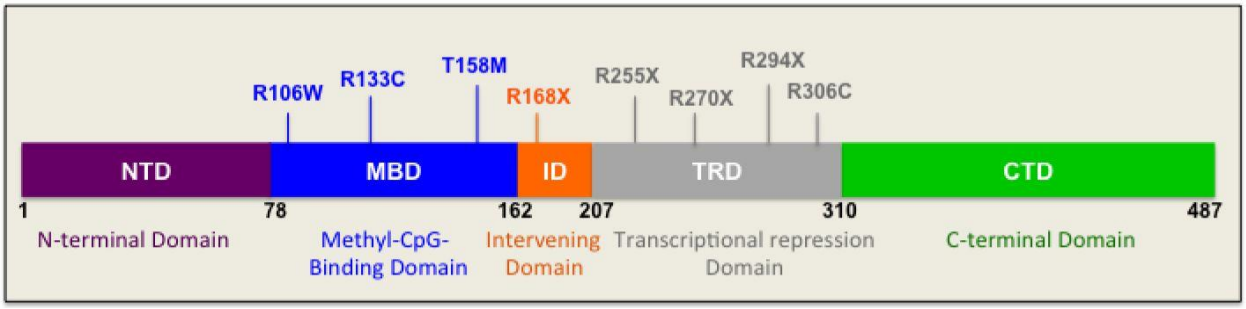

I.iii.b *MECP2* Duplication Syndrome

MECP2 Duplication Syndrome is observed in males and results from duplication or triplication of the *MECP2* gene.[2,112] Clinical features include severe intellectual disability, infantile hypotonia, mild dysmorphic features, absent or limited speech, motor abnormalities, choreiform movements, seizures, progressive spasticity, and severe infections. Patients succumb to an early death, 50% before age 25, most commonly from respiratory infections.[2,112,113] Developmental regression occurs in only half the population with highly variable age of onset.[113] Most cases are inherited from a carrier female. Females with duplication of the *MECP2* gene do not exhibit symptoms and this has been attributed to skewed X-inactivation whereby the X chromosome carrying the duplication is preferentially silenced in the large majority of cells.[112] MDS is 100% penetrant in males meaning that all males with duplication of the *MECP2* gene develop the symptoms of MDS. The shortest duplication sufficient for causing the core phenotype of MDS contains the *MECP2* and neighboring *IRAK1* genes. Larger duplications that include additional neighboring genes are correlated with increasing disease severity.[113] MDS is rare, with approximately 200 cases described worldwide but it is suspected to be underdiagnosed.[113]

From these two disorders, Rett Syndrome and *MECP2* Duplication Syndrome, it is clear that MeCP2 expression in the brain is a tightly controlled process during neurodevelopment and both too low or too high a level of the protein has serious consequences. The mechanism by which MeCP2 loss- and gain-of-function mutations result in a combination of similar and unique symptoms is still not fully understood.

I.iv. Investigating the cellular processes and mechanisms behind neurodevelopmental disorders resulting from MECP2 mutations

In this section, the models used to study MeCP2 functions will be described and the findings to date on three areas of MeCP2 regulation: transcription, protein translation and metabolism.

I.iv.a. *In vitro* and *in vivo* models developed to study MeCP2

The effects of MeCP2 mutations have been studied in a variety of *in vitro* and *in vivo* models. The most commonly used mouse models are the *Mecp2*-null mice which have been generated through deletion of exons 3 and 4,[114,115] as well as deletion of exon 3.[116] Male *Mecp2*-null mice show a similar disease progression to that seen in Rett Syndrome patients, developing normally until 4-6 weeks of age and then becoming uncoordinated in their gait and exhibiting tremors, hindlimb clasping and irregular breathing. Symptoms increase in severity until death between 8 to 12 weeks of age.[114,116] Female mice heterozygous for the null mutation begin showing hindlimb clasping after 3 months and approximately 50% develop the full phenotype by 9 months yet some are still healthy at 1 year. Variable X-inactivation patterns in the female mice result in the variable onset of symptoms. Obesity is observed in heterozygous female mice which is not a phenotype seen in human RTT patients.[114] The majority of RTT research using mouse models has been done using the male *Mecp2*-null mice, since they develop symptoms in a more consistent pattern.

Deletion of *Mecp2* specifically in post-mitotic neurons of mice also leads to development of the RTT-like phenotype at a delayed age indicating the importance of MeCP2 in maintaining neurons.[116] Inactivation of the *Mecp2* gene in mice at 8 weeks and 20 weeks of age has also been demonstrated to result in RTT-like symptoms.[117,118] A significant discovery made in RTT mouse models is that gradual reactivation of the previously silenced *Mecp2* gene in male or female mice with symptoms is capable of reversing the RTT phenotype.[119] This has also been shown *in vitro*.[63,120] This has created hope for Rett Syndrome patients and their families that there is potential for treatment of the disorder even after diagnosis.

There are also a number of mouse models created to probe the role of MeCP2 in specific regions or cell types of the brain such as deletion of MeCP2 from GABAergic inhibitory neurons, which almost completely reproduces the null phenotype.[121] The RTT phenotype could be reversed by

reactivating the previously silenced gene within GABAergic neurons.[122] Isoform-specific mutant mice have also been generated for E1[123] and E2.[124] A number of *Mecp2* knock-in mutant mouse models have been produced to represent Rett Syndrome patients more accurately by introducing mutations commonly occurring in patients such as R168X,[125] T308A, R306C,[107,126] T158A,[127] and T158M.[128]

The MeCP2^{Tg1} mouse model overexpresses MeCP2 at twofold the wild-type level. The model was created as a gain-of-function model to seek to understand MeCP2 function, but the overexpression was found to negatively impact the mice. Although their motor learning and synaptic plasticity were initially enhanced, the mice develop neurological symptoms at approximately 10 weeks and after 20 weeks develop seizures. This model was subsequently used to model MDS following the discovery of *MECP2* duplications in male patients with severe intellectual disability.[2,129] MeCP2^{Tg1} mice have increased dendritic spine density in layer 5 pyramidal neurons before they are 12 weeks of age but after this the density decreases below control levels, coordinating with the onset of symptoms.[87]

Monkey models of RTT have also been established which show similar symptom progression to humans.[130,131] *In vitro* models to study RTT and MDS include human induced pluripotent stem cells[132,133] and human embryonic stem cells differentiated to RTT neurons.[84] Brain cancer cell lines have also been used including the human neuroblastoma SH-SY5Y cell line which can undergo differentiation to mature neurons and the Daoy human medulloblastoma cell line derived from the cerebellum which have been used to study MeCP2 targets and regulators of MeCP2 stability.[134–136]

The decision of parents of patients to donate postmortem brain tissue of the patient is extremely important in gaining greater understanding of the effects of *MECP2* mutation in the patients, since there are differences between the mouse and human contexts.[56,61,137] Post-mortem tissue analysis presents only a snapshot of the final stages of the disease and both *in vitro* and *in vivo* models still remain valuable in understanding the dynamics and progression of the disease and for testing potential drug treatments.

I.iv.b. MeCP2 as an activator and repressor of transcription

MeCP2 was originally expected to act as a transcriptional repressor since DNA methylation was associated with gene repression and MeCP2 was shown to form complexes with other repressive proteins. However large-scale gene expression studies redefined MeCP2 as a transcriptional modulator that both represses and activates gene expression. Analysis of whole brain tissue of *Mecp2*-null mice revealed subtle changes in gene expression[138] but microarray analysis of individual brain regions such as the hypothalamus and cerebellum identified expression changes in hundreds of genes.[80,139,140] The fold changes in gene expression tended to be moderate, ranging from decreases of 0.5-fold to increases of 1.5-fold.[80] The studies of hypothalamus and cerebellum were performed in male *Mecp2*-null mice, which lack MeCP2, and MeCP2^{Tg1} mice, which overexpress MeCP2, at 6 weeks of age. At this time point, the null mice are showing symptoms but MeCP2^{Tg1} mice have not yet developed the phenotype. In the hypothalamus, 2582 genes were misregulated in both models and of these 85% were upregulated in MeCP2^{Tg1} and downregulated in *Mecp2*-null mice, suggesting MeCP2 activates their transcription. Of the remaining 15% of genes, the majority were downregulated in MeCP2^{Tg1} and upregulated in null, suggesting MeCP2 represses their transcription. A small number of genes were misregulated in the same direction in both models. There were 1187 genes altered only in the MeCP2^{Tg1} mice and 369 altered only in *Mecp2*-null mice which suggests the effects of overexpression and knockout do not produce a completely inverse effect. The cerebellum followed a similar trend with 583 genes misregulated in both models and of these 75% were upregulated in MeCP2^{Tg1} and downregulated in *Mecp2*-null again suggesting MeCP2 activates the majority of genes. 20% were downregulated in MeCP2^{Tg1} and upregulated in *Mecp2*-null, with the remaining 5% altered in the same direction. There were 597 genes that were altered only in MeCP2^{Tg1} mice and 519 genes were misregulated only in *Mecp2*-null mice.[139] A select number of gene expression changes were confirmed by qRT-PCR. ChIP analysis revealed that MeCP2 binds the promoters of genes that were misregulated in opposite directions in the two models, but not genes that were misregulated in the same direction.[80,139] Enhanced binding was observed in MeCP2^{Tg1} mice compared to wild-type indicating enhanced function.[80] MeCP2 has been shown to associate more frequently with activated promoters than repressed.[141]

One of the genes identified as a target of MeCP2 activation in the hypothalamus was the *Creb1* gene which encodes CREB1, a major transcriptional activator. MeCP2 binds the *Creb1* promoter and the two proteins also interact and bind at gene promoters of genes activated by MeCP2.[80] Another study performed in the cortex, midbrain, hypothalamus and cerebellum regions of *Mecp2*-null mice at 6-10 weeks of age found a much smaller number of gene expression changes compared to the studies in hypothalamus and cerebellum described above. This could be due to the fact that samples were collected at a variety of ages. However, this study also found that *Mecp2* deletion leads to both upregulation and downregulation of gene expression, and also identified the *Creb1* gene as a target of MeCP2 regulation.[142] This demonstrates that MeCP2 not only interacts with transcriptional repressors but also transcriptional activators.

The role of MeCP2 as a transcriptional modulator is dynamic. MeCP2 was found to function as a global activator of transcription in neurons, but not in neural precursors.[84] Neurons produced by differentiation of *MECP2* loss-of-function human embryonic stem cells display significant reductions in total RNA levels, while neural precursors do not. After 2 weeks of differentiation *MECP2* male and female mutant neurons showed greater than 1.2-fold reductions in 62.3% of genes 37.9% of genes, respectively. After 4 weeks reductions greater than 1.2-fold were seen in 54.1% of genes in male neurons and 64.6% in female neurons. A small percentage of genes were upregulated by more than 1.2-fold at 2 and 4 weeks. At the neural precursor stage, small percentages of genes were misregulated in either direction. Genes that were highly expressed in wild-type neurons were more susceptible to downregulation in mutant neurons indicating MeCP2 has a significant role as a transcriptional activator in neurons.[84]

The methylation landscape of promoters has a significant influence on the role of MeCP2 as a transcriptional modulator.[142] The 5kb upstream region of genes upregulated by MeCP2 were observed to be enriched in CpG islands, while downregulated genes were not. Analysis of DNA methylation levels indicated that CpG islands within promoters of genes which are activated by MeCP2 are not heavily methylated compared to CpG islands of promoters of repressed genes.[80] The DNA methylation landscape changes as neurons mature, which contributes to the dynamic role of MeCP2 in transcription modulation. In mouse hypothalamus, non-CG methylation (mCpH, H=A, C, or T) levels increases as neurons mature which MeCP2 also binds, influencing its

mechanism of regulation.[140] In human neurons, genes with high 5hmC/5mC ratios are more highly expressed in control neurons and more likely to be downregulated in *MECP2* mutant neurons. This correlation is not seen in neural precursors, suggesting that this mode of regulation is specific to neurons.[84]

The numerous genes misregulated upon *Mecp2/MECP2* mutation can be linked to a number of biological processes. The hypothalamus is relevant to Rett Syndrome and MDS phenotypes of anxiety, growth deceleration, sleep-wake rhythms and autonomic dysfunctions and the cerebellum relevant due to its role in regulating normal movement and coordination.[80,139] In the hypothalamus, genes identified as potential targets included those implicated in phenotypes of RTT including epilepsy, abnormal splicing of neuronal genes, intellectual disability, creatinine biosynthesis, speech, seizures, and hypotonia. Most neuropeptide receptors in the hypothalamus are G-protein coupled receptors (GPCRs) and expression of these genes was significantly affected. The expression of brain-derived neutrophic factor (*Bdnf)* was also identified as a target of MeCP2 activation.[80] In comparing the gene expression results of the cerebellum and hypothalamus, the authors found that 244 genes were commonly altered between the regions indicating MeCP2 has unique and shared functions between the regions. The majority of these commonly altered genes were those proposed to be activated by MeCP2 and were linked to biological processes including dendrite development, CNS neuron development, ion transport, synaptic transmission, neurotransmitter transport, generation of precursor metabolites and energy. One biological process, carbohydrate transport, was linked to genes repressed by MeCP2.[139] In *MECP2* loss-of-function neurons derived from human embryonic stem cells, gene ontology analysis showed that the downregulated genes were enriched for genes involved in the biological processes of transcription and translation as well as nervous system development and synapse formation. Immediate early genes *Arc*, *Fos*, *NPAS4* and *BDNF* were downregulated and confirmed by qRT-PCR. Ribosomal protein genes were downregulated in neurons as well as ribosomal RNAs.[84]

Increases and decreases in gene expression have also been observed in post-mortem RTT patient brain tissue,[143] human MeCP2 mutant fibroblast clones,[144] patient T-lymphocytes,[145] and SH-SY5Y neuronal cells.[134] The global gene expression analyses have provided a starting point, but more

research is required to pinpoint which genes MeCP2 regulates the transcription of directly, which genes are affected by secondary effects of mutations and whether the changes in transcript levels translate to changes in protein levels. Our lab has performed analysis of select targets in the *Mecp2*-null, MeCP2^{Tg1} and MeCP2^{Tg3} mouse models and RTT post-mortem brain tissue in order to also begin the important process of comparing common RTT models with the human context to assess disease relevance, which will be discussed in further detail in the upcoming sections.

I.iv.c. Regulation of the *BDNF* gene by MeCP2

Regulation of the *BDNF* gene has been studied quite extensively in connection with MeCP2. *BDNF* was one of the first targets studied in connection with Rett Syndrome and MeCP2 research since it is a member of the activity dependent genes which play an important role in neurons.[146] *BDNF* expression is regulated by activation of voltage-sensitive calcium channels in neurons, responding through calcium-response factor binding enhancer elements in the gene promoter. BDNF expression promotes cell survival of cultured embryonic cortical rat neurons.[147] Gamma-aminobutyric acid (GABA) inhibits neuronal activity and is known to decrease *Bdnf* mRNA levels.[146] BDNF is secreted from neurons and binds to its target receptor TrkB, which then forms homodimers that become auto phosphorylated.[148] BDNF promotes cell survival, neurite outgrowth, synaptic transmission, synaptic plasticity and cell migration in neurons,[149] processes which are defective in RTT and MDS.

The rat, mouse, and human *Bdnf*/*BDNF* genes are similar in structure. The rodent *Bdnf* gene has nine exons with the ninth containing the coding region of the gene. Exons one through eight have distinct promoters which are uniquely regulated.[146] In humans, the *BDNF* gene has eleven exons and nine functional promoters with the last exon again containing the coding region.[150] Promoter IV in the rodent and human genes was known as promoter III in some earlier studies but will be referred to as IV here. Previous studies have identified many transcription factors regulating *BDNF* promoters.[146] MeCP2 binds to the *Bdnf* promoter IV in rodents and humans, interacting with CCCTC-binding factor CTCF once bound.[141,146,151] Promoter IV is the most active promoter in the developing brain and also strongly linked to activation by neuronal activity. CREB, a transcriptional activator also binds *Bdnf* promoter IV, activating transcription.[146] MeCP2 also

binds broadly across the *Bdnf* gene in mice but with lower binding in exonic regions compared to intronic regions.[60]

In cultured neonatal rat neurons, MeCP2 was found to repress *Bdnf* expression until phosphorylation of MeCP2 following membrane polarization releases MeCP2 from the *Bdnf* promoter.[151] Yet in *Mecp2*-null and MeCP2^{Tg1} mouse models and in various other *in vitro* studies knocking out or overexpressing MeCP2, MeCP2 is implicated as an activator of *Bdnf* expression. The differences in effect *in vivo* may be due to the fact that neuronal activation is impaired in *Mecp2* mutant mice and this was being artificially modulated in the *in vitro* study in rat neurons.[151,152]

BDNF protein levels in RTT patient CSF and blood serum have been shown to be unchanged,[153,154] but *BDNF* mRNA levels are decreased in post-mortem RTT patient brain tissue.[56,155,156] BDNF protein levels were not significantly changed in Western blot and ELISA analysis of extracts of post-mortem brain tissues.[56] However, IHC analysis indicated elevated BDNF in the Purkinje cells of the cerebellum of RTT patients, while BDNF staining in the frontal cerebrum and hippocampus regions were unchanged compared to controls.[61] *BDNF* mRNA and BDNF protein levels are both found to be misregulated in *in vitro* and *in vivo* models during periods of neuronal differentiation. BDNF is also expressed in endothelial and astroglial cells in the brain and it is unclear how MeCP2 regulates BDNF in various cell types and in the context of the human RTT brain.[61]

Bdnf gene expression in the hypothalamus is upregulated in MeCP2^{Tg1} mice and downregulated in *Mecp2*-null mice, in the adult mice at 6 weeks but not in juvenile mice at 3 weeks of age.[80,140,152] Mouse neurons differentiated from *Mecp2*-null embryonic stem cells have decreased *Bdnf* transcripts and protein.[120] *BDNF* transcripts and protein are also decreased in human *MECP2*-null neurons derived from hESCs.[84] Nascent *BDNF* transcription is increased approximately 20-25 fold in human neurons compared to hESCs. MeCP2 protein levels also increase as hESCs differentiate to neural precursors and then neurons.[33] The *Bdnf* gene promoter undergoes dynamic changes in the levels of methylated CpH sites during rodent brain maturation, which may be the mechanism by which MeCP2 increases *Bdnf* in mature neurons.[140]

I.iv.d. The homeostasis network of MeCP2, BDNF, and *miR-132*

The homeostasis network involving MeCP2, BDNF, and *miR-132* has been demonstrated dynamically in primary rat cortical and hippocampal neurons isolated close to birth. The transcriptional activator CREB induces *miR-132* expression through binding its promoter, and BDNF also induces *miR-132* through CREB. Elevated *miR-132* levels increased the sprouting of neuronal processes in rat neonatal cortical neurons.[157] Augmented *miR-132* leads to decreased *Mecp2* transcripts, MeCP2 protein and BDNF protein. Decreased *miR-132* has the opposite effect.[68,157] Overexpression of MeCP2 results in increased levels of *BDNF* transcript IV. Increased *BDNF* can also be achieved through decreasing *miR-132* but if MeCP2 protein is decreased at the same time there is no change in *BDNF* transcripts indicating that *miR-132* acts through MeCP2 to induce *BDNF* expression.[68,158] This has also been shown by a Dual Luciferase experiment, where a reporter is fused with the 3'UTR sequence of *Mecp2* or *Bdnf.* Increased *miR-132* decreases expression of the *Mecp2* 3'UTR reporter but not the *Bdnf* reporter indicating *miR-132* directly affects *Mecp2* expression, not *Bdnf*.[158]

Mecp2-null mice have decreased *Bdnf* transcript IV in the cortex compared to wild-type mice.[68] The hippocampi of depressed rats have elevated *miR-132* with decreased MeCP2 and BDNF protein levels. Blood samples of patients with Major Depressive Disorder showed the same pattern.[158] Our lab has aimed to characterize this network in the context of Rett Syndrome research. In post-mortem brain tissue of three Rett Syndrome patients with unique mutations the transcript levels of *MECP2, BDNF* and *miR-132* are decreased in the frontal cerebrum, hippocampus, and amygdala. Only *MECP2 and BDNF* transcript levels are reduced in the cerebellum, not *miR-132*, and *miR-132* was also detected at lower levels in the cerebellum, indicating the homeostasis network function differently between brain regions. The protein levels of BDNF and MeCP2 were not significantly changed in the post-mortem brain tissue from RTT patients that were tested in this study.[56] Further research is needed to analyze this network dynamically in human cells and this will be one of the focuses of this thesis.

I.iv.e. MeCP2 and protein translation

Another cellular process adversely affected by *MECP2* mutations is the mTOR pathway, a crucial regulator of metabolism, growth, proliferation, and survival of eukaryotic cells. The protein mTOR is a serine/threonine protein kinase which phosphorylates key targets to regulate a number of cellular processes.[159] Two mTOR complexes are assembled in cells, mTORC1 and mTORC2, which contain three core components. The proteins mTOR and GβL are common to both complexes while the proteins Raptor and Rictor are unique to mTORC1 and mTORC2, respectively. mTORC1 responds to environmental conditions and regulates the balance of anabolism and catabolism in cells, controlling production of proteins, lipids and nucleotides and suppressing catabolic pathways such as autophagy. mTORC2 regulates the proliferation and survival of cells.[159] Of these, the impact of *MECP2* mutations on the regulation of protein translation and ribosome biogenesis by mTORC1 has been largely studied. AKT, also known as Protein Kinase B (PKB), is a positive upstream regulator of mTOR and promotes cell survival, proliferation, and growth.[160] The direct downstream targets of mTORC1 connected to protein translation initiation are p70S6 Kinase 1 (S6K1) and eIF4E binding protein (4EBP).[159,161] S6K1 phosphorylates and activates ribosomal protein S6 (RPS6). Phosphorylation of 4EBP leads to its release from eIF4E allowing translation initiation.

The levels of phosphorylated RPS6 are reduced in the cortex, cerebellum, and hippocampus of 8-week-old *Mecp2*-null male mice and are also reduced in the cortex and hippocampus of 10-month-old symptomatic heterozygous *Mecp2*$^{+/-}$ female mice. *Mecp2*-null mouse brain also exhibits reduced levels of actively translating ribosomes indicating reduced protein translation.[162] *MECP2*-null neurons derived from human ESCs have significantly reduced levels of activated AKT and RPS6, reductions in nascent protein synthesis and reduced soma size and dendritic complexity.[84] BDNF is an activator of mTOR and this may be compromised in RTT due to decreased BDNF levels.[163] Three-week treatment of *MECP2*-null neurons with growth factors BDNF or insulin-like growth factor 1 (IGF-1) elevated nascent protein synthesis, and significantly increased phospho-AKT and phospho-S6 and rescued soma size and dendrite complexity. Knockdown of PTEN, an inhibitor of the AKT/mTOR pathway, could similarly achieve rescue.[84,164] The mouse model of MeCP2 Duplication Syndrome, MeCP2^{Tg1} also show impaired dendritic

complexity and it is not yet fully understood how opposite MeCP2 mutations result in this similarity in phenotype. It has been suggested that elevated mTOR signaling in MDS mice may increase dendritic spine turnover, negatively impacting dendritic complexity.[87] In human RTT post-mortem cerebellum, components of the mTOR pathway were overactivated.[137] The effects of *Mecp2*/*MECP2* mutations on the mTOR pathway in the human context compared to mouse at different stages of disease progression with different mutations is still not fully understood.

The mechanism by which mTORC1 regulates ribosome biogenesis involves the activation of TIF-IA, a transcription factor involved in ribosomal DNA transcription.[165] Nucleolin is another factor involved in ribosome biogenesis in the nucleolus.[166] Nucleolar structure is impaired in *Mecp2*-null mice which show reduced growth of nucleolar structures during neuronal maturation.[167] The nucleolus is the primary location of nucleolin.[166] The localization of nucleolin to the nucleolus is significantly impaired in human RTT patient post-mortem cerebellum with the T158M mutation, which show nucleolin distributed through the nucleus and cytoplasm and do not show nucleolin concentrated in the nucleolus as is observed in control tissue.[137] In *Mecp2*-null mice the defects in nucleolin localization and structure are no longer observed in adulthood but in human RTT T158M patients this defect appears to persist.[137,167] Ribosomal proteins and *ribosomal RNAs* are a set of genes downregulated in human *MECP2*-null neurons.[84] The *18S* and *28S ribosomal RNA* transcripts are reduced in *Mecp2*-null mouse cortical neurons,[168] but not in *Mecp2*-null cerebellar tissue.[137] MeCP2 binds to *rDNA* genes in the forebrain of mice.[137] My thesis will study the transcriptional role of MeCP2 in regulating the nucleolin and *rDNA* genes.

I.iv.f. Metabolism is compromised in Rett Syndrome models and patients

The regulation of metabolism in the brain is unique and delicate due to the presence of the blood brain barrier. Cholesterol must be synthesized in the brain as it cannot pass the blood brain barrier.[169] The blood brain barrier has selective permeability for glucose, which is the primary fuel source for the brain and can only be supplemented, not replaced as the source of energy for the brain.[170] Metabolic defects in RTT patients are observed both in the brain and systemically. RTT patients present with dyslipidemia, with elevated peripheral cholesterol, triglycerides and/or low-density lipoproteins early in disease onset.[171,172] Some RTT patients develop inflammation of

the gallbladder and gallbladder removal may be required.[171,173] Elevated plasma leptin and adiponectin have also been observed.[174,175] RTT patients tend to have lower than average BMI which indicates elevated lipids are not deposited as fat.[171]

A suppressor screen in *Mecp2*-null mice identified that knockout of the *Sqle* gene encoding squalene epoxidase significantly improved the health of the *Mecp2*-null mice and extended their lifespan.[176] Squalene epoxidase also known as squalene monooxygenase performs the second rate-limiting step and first committed step of cholesterol synthesis.[177] Brain and peripheral lipids were subsequently examined in mice. In the brain of pre-symptomatic mice (P28) cholesterol biosynthesis gene expression is elevated, cholesterol levels are elevated and the expression of the cholesterol turnover enzyme *Cyp46a1* is also elevated to facilitate removal of excess cholesterol from the brain. Pre-symptomatic mice show elevated expression of cholesterol biosynthesis genes in the liver and elevated serum cholesterol. In post-symptomatic mice (8-10 weeks) brain cholesterol is slightly elevated and cholesterol biosynthesis gene expression is now downregulated.[4,142,176] In post-symptomatic mice, peripheral lipid accumulation varies between genetic backgrounds of mice. Brain lipids are perturbed in *Mecp2*-null mice regardless of their genetic background, whether on the 129 or C57BL/6 background. However, peripheral lipid accumulation varies between *Mecp2*-null mice on the 129, C57BL/6, and CD1 backgrounds with mice of the 129 background exhibiting elevated cholesterol and triglycerides in both serum and liver. *Mecp2*-null CD1 mice have only elevated serum triglycerides and peripheral lipids are unchanged in the *Mecp2*-null C57BL/6 mice.[4,176] RTT patients and mouse models may also develop fatty liver disease post-symptomatically.[4,101] These findings should be considered in evaluating lipid-altering drugs in the various RTT mouse models.

RTT patients and *Mecp2* mutant mice both have perturbed glucose tolerance levels and mutant mice show insulin resistance.[178–180] In RTT patients brain carbohydrate metabolism changes have been detected in CSF[181] and by altered glucose uptake in brain regions measured by PET. RTT patients aged 4 to 15 years old had elevated glucose uptake in the cerebellum and decreased uptake in occipital visual association areas, which resembles uptake rates seen in healthy children less than 1 year old indicating a defect in maturation.[182]

Additional metabolic defects include neurometabolite changes such as decreased N-acetylaspartate, a marker of healthy neurons,[183] mitochondrial abnormalities,[84,184] increased oxidative stress,[185] and elevated lactate and pyruvate in the blood and CSF.[181]

The multitude of abnormalities in cellular processes described in this section indicate a multi-pronged treatment plan is likely needed for RTT and MDS patients. An ideal therapy would correct MeCP2 levels, but this is challenged by the requirement for very precise MeCP2 levels. The MeCP2E1 isoform is considered the major isoform in the brain and most studies consider total MeCP2 rather than studying each isoform separately. Yet a number of studies indicate a more comprehensive understanding of MeCP2 function and treatment plans could be achieved if both isoforms are distinguished in research and this will be discussed in the following section prior to discussion of current therapeutic strategies.

I.v. The two isoforms of MeCP2

Alternative splicing of the *Mecp2*/*MECP2* gene produces the two isoforms E1 and E2. A patient with typical Rett Syndrome was found to have an 11 base pair deletion in exon 1 which resulted in a frameshift and premature stop codon, ablating *E1* transcript expression but not affecting *E2* transcripts.[44] However, this 11 bp deletion was shown to affect translation of E2.[186] Additional E1-specific mutations have been identified and these are estimated to occur in 1% of RTT patients.[187–189] To date no E2-specific mutations in RTT have been identified.

The expression patterns of the isoforms have been studied in human and mouse tissues. *E1* transcripts were found to be more abundant than *E2* in mouse and human brain,[54,56] and *E1* transcripts appeared to increase during neuronal differentiation of mouse ESCs.[43] *E1* transcripts are estimated to be ten times higher than *E2* transcripts in adult human brain.[44] At the protein level it has been estimated that 90% of the MeCP2 protein in mouse brain is the E1 isoform.[43] Both E1 and E2 are nuclear and colocalize with densely methylated heterochromatin foci in mouse cells.[43,54] The transcripts and protein levels of E1 are significantly higher than E2 in mice from embryonic day 14 till birth but E2 expression increases postnatally.[54] E1 expression is quite uniform in different brain region of mice such as the olfactory bulb, striatum, cortex, hippocampus, thalamus, brainstem and cerebellum, while E2 is more differentially enriched in

specific parts of the brain. The highest levels of E2 protein are seen in olfactory bulb and cerebellum, and lowest in brainstem.[54]

Before E1 was discovered, *Mecp2*-null male mice were rescued by expression of a *Mecp2E2* transgene under the control of a neuronal-specific promoter. Wild-type mice heterozygous for *Mecp2E2* transgene were found to express MeCP2 2- to 4-fold higher than the endogenous level but were unaffected and healthy. However, wild-type and mutant mice homozygous for the E2 transgene developed severe motor dysfunction.[190] This indicates the importance of *Mecp2* dosage, and also how E2 may be able to rescue deficits on its own, even if slightly overexpressed. A different model system from same group also showed partial rescue by E2 expression in null mice, with activation of expression during embryogenesis leading to the highest level of rescue.[191] However, overexpression of *Mecp2* to 2-fold levels by a transgene which includes the entire human *MECP2* gene results in a progressive neurological phenotype in male mice of the *Mecp2*^{Tg1} model.[129]

Deletion of exon 2 in mice resulted in no neurological symptoms, when the E1 isoform was still expressing. However, E2 null mice did have reduced embryonic viability, which was linked to placenta integrity.[124] Inhibiting E2 expression in PC12 cells during differentiation inhibited neurite extension and proper localization of synapsin I, a marker for synapse formation.[192] An E1 ablating mutation in mice results in RTT phenotypes. Authors showed that in this E1-deficient mouse model, E2 protein levels are increased 2-fold but overall MeCP2 protein was still 50% of the wild-type level, which isn't sufficient to rescue the symptoms.[123] In SHSY-5Y cells E1 protein was found to be more stable than E2.[123] E2 overexpression in cerebellar rat granule neurons promotes apoptosis, while E1 does not.[193] Interestingly in mouse adult brain, E2 is higher than E1 in the granule layer of cerebellum.[54]

The transcripts encoding E2 include all four of the exons. There is an open reading frame upstream of the start codon for E2, using the start codon for E1 and terminating in the 5' UTR of exon 2. This may hamper translation of E2 transcripts. Mutation of the exon 1 ATG to AAG in an E2 expression vector led to increased levels of E2, when transfected in *Mecp2*-null mouse fibroblasts, compared to vector with the WT sequence.[43] The likelihoods of the ATG codons in exons 1 and 2 to be used as initiation codons has previously been analyzed and the exon 1 ATG

gave a score of 97% while exon 2 showed 64%. This is determined by analyzing surrounding Kozak nucleotide contexts and indicates exon 1 is more likely to be used as the exon with initiation codon.[44] The N-terminus of E1 has a unique serine that can be phosphorylated.[123] The two isoforms have unique biophysical properties, DNA binding properties and protein interaction partners,[69] and show differential sensitivity to DNA methylation.[65]

Further studies are required to assess the unique roles of E1 and E2. Evaluating the isoforms separately may allow greater sensitivity in the analyses performed and provide a clearer picture of avenues for therapy.

I. vi. Potential therapeutics for RTT Syndrome

Phenotypic rescue of *Mecp2* knockout mice was achieved by reactivation of the gene indicating that RTT Syndrome may also be reversible. In the case of drug-based therapeutic strategies, the broad effects of *MECP2* mutation indicate a multi-pronged treatment plan is likely required. While correcting the expression of MeCP2 itself is the most desirable approach, the dosage delivery of the protein must be precise, which is still a challenge to gene therapy strategies, along with the targeted delivery into the brain and correct brain cells.[63] Research of therapeutics for MDS has not been as extensive but has included screening for compounds that reduce the stability of the MeCP2 protein to normalize its levels.[136]

One therapeutic strategy for RTT involves screening for small molecules capable of reactivating the wild-type copy of the *MECP2* gene from the inactive X chromosome, which has been demonstrated for the *Ube3a* gene in a mouse model of Angelman syndrome.[194] Gene therapy delivered by the adeno-associated virus (AAV) system is being optimized in mice,[195,196] in which liver toxicity was avoided by inclusion of additional 3'UTR elements of the *MECP2* gene. AAV vectors can be delivered across the blood brain barrier, yet direct injection to the brain provides the highest transduction efficiency to the brain and greatest amelioration of phenotypes.[196]

Another strategy demonstrated in mice is overexpression of a mutant form of the protein. Mutated forms may retain some functions, but the protein commonly tends to be less stable, such as in the case of T158M mutations. Increasing the expression of the T158M mutant form of MeCP2 could partially rescue the mice without negative impacts of overexpression.[197] Screening

for drugs which cross the blood brain barrier and increase expression of the gene in patients or stabilize the protein could be performed, yet there is the complicating factor that RTT patients have a proportion of cells expressing the wild-type protein.

The most extensive testing of RTT therapeutics have been in the areas of drugs which correct dysfunctions in neurotransmitters and excitatory/inhibitory signaling, growth factor signaling pathways, and metabolism. Low dose ketamine, an NMDA receptor antagonist, extended the lifespan of *Mecp2*-null mice and has entered into clinical trials for RTT patients. Ketamine inhibits the binding of glutamate, an excitatory neurotransmitter, to NMDARs.[198] Correction of growth factor signaling has been attempted through induced BDNF and IGF-1, which improves symptoms in *Mecp2*-null mice[152,199,200] and patient iPSC derived neurons.[132] Increasing BDNF expression rescued dendritic morphology in *Mecp2*-null neurons.[86] BDNF itself has low blood brain barrier permeability, making BDNF supplementation unfeasible.[201] In contrast, IGF-1 can cross the blood brain barrier and has been tested in clinical trials. The phase 1 trial demonstrated that IGF-1 was safe, well tolerated and resulted in some improvements in anxiety and breathing abnormalities.[202] However, phase 2 trials did not demonstrate amelioration of symptoms.[203]

Drug therapies to correct BDNF levels include fingolimod, a sphingosine-1 receptor agonist, which crosses the blood brain barrier and increases *BDNF* transcript and protein in cultured neurons and in mouse cortex, hippocampus, and striatum. Fingolimod extended survival of *Mecp2*-null mice but treatment must be initiated before symptom onset, while treatments for RTT patients will most likely be initiated following symptom onset.[204] In addition to the defects in BDNF expression, there is also evidence that *Mecp2* knockout mice show impaired BDNF trafficking between brain regions which involves the protein Huntingtin.[205] A calcineurin inhibitor, FK506 which increases Huntingtin phosphorylation was found to rescue BDNF trafficking, improve respiration and motor function in mice with treatment beginning after symptom onset.[205]

Two FDA-approved drugs which show promise in targeting two areas of therapeutic strategies for RTT, growth factor signaling and metabolism, are simvastatin and metformin, which will be the focus of this thesis. Statin drugs inhibit HMG-CoA reductase, the first rate-limiting step of cholesterol biosynthesis, and are widely used to treat dyslipidemia, providing primary and secondary prevention of cardiovascular disease and stroke.[206,207] Statins are competitive,

reversible inhibitors of HMG-CoA reductase and bind the catalytic domain of the enzyme causing steric hindrance.[206] Additional health benefits of statins have been observed in patients with cognitive and neurological disorders such as dementia, depression, multiple sclerosis, epilepsy and stroke. Mechanism based studies are needed to elucidate the mechanisms of action of statin drugs in the brain.[207,208]

Statins are taken orally and absorbed well, but metabolism of the drug in the liver reduces systemic bioavailability.[209] Simvastatin and lovastatin are reported to have low system bioavailability of 5% or less, yet this has been improved on recently, through delivery of the drug within various mixtures and complexes.[210,211] Statin doses range from 10-80 mg daily.[212,213] The liver is the primary site of cholesterol metabolism in the peripheral system. High cholesterol synthesis occurs in the CNS during early neural development for active myelination, performed by oligodendrocytes. Cholesterol turnover in the mature adult brain is very low and cholesterol is present at low basal levels. Synthesis of cholesterol occurs primarily by *de novo* mechanisms in astrocytes, but also occurs in neurons.[208,214,215] Brain cholesterol has a half-life of 6 months to 5 years,[216,217] which indicates longer term statin treatment may be needed before CNS effects become evident.

Simvastatin is lipophilic and likely enters the cells by passive diffusion. More hydrophilic statins may be taken up by active transport.[218] Lipophilic statins cross the blood brain barrier by passive diffusion. Hydrophilic statins cross less effectively and may cross *via* transporters.[207] The majority of clinical trials are supportive of a protective role for statins against cognitive impairment and dementia in patients. Increased low density lipoprotein (LDL) and total cholesterol have been associated with cognitive impairment.[219] Therefore statin treatment may act by correcting elevated lipid levels in the brain, but the effects of statins have also been seen to be independent of lipid levels.[220]

Statins also inhibit isoprenoid production such as farnesylpyrophosphate and geranylgeranylpyrophosphate, which are suggested to impact cognitive function. Inhibition of farnesylation by simvastatin has been associated with the enhancement of long-term potentiation between neurons in mice.[221] Simvastatin was shown to promote neurogenesis in cultured adult neural progenitor cells and in the dentate gyrus of adult mice through enhanced

Wnt signaling.[222] Statins also promote neurogenesis in some models of traumatic brain injury, both simvastatin and atorvastatin achieve this in the dentate gyrus.[223,224] This was associated with increased vascular endothelial growth factor (VEGF) and BDNF expression, and improved spatial learning.[224] Statins have also been associated with reduced risk of developing epilepsy, a major debilitating phenotype of RTT,[225] with simvastatin and lovastatin both performing the best in this regard *in vitro* and *in vivo*.[226,227]

Lovastatin treatment of *Mecp2*-null mice resulted in improved phenotypes in mice on the 129 background but not those of the C57BL/6 background.[176] These variations will be important to consider if clinical trials are performed in RTT patients and may indicate these drugs may have patient-specific effects. Simvastatin has not yet been evaluated in the context of RTT. Side-by-side comparison of lovastatin and simvastatin was performed in a mouse model of Fragile X Syndrome (FXS). FXS results from mutations in the FMR1 gene resulting in autistic features and intellectual disability. *Fmr1* knockout mice display elevated protein synthesis in the brain and audiogenic seizures.[228,229] Lovastatin normalized protein synthesis and reduced audiogenic seizures, but simvastatin increased protein synthesis and did not ameliorate seizures in *Fmr1* knockout mice.[229,230] These studies indicate that lovastatin and simvastatin have unique mechanisms of action in the brain. Simvastatin may be a promising drug for *Mecp2*-null mice, which show reduced protein synthesis. However, it is important to note that this may differ in the human context. Post-mortem RTT brain analysis showed slightly elevated activation of the mTOR pathway; however, it is still unknown how protein translation is affected in RTT patients during early development.[137] It is also important to investigate the mechanism by which statins influence BDNF expression as well as how they influence MeCP2 expression, which will be a focus of this thesis.

The drug metformin is a synthetic derivative of the compound galegine from the plant *Galega officinalis.* As a natural remedy it was found to benefit type 2 diabetes patients before its mechanism of action was known and has been used for approximately 60 years.[231] Diabetic patients typically receive a dose ranging from 500-2500 mg daily.[232] The mechanisms by which metformin reduces hepatic glucose production was subsequently discovered but is still debated

and suspected to act in a variety of ways in other tissues as well. There are also differences in the acute and chronic effects of metformin treatment.[231]

The mechanism of action of metformin in the liver is characterized the most thoroughly. Metformin is taken up into hepatocytes through organic cation transporter I,[233] and enters the mitochondria due to its positive charge where it inhibits complex I of the electron transport chain.[234] This leads to decreased ATP production, increasing the ADP:ATP and AMP:ATP ratios, which activates AMP-activated protein kinase (AMPK) and leads to inhibition of gluconeogenesis, expression of gluconeogenic genes including *CREB*, and lipid synthesis.[235] Metformin can activate AMPK through mitochondrial mechanisms as well as through a lysosomal mechanism. The latter involves lysosomal protein complex LAMTOR1.[236]

Metformin crosses the blood brain barrier.[237] The mechanism of action of metformin in the brain is not well characterized. The effect of metformin treatment on the human brain has not been characterized as extensively as statins, yet there is evidence in mouse models that metformin has some neuroprotective effects.[232] Metformin enhances neurogenesis and spatial memory formation in the adult mice. CREB binding protein (CBP) is a transcriptional coactivator and histone acetyltransferase and is required for optimal differentiation of embryonic neural precursors. CBP is required to be phosphorylated by atypical protein kinase C (aPKC) to promote differentiation[238] Metformin increases phosphorylation of aPKC in mouse cortical precursors and nearly doubled the number of neurons formed in culture. This was also shown in human ESC differentiation, mouse embryos and adult mice.[239] Mice treated with 200 mg/kg metformin daily for 38 days didn't have affected body weight; metformin selectively enhanced ability to update spatial memory in reversal phase of the water maze task.[239] Protective effects of metformin are being studied in mouse models of Parkinson's Disease with promising results of inhibiting the loss of dopaminergic neurons and elevated BDNF.[232,240] Metformin has also been shown to reduce mTOR phosphorylation in the substantia nigra, and increase BDNF.[240] Metformin also increased BDNF expression in a mouse model of depression, through increasing histone acetylation of the *BDNF* promoter, due to AMPK and CREB activation.[241]

These results indicate metformin may be a promising treatment for RTT, which shows reduced neuronal maturation, and reduced *BDNF*. Metformin is reported to inhibit mTOR in hepatocytes,

but it is still unclear how metformin affects signaling pathways in neurons. Metformin ameliorates the defects observed in the Fragile X Syndrome mouse model by correcting overactivated mTOR signaling.[228] As mentioned earlier RTT mouse models indicate decreased mTOR signaling but post-mortem RTT brain tissue indicated slightly increased mTOR phosphorylation and further studies will be required to determine whether metformin would be beneficial for this aspect of the disease. Metformin improved glucose homeostasis in *Mecp2*-null mice[242] and rescued mitochondrial defects and reduced oxidative damage in the brain of fully symptomatic MeCP2-308 mutant mice[243] but was not able to extend lifespan or ameliorate the motor abnormalities of the mice indicating metformin may need to be used in combination with other drugs and/or at an earlier time point.

Figure 5. Modes of action of simvastatin and metformin. The principal metabolic actions of the drugs are summarized through which simvastatin corrects dyslipidemia and metformin corrects glucose levels. The mechanisms of these drugs observed in neuroprotection are summarized.

<table>
<tr><th>Metabolic mechanisms of simvastatin</th><th colspan="2">Mechanisms of simvastatin in the brain</th></tr>
<tr><td>Inhibition of HMG-CoA reductase
➔ ↓cholesterol synthesis</td><td>Lipid dependent
↓ LDL
↓ cholesterol
↓ cognitive impairment</td><td>Lipid independent
↑Wnt signaling
↑VEGF
↑BDNF
↓Epilepsy</td></tr>
<tr><th>Metabolic mechanisms of metformin</th><th colspan="2">Mechanisms of metformin in the brain</th></tr>
<tr><td>Inhibition of Complex I of ETC
➔ ↓ATP, ↓ADP/ATP and AMP/ATP ratios
➔ ↑ activation of AMPK
➔ Inhibition of gluconeogenic genes, gluconeogenesis, and lipid synthesis</td><td colspan="2">↑activation of aPKC → ↑activation of CBP
➔ promotion of differentiation

↑CREB activation → ↑BDNF</td></tr>
</table>

I.vii. Rationale, hypothesis and objectives

I.vii.a. Aim 1: Investigate the effects of MeCP2E1/E2 overexpression in Daoy cells by lentiviral transduction with *MECP2E1/E2* isoform-specific vectors.

There is an extensive range of research on the broad effects of *MECP2* mutations, which will be used as a guide to investigate whether MeCP2E1 and E2 isoforms have unique and/or synergistic effects on transcription. This research aim will establish *in vitro* cellular models of MeCP2 isoform-specific overexpression. The Daoy cell model was selected for this aim, a human cell line reported to express MeCP2 endogenously and used previously in mechanistic studies to screen for MeCP2 targets.[136] Daoy cells are a human brain cancer cell line derived from a medulloblastoma brain tumor in the cerebellum. Overexpression of E1 and E2 through lentiviral transduction was performed to create stable overexpression in cells, which were validated and subsequently investigated for changes in nascent RNA production of selected confirmed MeCP2 genes. These selected genes are: *BDNF* and *miR-132-3p* (components of MeCP2 homeostasis regulation), *Nucleolin* and the *45S, 28S,* and *18S* ribosomal RNAs. This is the first study to examine MeCP2-isoform-specific regulation of these genes at the transcriptional levels.

I.vii.b. Aim 2: Investigate the effect of metformin and simvastatin treatment of Daoy cells on *de novo* transcription of *MECP2* and *BDNF* by nascent RNA analysis.

Metformin and simvastatin are well established metabolism modulating drugs, whose effects are suggested to correct the metabolic defects detected in RTT patients. The second aim of this thesis seeks to investigate the effects of these drugs on the transcription of the *MECP2* and *BDNF* genes, as this will be key knowledge in evaluating the promise and suitability of these drugs as RTT therapies. The mechanistic effects of metformin in liver cells are well known, and of simvastatin on cholesterol biosynthesis but there is limited knowledge of the mechanistic effects of these drugs in brain cell models. The Daoy cell model was also used in addressing this objective and nascent RNA analysis of *MEPC2E1, MECP2E2, BDNF, 45S pre-rRNA, 28S rRNA,* and *18S rRNA* was performed.

Chapter II: Materials and Methods

II.i. Cell Culture

Daoy cells (ATCC HTB-186) were cultured in MEM supplemented with 10% FBS, 1 mM sodium pyruvate, and 1% penicillin-streptomycin-glutamine (Gibco, Thermo Fisher Scientific). HEK-293T cells (ATCC CRL-3216) were cultured in DMEM supplemented with 10% FBS and 1% penicillin-streptomycin-glutamine. Cells were grown in a humidified incubator at 37°C and 5% CO_2.

Daoy and HEK-293T cells were detached from culture plates by rinsing twice with warm PBS followed by incubation with 0.25% Trypsin-EDTA for 1-2 minutes at 37°C. Fresh media was then added to the cells, they were collected into a conical tube, centrifuged at 1300 x g for 5 minutes and the supernatant removed. Cells were resuspended in fresh media and passaged by plating at dilutions ranging from 1:4 to 1:8. To achieve specific seeding densities for an experiment, live cells were counted using Trypan Blue stain. When collecting cell samples for analysis, cells were detached and centrifuged as described above, then resuspended in room temperature PBS and centrifuged at 5000 x g for 5 minutes at 4°C. The supernatant was removed, and cell pellet snap frozen on dry ice and stored at -80°C.

II.ii. Lentivirus Production and Transduction

Construction of *MECP2* and *EGFP* PL-cHS4-EF1α lentiviral vectors has been described previously.[63] Plasmid preparation was done with the PureLink HiPure Plasmid Midiprep kit (Invitrogen, Thermo Fisher Scientific). Transformed DH5α cells were cultured in LB broth with 100 µg/mL ampicillin at 37°C with shaking. A starter culture was incubated for 8-14 hours, then scaled up and cultured for 18 hours. Plasmid purification was done according to the kit protocol.

All lentiviral procedures were completed in a Class II Biosafety Cabinet. Lentiviral particles were produced in HEK-293T cells which were seeded at a density of $2.3x10^6$ cells in T25 flasks. The media was changed two hours prior to transfection. Four vector mixes were prepared in Opti-MEM (Gibco, Thermo Fisher Scientific). The first mix contained 5 µg Lenti-EF1α-*MECP2E1*, the second 5 µg Lenti-EF1α-*MECP2E2*, the third 2.5 µg Lenti-EF1α-*MECP2E1* + 2.5 µg Lenti-EF1α-*MECP2E2* and the fourth 5 µg Lenti-EF1α-*EGFP*. All mixes contained 3.33 µg each of REV, TAT and GAG/POL plasmids and 1.7 µg VSVG plasmid. Lipofectamine 2000 (Thermo Fisher Scientific) was

added to Opti-MEM at a 1:25 ratio and incubated for five minutes at room temperature. Then an equal volume of the Lipofectamine mix was added to each vector mixture to produce the transfection mixture, which was mixed and incubated for 20 minutes at room temperature. The transfection mixture was gently added to the media of the HEK-293T T25 flasks and mixed thoroughly but gently. The flasks were incubated overnight for 16 hours. The following morning the HEK-293T media was removed from the transfected cells and Daoy cell media added. The cultures were incubated for 48 more hours.

Daoy cells were seeded the day prior to transduction in 6 well plates, one set at $5.0x10^4$ cells per well and another set at $7.5x10^4$. On the day of transduction, viral supernatants were removed from HEK-293T cells, transferred to a falcon tube and filtered through a 0.45 µm syringe filter. Polybrene was added at a concentration of 6 µg/mL similar to what has been used previously.[244–246] Daoy media was removed from Daoy cells and replaced with viral supernatant. Control cells received new media with polybrene only. Transduced cells were then incubated overnight for 16 hours, and media changed the next morning. Then cells were incubated for another 48 hours. EGFP expression was monitored by fluorescence microscopy with the Axio Vert.A1 inverted microscope (Carl Zeiss Microscopy). Cells were passaged to 10 cm plates for expansion and collection of samples.

II.iii. Flow cytometry

Lenti-EF1α-EGFP transduced Daoy cells were analyzed by flow cytometry. Cells were trypsinized and resuspended in 2% FBS in PBS and a sample added to a well of 96 well plate. The polybrene treated cells were used as control. Flow cytometry was performed on the Guava easyCyte 8HT system (Millipore, Guava Technologies) and analyzed using FlowJo software as a paid service provided at the Regenerative Medicine Program Flow Cytometry core, University of Manitoba.

II.iv. Cell viability assay

Cells were seeded in 96 well plates at 5,000 cells per well and cell viability assessed at 24, 48, and 72 hours by MTT assay, as previously reported.[247–250] At the time of each assay, 27.5 µL of MTT reagent (Sigma-Aldrich) was added to the media in the culture wells. The plate was incubated in

the 37°C cell culture incubator for 3 hours. The media and reagent were then carefully and fully removed and 200 µL Dimethyl Sulfoxide (DMSO) added per well. The wells were mixed by pipetting and absorbance at 570 nm measured. DMSO alone was used as the blank and the absorbance at 570 nm subtracted from sample absorbances.

II.v. Western blot

Protein was extracted from snap-frozen cell pellets using ice cold NP-40 lysis buffer consisting of 50 mM Tris-HCl (pH 8.0), 150 mM NaCl, and 1% NP-40 in H_2O, with Roche protease inhibitor cocktail added to the lysis buffer immediately before lysis. The pellet was lysed by pipetting up and down in lysis buffer, then sonicated at 50 Hz for five 1 second pulses. The lysate was centrifuged at 10,000 x g for 8 minutes at 4°C and the supernatant containing protein removed. The protein concentration was determined by the Bradford protein assay with absorbance measured at 595 nm.

Protein samples were prepared for Western blot in Laemmli Buffer, NP-40 lysis buffer and 10% β-mercaptoethanol and boiled for five minutes before loading 10 µg per lane on the gel. Proteins were separated by SDS-PAGE using freshly prepared polyacrylamide gels and the BIO-RAD Mini-PROTEAN Tetra System. The Precision Plus Protein Dual Color Standards (Bio-Rad) were used as the ladder. Proteins were transferred to 0.2 µm PVDF membrane by wet transfer using ice-cold transfer buffer for approximately two hours. Membranes were blocked with 5% milk in TBST for one hour at room temperature. Primary antibody incubation was performed overnight at 4°C in 3% milk in TBST (see Table 1 for list of primary antibodies). Membranes were washed three times with 0.05% TBST, incubated with secondary antibody for 1 hour at room temperature (see Table 2 for list of secondary antibodies), followed by three washes. The signal was detected by ECL (enhanced chemiluminescence) and developed on HyBlot CL Autoradiography Film.

Table 1: Primary antibodies used in Western blot and immunofluorescence

Primary antibody	*Application and dilution*	*Description*	*Source*
c-Myc	WB 1:1000	mouse monoclonal	Thermo Fisher Scientific, A21280
c-Myc	IF 1:50	mouse monoclonal	Thermo Fisher Scientific, MA5-12080
MeCP2-E1	WB, IF 2 µg/mL	chicken polyclonal	Custom-made[53]
MeCP2-E2	WB, IF 2 µg/mL	chicken polyclonal	Custom-made[54]
MeCP2 (C-terminal)	WB 1:1000 IF 1:200	rabbit polyclonal	Thermo Fisher Scientific, PA5-12234
GAPDH	WB 1:7500	mouse monoclonal	Santa Cruz Biotechnology, sc-47724

Table 2: List of secondary antibodies used in western blot and immunofluorescence

Secondary antibody	*Application and dilution*	*Source*
HRP-conjugated anti-rabbit IgG	WB 1:5000	Sigma A6154
Peroxidase-AffiniPure sheep anti-mouse IgG	WB 1:7500	Jackson ImmunoResearch 115-035-174
Peroxidase-AffiniPure goat anti-chicken IgY	WB 1:7500	Jackson ImmunoResearch 103-035-155
Alexa Fluor 594 conjugated goat anti-chicken IgY	IF 1:1000	Invitrogen, Thermo Fisher Scientific, A11042
Alexa Fluor 594 conjugated goat anti-rabbit IgG	IF 1:1000	Invitrogen, Thermo Fisher Scientific, A11037
Alexa Fluor 488 conjugated goat anti-mouse IgG	IF 1:1000	Invitrogen, Thermo Fisher Scientific, A11017
Alexa Fluor 594 conjugated goat anti-mouse IgG	IF 1:1000	Invitrogen, Thermo Fisher Scientific, A11032
Alexa Fluor 488 conjugated goat anti-chicken IgG	IF 1:1000	Invitrogen, Thermo Fisher Scientific, A11039
Alexa Fluor 488 conjugated goat anti-rabbit IgG	IF 1:1000	Invitrogen, Thermo Fisher Scientific, A11034

II.vi. Immunofluorescence

Cells were seeded in Nunc Lab-Tek II 8 well chamber slides (Thermo Fisher Scientific) or on glass coverslips in 24 well plates, as reported.[251] The chamber slides or coverslips were first coated with 0.1% gelatin. At the time of fixation, cells were rinsed twice with room temperature PBS, then placed on ice and fixed with ice cold 4% paraformaldehyde (Electron Microscopy Sciences) in PBS for 10 minutes. Cells were then washed by three 5-minute washes with ice cold PBS and stored in PBS at 4^{o}C in the sealed culture dish.

Before immunostaining, the storage PBS was removed, and cells were rinsed once with room temperature PBS. Cells were permeabilized for 10 minutes with 2% NP-40 in PBS, followed by three 5-minute washes with PBS. Blocking was done with 10% normal goat serum (NGS, Jackson ImmunoResearch) in PBS for 1 hour at room temperature. Primary antibody was prepared in 10% NGS in PBS and incubated overnight at 4^{o}C (Table 1). Cells were washed by three 5-minute washes

with PBS. Secondary antibody was prepared in 10% NGS in PBS and incubated for 1 hour at room temperature in the dark (Table 2). After three 5-minute washes with PBS, DAPI (Calbiochem) was added at a concentration of 0.5 µg/mL in PBS for 10 minutes in the dark. Cells were washed by three 5-minute washes with PBS. Coverslips were mounted on slides with Mowiol antifade mounting medium. Imaging was performed on the Zeiss Axio Observer.Z1 equipped with the AxioCam MRm. Images were acquired using Zen Blue software.

Immunofluorescence images were analyzed with ImageJ in order to quantify the fluorescence intensity of c-Myc staining in individual cells. Images were converted to 16-bit grayscale images for analysis. The threshold values were set using polybrene-treated control images, which displayed the lowest intensity of c-Myc staining, in order to ensure cells of similar or greater fluorescence intensity were appropriately selected and measured by ImageJ for all images. The same threshold values were used for transduced cell populations to allow comparison of fluorescence intensity between control and transduced populations. For each image, the threshold was applied and then measurements obtained for the area of each cell, its mean grey value and integrated density. The integrated density is obtained by multiplying the area by the mean grey value of each cell. Six background measurements were made, and the six mean grey values averaged. The measurements made in ImageJ were used to determine corrected total cell fluorescence (CTCF) values for each of the cells in an image.[252] The CTCF is calculated by subtracting the background integrated density from the integrated density of the cell of interest. The background integrated intensity was calculated for each cell of interest by multiplying the area of the cell by the average mean grey value of the background measurements (Equation 1).

Eq.1: CTCF = (*integrated density of cell*) – [(*area of cell*) x (*average mean grey value of background measurements*)]

The CTCF values for transduced cells were compared to polybrene-treated control cells to determine whether the c-Myc fluorescence intensity in transduced cells was greater than endogenous levels. The CTCF values were also used for counting cells to estimate the percentage of overexpressing cells. Counting cells could not be performed visually by assessing presence or

absence of detection of the c-Myc tag since Daoy cells express c-Myc endogenously and low levels of c-Myc were also detected in polybrene-treated control cells. The CTCF value for each cell in images of transduced cells was compared to the average CTCF value of polybrene-treated control cells and if the CTCF value was greater, the cell was counted as overexpressing. The total number of cells determined to overexpress was divided by the total number of cells in the image to calculate the percentage.

II.vii. Genomic DNA analysis

The DNeasy Blood & Tissue kit (Qiagen) was used to extract genomic DNA from snap-frozen cell pellets according to the manufacturer protocol for purification of total DNA from animal blood or cells (spin-column protocol). The pellet was suspended in 200 µL PBS followed by addition of 20 µL proteinase K, then 200 µL Buffer AL. The sample was vortexed by 2-3 short pulses, and the sample tube incubated at 56^{o}C for 10 minutes. Then 200 µL ethanol was added and gently mixed. The mixture was pipetted onto a DNeasy Mini spin column and centrifuged at 6000 x g for 1 minute and flow through discarded. The column was washed with Buffer AW1, centrifuged at 6000 x g for 1 minute, then wash with Buffer AW2 and centrifuged at 14,000 x g for 3 minutes. The DNA was eluted in 200 µL Ultra-pure water and concentration determined with the Nanodrop 2000.

Genomic DNA was analyzed for insertion of lentiviral vectors by qRT-PCR. The reaction mix contained 10 ng genomic DNA, gene-specific primer, PowerUp SYBR Green Master Mix (Applied Biosystems, Thermo Fisher Scientific), and water. Then qRT-PCR was performed on the Applied Biosystems 7500 Fast Real-Time PCR System. The *GAPDH* gene was used as control. See Table 3 for the list of primers. The run methods used for *GAPDH, MECP2E1,* and *MECP2E2* genes were as follows: hold at 95^{o}C for 10 minutes followed by 40 cycles of denature at 95^{o}C for 15 seconds and anneal/extend at 60^{o}C for 1 minute.

Table 3: Primer sequences used for qRT-PCR

Primer Name		*Sequence*	*Reference*
GAPDH	Forward	CCACTCCTCCACCTTTGAC	253
	Reverse	ACCCTGTTGCTGTAGCCA	
MECP2E1[a]	Forward	AGGAGAGACTGGAAGAAAAGTC	254
	Reverse	CTTGAGGGGTTTGTCCTTGA	
MECP2E2[a]	Forward	CTCACCAGTTCCTGCTTTGATGT	
	Reverse	CTTGAGGGGTTTGTCCTTGA	
MECP2E2[b]	Forward	GGTAGCTGGGATGTTAGGGC	
	Reverse	CTTGAGGGGTTTGTCCTTGA	
MECP2E2[b]	Forward	GCTGGGATGTTAGGGCTC	
	Reverse	CTTGAGGGGTTTGTCCTTGA	
BDNF	Forward	TAACGGCGGCAGACAAAAAGA	255
	Reverse	GAAGTATTGCTTCAGTTGGCCT	
Nucleolin	Forward	AGCAAAGAAGGTGGTCGTTT	137
	Reverse	CTTGCCAGGTGTGGTAACTG	
45S rRNA	Forward	CTCCGTTATGGTAGCGCTGC	256
	Reverse	GCGGAACCCTCGCTTCTC	
28S rRNA	Forward	AGAGGTAAACGGGTGGGGTC	257
	Reverse	GGGGTCGGGAGGAACGG	
18S rRNA	Forward	GATGGTAGTCGCCGTGCC	
	Reverse	GCCTGCTGCCTTCCTTGG	

a. Used for analyzing endogenous levels of *MECP2*.
b. used for analyzing *MECP2E2* for genomic DNA and mRNA from lentivirus transduced cells overexpressing *MECP2*.

II.viii. Metformin and Simvastatin Treatments

Daoy cells were treated with metformin and simvastatin. Metformin (Sigma-Aldrich, PHR1084, Lot#LRAA8975 and Lot#P500240) was dissolved in H_2O and filtered. Simvastatin (Sigma-Aldrich, S6196, Lot#116M4716V) was dissolved in DMSO. Daoy cells were seeded in 6 well plates at 50,000 cells per well. Drug treatment was performed both with and without prior serum starvation. Cells which underwent serum starvation were cultured in serum-free media for 24 hours prior to drug treatment. Drug treatment was performed using media containing serum.

Type 2 diabetes patients receiving an 850 mg metformin dose have a plasma metformin concentration of approximately 8-24 µM 3 hours after the dose.[258] Caution is required with increasing metformin dosages, since patients with plasma metformin concentrations of 150-820 µM may develop lactic acidosis due to increased plasma lactate levels.[259] Plasma concentrations of approximately 2.5 mg/L, or 20 µM are generally considered to be safe.[259] For this study Daoy cells were treated with 250, 1000 and 2000 µM metformin which are higher compared to what is recommended for patient plasma levels. The purpose of this study was to evaluate the effects of metformin on gene transcription *in vitro* over a short time period. Concentrations of metformin in this range have previously been used *in vitro* to analyze the impact of metformin on cell signaling.[239,260] Future study could investigate the effects of prolonged metformin treatment at lower concentrations.

Simvastatin concentrations of 2.5 and 5.0 µM were selected for this study, for a 24 hour treatment, based on cell viability data at 24 hours performed previously in Daoy cells.[250] This is a greater concentration than what is typically found in the plasma of patients taking statins, which tends to peak at the nanomolar range, ranging from 6-80 nM.[212,261] *In vitro* studies have commonly employed statins in the micromolar range.[261]

II.ix. RNA extraction

II.ix.a. RNeasy Plus Mini Kit

RNA extraction for drug treated samples was performed with the RNeasy Plus Mini Kit (Qiagen) according to the kit protocol. Steps were performed at room temperature. Buffer RLT Plus was prepared fresh for each extraction by addition of β-mercaptoethanol. Snap-frozen cell pellets were lysed by addition of 350 µL RLT Plus and pipetting up and down. The lysate was loaded on a gDNA eliminator column and centrifuged at 11,000 rpm for 30 seconds. 350 µL of 70% ethanol was added to the flow-through, pipetted well to mix and the total volume transferred to and RNeasy spin column. The column was centrifuged at 11,000 rpm for 15 seconds and the flow-through discarded. The column was washed with Buffer RW1 and Buffer RPE. RNA was eluted in 30 µL commercial RNase-free H_2O.

II.ix.b. TRIzol

RNA extraction was done as reported[28] using TRIzol (ThermoFisher Scientific). Snap-frozen cell pellets were lysed with 250 µL TRIzol by pipetting followed by incubation at room temperature for five minutes. 50 µL chloroform was added, the sample shaken vigorously for 15 seconds and then incubated at room temperature for 2-3 minutes. Samples were centrifuged at 12,000 x g for 15 minutes at 4°C. The upper aqueous layer was isolated and transferred to a new tube. Then 0.25 µL glycogen and 125 µL of isopropanol were added followed by pipetting to mix a few times. The sample was incubated in ice for 10 minutes, then centrifuged at 12,000 x g for 10 minutes at 4°C. The supernatant was discarded, the pellet washed with 250 µL 75% EtOH and centrifuged at 7,500 x g for 5 minutes at 4°C. The supernatant was discarded, the pellet allowed to dry for 5-10 minutes then resuspended in H_2O. RNA extracted with TRIzol was treated with DNase using TURBO DNase (Ambion Life Technologies).

II.ix.c. MagMAX *miR*Vana Kit

Total RNA was extracted from snap-frozen cell pellets with the MagMAX *mir*Vana Total RNA Isolation Kit (Applied Biosystems, Thermo Fisher Scientific). The extraction was performed manually at room temperature. Each sample was lysed in 200 µL Lysis Binding Mix consisting of 99 µL Lysis Buffer, 100 µL isopropanol and 1 µL 2-mercaptoethanol. The sample was pipetted several times to homogenize and incubated for five minutes. Then 20 µL of Binding Beads Mix was added to each sample, containing 10 µL RNA Binding Beads and 10 µL Lysis/Binding Enhancer, and samples were incubated for five minutes while tapping to mix. The Qiagen magnetic tube rack was used to immobilize RNA Binding Beads for washes. The beads were washed with Wash Solution 1, then Wash Solution 2, then allowed to dry for two minutes. 30 µL TURBO DNase Solution was added, containing 28 µL MagMAX TURBO DNase Buffer and 2 µL TURBO DNase, and incubated for 15 minutes while tapping. 50 µL Rebinding buffer was added, followed by addition of 100 µL isopropanol and incubation for three minutes. The beads were washed twice with Wash Solution 2 and dried for two minutes. RNA was released by addition of 30 µL Elution buffer, preheated to 37°C, and incubation for three minutes. The beads were then immobilized and the supernatant containing RNA collected.

II.x. Preparation of cDNA from Total RNA

RNA samples were quantified using the Nanodrop 2000. To synthesize cDNA, 500 ng of RNA template was combined with random primers, dNTPs, and water and incubated at 65^{o}C for 5 minutes. Samples were then immediately transferred to ice for 1-2 minutes. A Master Mix of 5X first strand buffer, 0.1 M DTT, RNaseOUT and Superscript III Reverse Transcriptase (Thermo Fisher Scientific) was prepared and 7 uL added to each sample. Samples were incubated for five minutes at room temperature, then 1 hour at 50^{o}C, and finally 15 minutes at 70^{o}C.

II.xi. Nascent RNA collection and cDNA synthesis preparation

The method of choice for this study was to perform metabolic labelling and isolate RNA for targeted gene-specific transcript analysis. Cells are incubated for a specific period of time in media supplemented with cell-permeable uridine nucleoside analogues such as bromouridine, 4-thiouridine, or 5-ethynyl-uridine. These nucleosides are taken up by the cells and converted into UTPs *via* enzymatic reactions.[18] Isolation of bromouridine labeled RNAs is an antibody-based method.[30,32]. The 4-thiouridine labeled RNAs are purified by biotin/streptavidin interaction.[34] The 5-ethynyluridine (EU) is detected with click chemistry by a copper(I)-catalyzed cycloaddition reaction.[30] Labeling with EU was selected for this study. EU is incorporated into RNA transcripts generated by RNA polymerases I, II and III, labels RNA specifically and labels approximately 1 in every 35 uridines. EU labeling could be applied to both *in vitro* and *in vivo* studies. *In vitro* studies that used this technique include imaging of the nascent RNA production in cultured NIH-3T3 cells[30] as well as in dendrites of cultured hippocampal neurons.[31] Targeted gene transcript analysis has also been reported *in vitro* for *NEAT1* transcripts in HeLa cells[29] and to study *MECP2* post-transcriptional regulation in a hESC differentiation model of neurodevelopment.[33] *In vivo* studies have been performed by injecting EU into mice and zebrafish.[30,31]

Nascent RNA was isolated with the Click-iT Nascent RNA Capture Kit (Invitrogen, Thermo Fisher Scientific). Daoy cells were labelled with 0.1 mM ethynyl-uridine (EU) in the culture media for 1 to 48 hours, depending on the experiment. Cells were harvested, snap frozen and RNA extracted with the RNeasy Mini Kit or MagMAX *mir*Vana Total RNA isolation kit as described earlier. Then

1 µg of EU-RNA was biotinylated by a copper-catalyzed click reaction, using 0.5 mM azide-modified biotin. Biotinylated RNA was precipitated by overnight incubation at -80^{o}C.

400 ng of biotinylated EU-RNA was bound to Dynabeads MyOne Streptavidin T1 magnetic beads according to the manufacturer protocol. The Qiagen magnetic tube rack was used for steps requiring immobilization of the beads. This was followed immediately by cDNA synthesis on the beads. The beads were heated for five minutes at 68-70^{o}C followed immediately by addition of cDNA synthesis mix containing random primers, dNTPs and water. The mix was brought to room temperature, then the enzyme master mix added containing 5X first strand buffer, Superscript III Reverse Transcriptase, and RNase OUT. The reaction was incubated at 50^{o}C for one hour while gently mixing. The reaction was terminated and cDNA released from the beads by heating at 85^{o}C for five minutes. The beads were immobilized and supernatant containing cDNA collected.

II.xii. qRT-PCR

Gene expression analysis was performed by qRT-PCR on the Applied Biosystems 7500 Fast Real-Time PCR System. Reactions were composed of 25 ng template cDNA, gene-specific primers (Table 3), PowerUp SYBR Green Master Mix (Applied Biosystems, Thermo Fisher Scientific), and water. Target gene C_T values were normalized to the housekeeping gene *GAPDH.* Fold change values were calculated by the $2^{-\Delta\Delta CT}$ method (Livak and Schmittgen, 2001).

The run methods for *GAPDH, MECP2E1, MECP2E2* and *BDNF* were: hold at 95^{o}C for 10 minutes followed by 40 cycles of denature at 95^{o}C for 15 seconds and anneal/extend at 60^{o}C for 1 minute. The run method for *28S ribosomal RNA* was hold at 50^{o}C for 20 seconds then 95^{o}C for 10 minutes followed by 35 cycles of denature at 95^{o}C for 30 seconds and anneal/extend at 65^{o}C for 1 minute. The run method for *18S ribosomal RNA* was hold at 50^{o}C for 20 seconds then 95 ^{o}C for 10 minutes followed by 35 cycles of denature at 95 ^{o}C for 15 seconds and anneal/extend at 60^{o}C for 1 minute and 72 ^{o}C for 30 seconds. The run method for *45S ribosomal RNA* was hold at 95^{o}C for 5 minutes followed by 35 cycles of denature at 95^{o}C for 30 seconds and anneal/extend at 60^{o}C for 30 seconds and 72 ^{o}C for 30 seconds.

II.xiii. miRNA analysis

RNA for miRNA analysis was prepared using TRIzol or *mir*Vana RNA extraction methods as described earlier. Analysis of microRNAs was done with TaqMan™ MicroRNA Assays (Applied Biosystems). For the reverse transcription (RT) reaction a master mix was prepared from 100 mM dNTPs, MultiScribe Reverse Transcriptase and 10X Reverse Transcription Buffer from the High-Capacity cDNA Reverse Transcription Kit (Applied Biosystems), with addition of RNase inhibitor. For total RNA, 5 ng was used in the RT reaction. For nascent RNA, the Click-iT Nascent RNA Capture Kit kit protocol was followed for binding biotinylated EU-RNA to Dynabeads, then 50 ng of bead-bound RNA was used in the RT reaction. The RT reaction was prepared by combining the RT master mix, RNA and assay specific TaqMan 5X RT primer and the reactions were run on the Eppendorf vapo.protect thermocycler. The steps of the RT reaction were as follows: 16°C for 30 minutes, 42°C for 30 minutes, 85°C for 5 minutes, hold at 4°C. For nascent RNA, the cDNA is released from the beads during the 85°C step. Then the beads were immobilized using the magnetic tube rack and the supernatant containing cDNA collected.

RT-PCR was then performed using the product of the RT reaction, assay-specific 20X TaqMan MicroRNA Assay, TaqMan Universal PCR Master Mix (Applied Biosystems), and water. 20 µL reactions were prepared which were split into duplicate wells of 9.5 µL each. The reactions were run on the Applied Biosystems 7500 Fast Real-Time PCR system with the following thermal cycling parameters: hold at 96°C for 10 minutes followed by 40 cycles of denature at 95°C for 15 seconds, anneal/extend at 60°C for 60 seconds.

The following assays were used: has-miR-132 (Assay ID 000457) and U6 snRNA (Assay ID 001973). Target gene *miR-132* C_T values were normalized to the housekeeping gene *U6.* Fold change values were calculated by the $2^{-\Delta\Delta CT}$ method (Livak and Schmittgen 2001).

II.xiv. Statistics

Statistical analysis was performed using GraphPad software. Comparisons between 3 or more groups were analyzed by one way ANOVA followed by the Tukey multiple comparisons test, with an alpha of 0.05. Comparisons between 2 groups were analyzed by unpaired t-test with Welch's

correction, with an alpha of 0.05. Levels of significance were considered as *p<0.05, **p<0.01, ***p<0.001, ****p<0.0001.

Chapter III: Results Aim 1: Investigate the effects of MeCP2E1/E2 overexpression in Daoy cells by lentiviral transduction with *MECP2E1/E2* isoform-specific vectors.

MeCP2 is a critical epigenetic regulator in the brain. Mutations in the *MECP2* gene cause Rett Syndrome and *MECP2* Duplication Syndrome. *MECP2* mutations have widespread effects on gene expression, which presents challenges to developing targeted therapies for these disorders. Mouse models with *Mecp2* loss- and gain-of function-mutations display broad gene expression changes in the brain.[80,139,140] There are two isoforms of MeCP2 termed E1 and E2, since they are generated by alternative splicing of exons 1 and 2 of the *Mecp2*/*MECP2* gene.[43,44] There is limited knowledge on whether these two isoforms have unique or common functional roles in regulating gene expression. The structure of these isoforms is identical, expect their extreme N-termini, which suggests the isoforms could have similar or redundant functions. Both E1 and E2 are nuclear proteins, and colocalize with densely methylated heterochromatin foci in mouse cells.[43] However, evidence points to unique functions of these isoforms and mechanisms regulating their differential expression. MeCP2E1 is the dominant isoform expressed in the brain.[53] E1-specific loss-of-function mutations are sufficient to cause Rett Syndrome while E2-specific mutations have not been observed in patients.[44,187,189] Mice with E2 isoform deletion display no adverse neurological symptoms, however a reduction in embryo viability was observed.[124] Mice with an E1-specific mutation develop a Rett Syndrome phenotype.[123] Expression of the E2 isoform alone was capable of ameliorating RTT symptoms in *Mecp2*-null mice.[190,191] Mice with the E1-specific mutation did have increased levels of E2, though not significant enough to rescue.[123] Differential expression of these isoforms during neuronal differentiation has been shown *in vitro* in mouse NSCs[65] as well as *in vivo* where E1 and E2 were both seen to increase during mouse brain development, but E1 showing an earlier onset of expression.[54] E1 expression was also found to be quite uniform across different mouse brain regions while E2 showed a differential expression pattern in brain regions.[54] Studies which have assessed gene expression changes in *Mecp2*-mutant mice have used mice with knockdown or overexpression of both isoforms.[80,139,140] Isoform-specific effects on gene expression have been studied by overexpression of each isoform in SK-N-SH cells, derived from a bone marrow metastasis of neuroblastoma.[262] In these cells E1 overexpression resulted in a greater number of gene expression changes compared to E2.[262] The

first aim of this thesis was to establish human brain cells which overexpress each MeCP2 isoform, as well as both isoforms together and evaluate transcriptional changes in previously identified targets of MeCP2.

MeCP2 isoform-specific overexpression was achieved through *in vitro* lentiviral transduction. The Daoy medulloblastoma human cell line was selected for this study. These cells originated from a tumor in the cerebellum of a 4-year-old boy. The cells express MeCP2 endogenously and have been used previously to study MeCP2 regulation and screen potential therapeutic targets for MeCP2-related disorders.[67,136] Daoy cells were transduced using isoform-specific lentiviral vectors developed previously to obtain stable long-term overexpression.[63] The procedure of lentiviral transduction has a number of biosafety features. Here, HEK-293T cells were transfected with the lentiviral vector containing the gene of interest and four separate plasmids encoding the *rev, tat, gag/pol* and *vsvg* genes. The lentiviral vector is packaged in viral particles in HEK293T cells. Therefore, the only genetic material packaged in the virus is that of the gene of interest, meaning the viral particles are incapable of reproducing inside a target cell. The *vsvg* gene encodes the vesicular stomatitis virus G glycoprotein (VSVG) envelope protein.[263,264] The *gag* gene encodes the matrix, capsid and nucleocapsid structural components of the virus and *pol* encodes reverse transcriptase and integrase enzymes. The Rev protein binds the Rev response element of the lentiviral vector sequence to facilitate nucleocytoplasmic transport of full-length vector RNA. The Tat transactivator is required to promote expression of the full-length vector RNA during viral production in HEK-293T cells.

The viral supernatant was harvested from the HEK-293T cells and used to transduce Daoy cells. The agent polybrene, a cationic polymer, was added at a concentration of 6 μg/mL to facilitate uptake of the viral particles into the target cells.[244] Three lentiviral vectors were used, Lenti-EF1α-EGFP, Lenti-EF1α-E1, and Lenti-EF1α-E2 (Figure 6A). The genes of interest are under control of the ubiquitous EF1α promoter, which was previously shown to maintain expression of MeCP2 in neural stem cells and differentiated neurons without silencing, and thus was most likely to obtain long-term overexpression.[63] The vectors were constructed using the PL-cHS4 lentivirus vector backbone[265] that are self-inactivating (SIN). SIN vectors also have increased biosafety through a deletion in the U3 regions of the 3'LTR. This becomes the 5' LTR following reverse transcription

in the host cell but the deletion abolishes transcription from the 5'LTR, meaning there is only gene expression from the promoter controlling the gene of interest, EF1α in this case.[266,267] The chicken *β-globin* locus Hypersensitive Site 4 (cHS4) core chromatin insulator element in the LTRs blocks position effects following integration that could affect expression of the gene of interest such as silencing through chromatin formation or interactions with other enhancers.[264,265] These lentiviral vectors also contain *cis*-elements central Poly Purine Tract (cPPT) and Central Terminal Sequence (CTS), which improve transgene expression and transduction efficiency during the reverse transcription step.[264]

The Lenti-EF1α-E1 and Lenti-EF1α-E2 vectors express MeCP2 tagged with c-Myc. EGFP wasn't used a tag to monitor expression since the EGFP DNA sequence contains 60 CpGs which could be a target for silencing by MeCP2.[63,268] Instead, the Lenti-EF1α-EGFP vector was used in a separate transduction to monitor efficiency of the transduction and to control for the non-specific effects of transduction in future studies. Cells treated with polybrene alone were included as an additional control. Daoy cells were transduced with Lenti-EF1α-E1 and Lenti-EF1α-E2 vectors separately to evaluate isoform-specific affects and were also transduced with a combination of the two vectors.

Transduced cells were validated by a number of methods including flow cytometry analysis of EGFP expression, Western blot and immunofluorescence analysis of protein expression, genomic DNA analysis to confirm integration of the lentiviral vectors, and finally transcript analysis to assess the effects on gene expression of selected target genes. Two main gene targets selected for analysis are *BDNF* and *miR-132,* which have been proposed to form a homeostatic regulatory network with MeCP2.[68] BDNF is also significantly reduced in Rett Syndrome models.[84,152] There is evidence that MeCP2 binds to the *BDNF* promoter in mouse neuronal cultures,[151] but isoform specific regulation is unclear. Expression of Nucleolin and ribosomal RNA genes was also evaluated. Nucleolin protein expression dysregulation has been observed in RTT mouse models as well as Rett Syndrome patients, but it is unknown whether MeCP2 regulates Nucleolin gene expression.[137,167] Ribosomal protein genes and *ribosomal RNA* genes were observed to be downregulated in MeCP2-knockout neurons derived from human embryonic stem cells, but isoform-specific regulation of these genes is not fully clear.

In order to study whether overexpression of the MeCP2 isoforms leads to direct transcriptional effects on the target genes of interest, nascent RNA production was analyzed. Transcript levels are regulated at multiple levels, from nascent RNA transcription of the gene to post-transcriptional regulation mechanisms. Nascent RNA analysis was performed through labeling nascent RNAs with ethynyl-uridine (EU), a uridine analogue utilizing the Click-iT Nascent RNA Capture Kit. Nascent RNA levels were compared with steady-state transcript levels to evaluate how overexpression of MeCP2 E1 and E2 isoforms impacts gene expression.

III.i. Flow cytometry of EGFP-transduced control cells indicates high transduction efficiency

Daoy cells that had been transduced with the Lenti-EF1α-EGFP control vector were analyzed by flow cytometry one week after transduction. Flow cytometry analysis of EGFP expression was a paid service provided by Regenerative Medicine Program Flow Cytometry core. EGFP expression was tested in two independent biological samples of EGFP-transduced cells and one polybrene-treated control sample. The two sets of EGFP-transduced cells were 97.5% and 98% positive for EGFP-expression. Graphs generated using FlowJo software indicated a clear shift in the number of EGFP expressing cells in the EGFP-transduced cells compared to the polybrene-treated control sample (Figure 6B). EGFP expression in EGFP-transduced cells was also confirmed by fluorescence microscope imaging (Figure 6B). These results indicated a high level of transduction efficiency. The EGFP-transduced cells were included in further molecular studies of the effects of MeCP2 overexpression to control for potential off-target effects of transduction.

Figure 6. Transduction of Daoy cells by lentiviral vectors expressing EGFP and MeCP2E1/E2. A) Schematic of lentiviral vectors used to express *EGFP*, *MECP2E1,* or *MECP2E2* under control of the EF1α promoter. MeCP2 isoforms are tagged with C-terminal c-Myc tag. cHS4: chicken *β-globin* locus Hypersensitive Site 4; cPPT: central Poly Purine Tract; CTS: Central Terminal Sequence; RRE: Rev-Responsive Element (adapted from Rastegar et.al.2009). B) Flow cytometry analysis and fluorescence microscope images of polybrene-treated control and EGFP-transduced cells. BF=bright field, scale bars represent 50 µm. C) Western blot analysis of total MeCP2, c-Myc tag, and MeCP2E1/E2 isoforms in polybrene-treated control, EGFP-transduced (EGFP), E1-transduced (E1), E2-transduced (E2) and E1+E2-tranduced (E1+E2) cells.

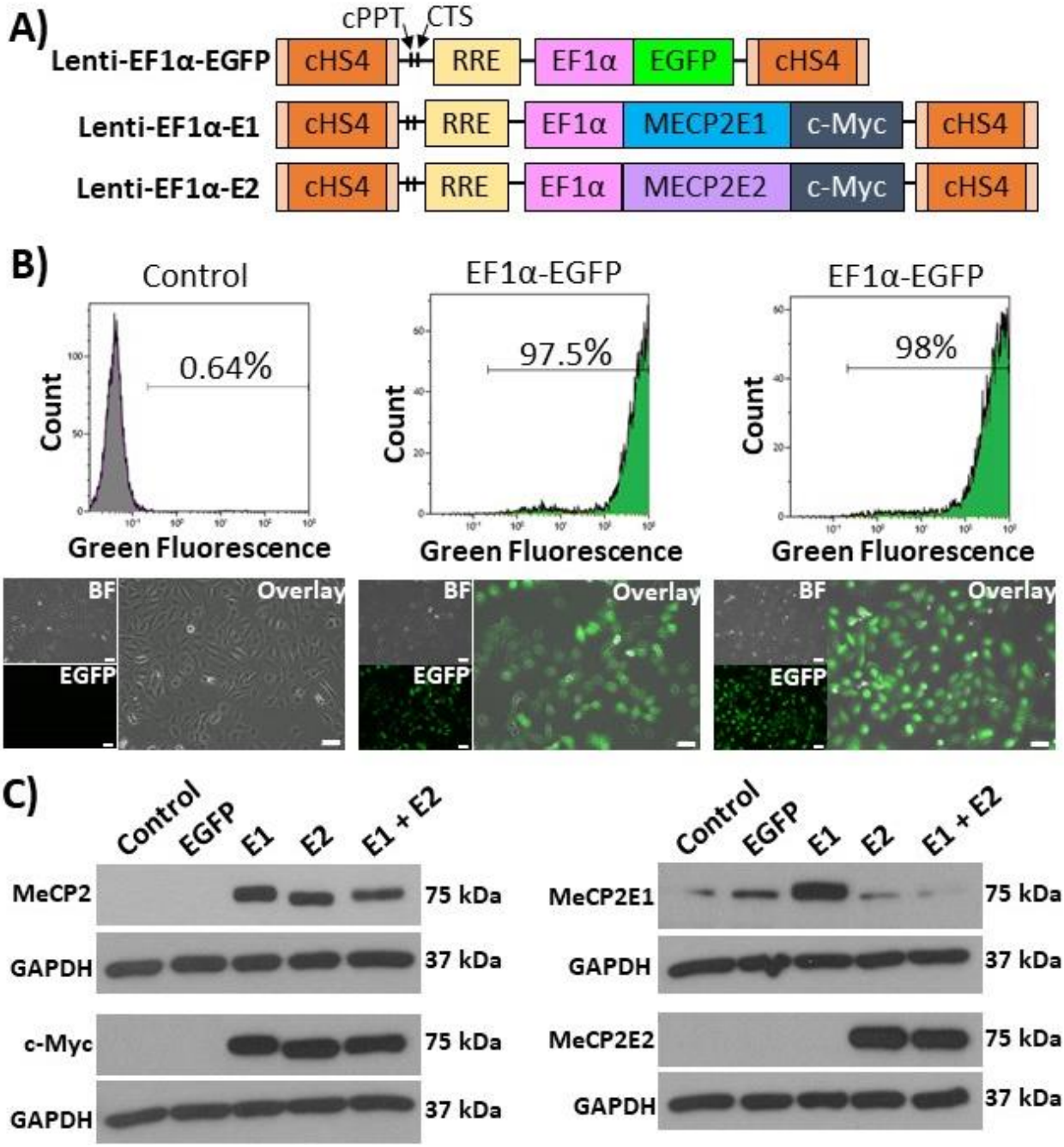

III.ii. Analysis of MeCP2 protein overexpression in MECP2 E1- and E2-transduced Daoy cells

The two MeCP2 isoforms, E1 and E2, were overexpressed in Daoy cells by transduction with Lenti-EF1α-E1 and Lenti-EF1α-E2 vectors (Figure 6A). Daoy cells overexpressing E1 alone, E2 alone, and E1+E2 in combination were generated by transduction with Lenti-EF1α-E1 alone, Lenti-EF1α-E2 alone, or a combination of Lenti-EF1α-E1 and Lenti-EF1α-E2 vectors, respectively. These cells will be referred to as E1-transduced, E2-transduced and E1+E2-transduced cells. After approximately two weeks in culture or three cell passages, samples of polybrene-treated, EGFP-transduced, E1-transduced, E2-transduced and E1+E2-transduced cells were collected for protein analysis by Western blot. Protein was prepared from whole-cell lysates and 10 μg of protein loaded per lane for separation by SDS-PAGE. Four sets of the samples were run in order to probe samples with four primary antibodies: total MeCP2, c-Myc, MeCP2E1 and MeCP2E2 (Figure 6C). The antibody detecting total MeCP2 binds to the C-terminus of MeCP2 and therefore recognizes both MeCP2 isoforms. This antibody detected MeCP2 at 75 kDa in E1-, E2- and E1+E2-transduced cells but not in polybrene-treated or EGFP cells. Probing with the c-Myc primary antibody was performed to confirm presence of the C-terminal c-Myc tag on MeCP2 expressed from the lentiviral vectors. The c-Myc tag was detected in E1-, E2-, and E1+E2-transduced cells at 75 kDa, the same molecular weight as total MeCP2, confirming detection of MeCP2 expressed from the lentiviral vectors. The samples were also tested for overexpression of MeCP2E1/E2 isoforms by probing with isoform-specific antibodies developed in our lab, which recognize the unique N-terminus of each isoform.[53,54] Probing with the E1-specific antibody indicated that MeCP2E1 was overexpressed in E1-transduced cells but not E1+E2-transduced cells. Endogenous levels of E1 were detected in polybrene-treated, EGFP-transduced, E2-transduced and E1+E2-transduced cells and a clear overexpression of E1 in E1-transduced cells. Probing with the E2-specific antibody indicated that MeCP2E2 was overexpressed in both E2-transduced and E1+E2-transduced cells, and E2 was not detected in polybrene-treated, EGFP-transduced and E1-transduced cells.

The size of the MeCP2 isoforms observed by Western blot was approximately 75 kDa, which has been observed previously.[53,54,56,63] Detection of MeCP2 with the total MeCP2 and c-Myc antibodies showed MeCP2 running at a slightly lower molecular weight in E2-transduced cells compared to E1-transduced cells. This is expected due to the slight size difference between the

two isoforms: MeCP2E1 is 498 amino acids, and MeCP2E2 486 amino acids and therefore E1 runs slightly higher than E2. This size difference has been detected by Western blot in previous studies.[53,54,63] In the E1+E2-transduced cell samples the band for total MeCP2 and c-Myc appears to be slightly higher than that of the E2-transduced cells, yet the E2 isoform was seen to be the predominant isoform overexpressed in the E1+E2-transduced cells. This could be due to uneven running of the lanes during electrophoresis since the GAPDH bands are not completely straight.

There were also differences observed in the detection of endogenous MeCP2 in Daoy cells by the antibodies for total MeCP2 and E1- and E2-isoform specific antibodies. Endogenous MeCP2 was only detected by the MeCP2E1 antibody in the polybrene-treated, EGFP-transduced, E2-transduced and E1+E2-transduced cells, and not by the total MeCP2 or MeCP2E2 antibodies. Endogenous MeCP2 in Daoy cells has been detected previously by a different total MeCP2 antibody, which is known to be from a different company, but the catalogue number was not provided in that study.[67] Another report detected overexpressed MeCP2 but not endogenous MeCP2 in Daoy cells by using a total MeCP2 antibody developed within the Zoghbi lab.[136] Unfortunately, due to the lack of information provided in these reports, it is not possible to compare the epitopes to which those antibodies bind with the anti-MeCP2 antibody that we used in this study. The differences in the detection of endogenous MeCP2 could also be due to differing antibody binding efficiencies. Increasing the amount of protein loaded per lane from 10 μg could lead to detection of the endogenous MeCP2 by the anti-MeCP2 antibody and of endogenous E2 by the anti-MeCP2E2 antibody. MeCP2E2 is known to be expressed at lower levels than MeCP2E1 in the brain but its endogenous levels in Daoy cells have not been studied previously.

MeCP2 overexpressing Daoy cells were also analyzed by immunofluorescence staining, approximately 14 weeks following transduction, after cells had been passaged 26-29 times. Polybrene-treated, E1-transduced, E2-transduced and E1+E2-transduced cells were seeded in chamber slides and fixed using paraformaldehyde to preserve proteins within the structural integrity of the cells. Following permeabilization of the cell membranes by NP-40 the cells were labelled with the same panel of antibodies used in Western blot. Cells were double-stained with three combinations of primary antibodies, total MeCP2 + c-Myc, MeCP2E1 + c-Myc, and MeCP2E2 + c-Myc.

Figure 7. Immunofluorescence imaging of total MeCP2 in Daoy cells transduced with lentiviral vectors expressing MeCP2 isoforms. Images show co-localization of total MeCP2 and c-Myc tag at DAPI-stained nuclei for A) polybrene-treated control cells, and cells transduced with B) EF1α-E1, C) EF1α-E2 and D) EF1α-E1+ EF1α-E2 vectors. Scale bar represents 20 µm.

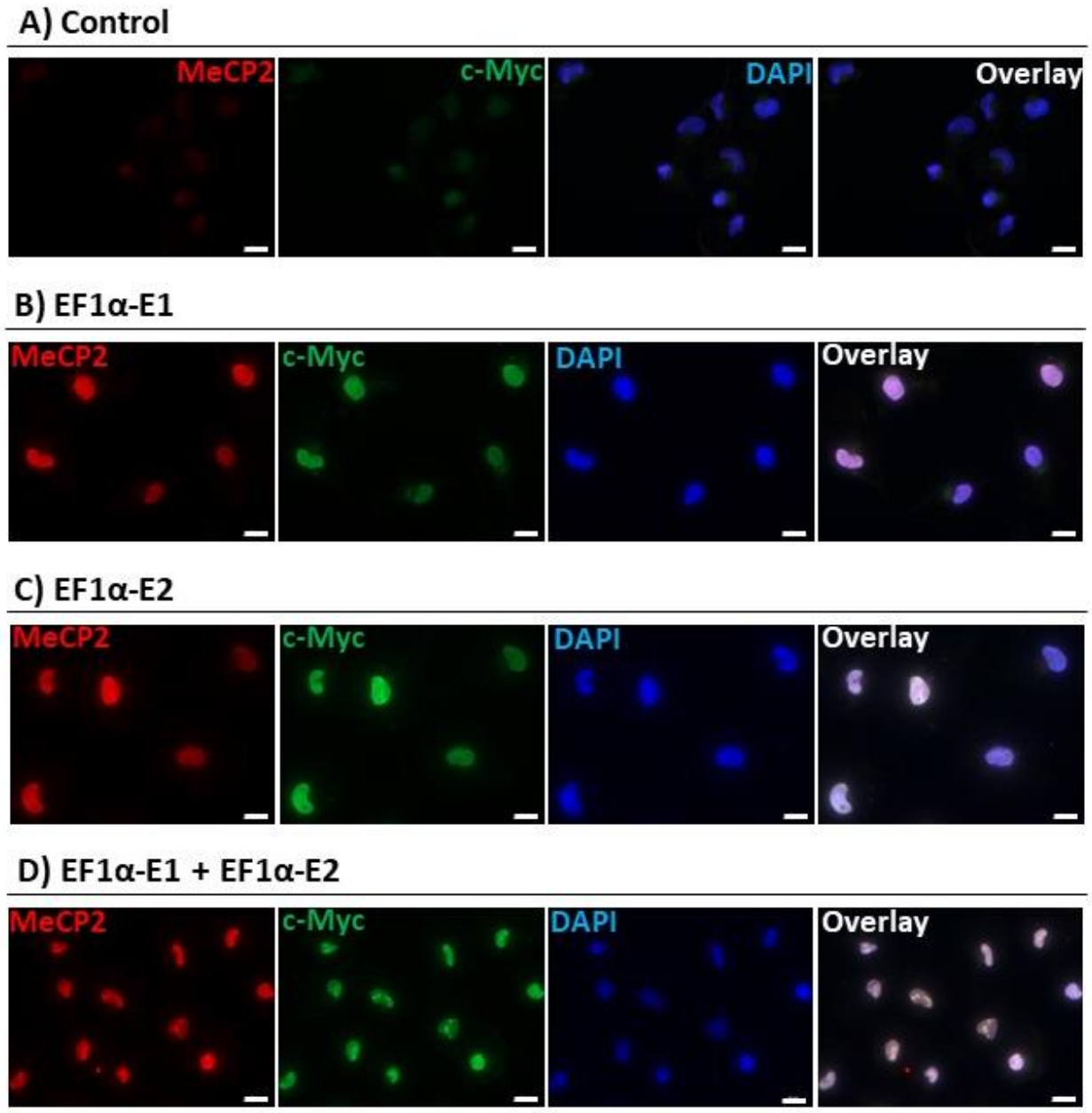

Double-staining with c-Myc antibody was performed to evaluate whether MeCP2 antibodies detected transduced proteins expressed from the lentiviral vectors. The two primary antibodies were distinguished by use of two secondary antibodies with different fluorophores, one

conjugated to the AlexaFluor 488 and the other to AlexaFluor 594. Cells were also counter-stained with DAPI to stain cell nuclei.

Total MeCP2 and c-Myc double-staining confirmed overexpression of MeCP2 from lentiviral vectors in E1-transduced, E2-transduced, and E1+E2-transduced cells (Figure 7B,C,D). Overlay images of antibody labeling with DAPI staining indicated that overexpressed MeCP2 is localized to the nucleus. A faint level of staining with both MeCP2 and c-Myc antibodies was observed in polybrene-treated control cells which could be due to endogenous MeCP2 as well as endogenous c-Myc protein, which is a transcription factor expressed in Daoy cells[5,6] (Figure 7A). Double-staining with MeCP2E1 + c-Myc antibodies in polybrene-treated control cells showed low detection of endogenous MeCP2E1 and c-Myc (Figure 8A). E1-transduced cells showed overexpression of MeCP2E1 accompanied by increased c-Myc staining (Figure 8B). Endogenous staining of MeCP2E1 was detected in E2-transduced and E1+E2-transduced cells along with overexpressed c-Myc due to the presence of MeCP2E2 overexpression in those cells (Figure 8C,D). The overlay images again confirmed localization of MeCP2E1 and c-Myc in the nucleus. Double-staining with MeCP2E2 + c-Myc antibodies in polybrene-treated control cells indicated lack of staining for MeCP2E2 and faint endogenous staining of endogenous c-Myc (Figure 9A). E1-transduced cells were negative for detection of MeCP2E2 but had elevated staining for c-Myc due to MeCP2E1 overexpression from lentiviral transduction (Figure 9B). E2-transduced and E1+E2-transduced cells both showed strong staining for MeCP2E2 and c-Myc (Figure 9C,D).

Figure 8. Immunofluorescence imaging of MeCP2E1 isoform in Daoy cells transduced with lentiviral vectors expressing MeCP2 isoforms. Images show co-localization of MeCP2E1 and c-Myc tag at DAPI-stained nuclei for A) polybrene-treated control cells, and cells transduced with B) EF1α-E1, C) EF1α-E2 and D) EF1α-E1+ EF1α-E2 vectors. Scale bar represents 20 µm.

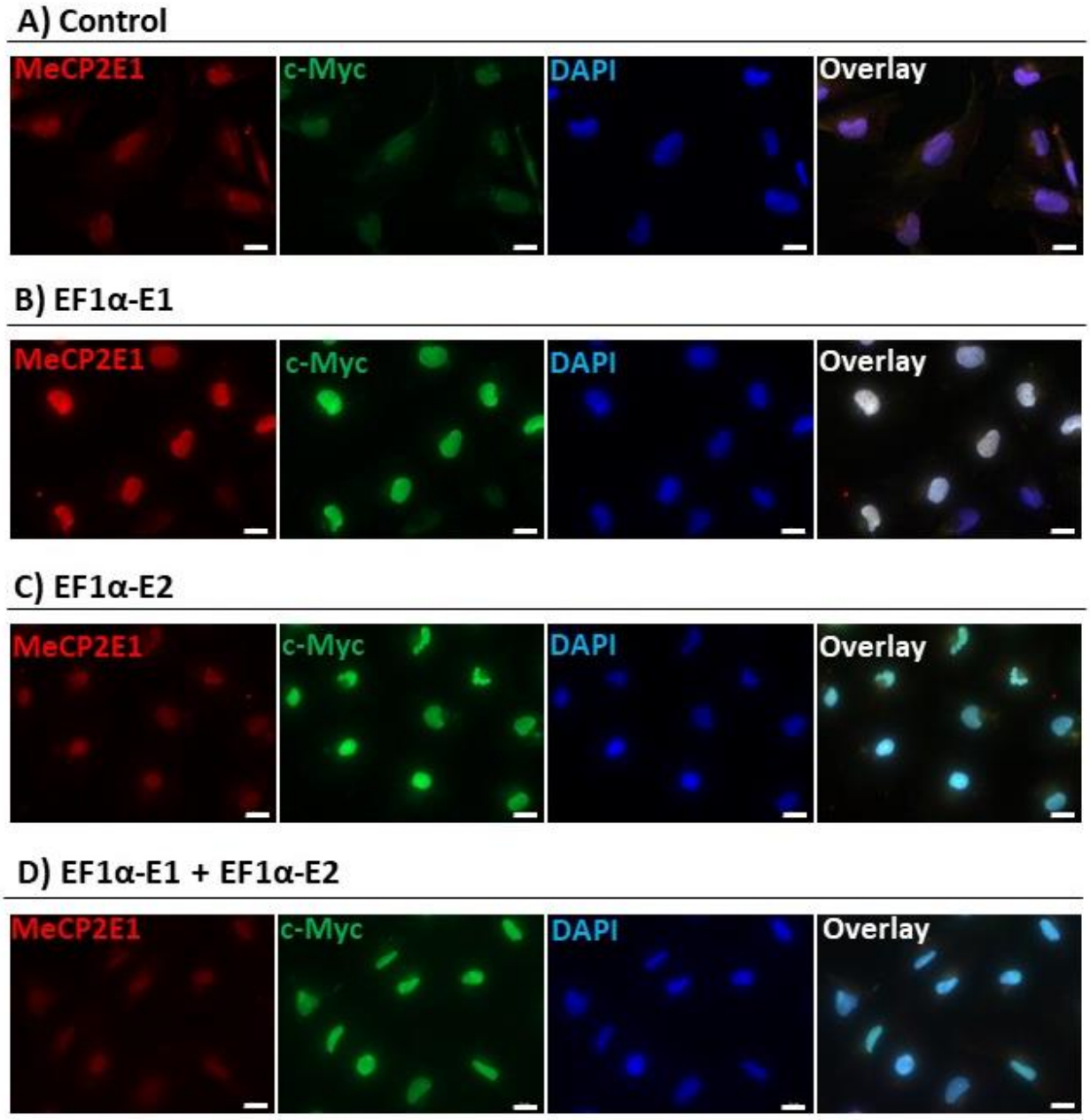

Figure 9. Immunofluorescence imaging of MeCP2E2 isoform in Daoy cells transduced with lentiviral vectors expressing MeCP2 isoforms. Images show co-localization of MeCP2E2 and c-Myc tag at DAPI-stained nuclei for A) polybrene-treated control cells, and cells transduced with B) EF1α-E1, C) EF1α-E2 and D) EF1α-E1+ EF1α-E2 vectors. Scale bar represents 20 µm.

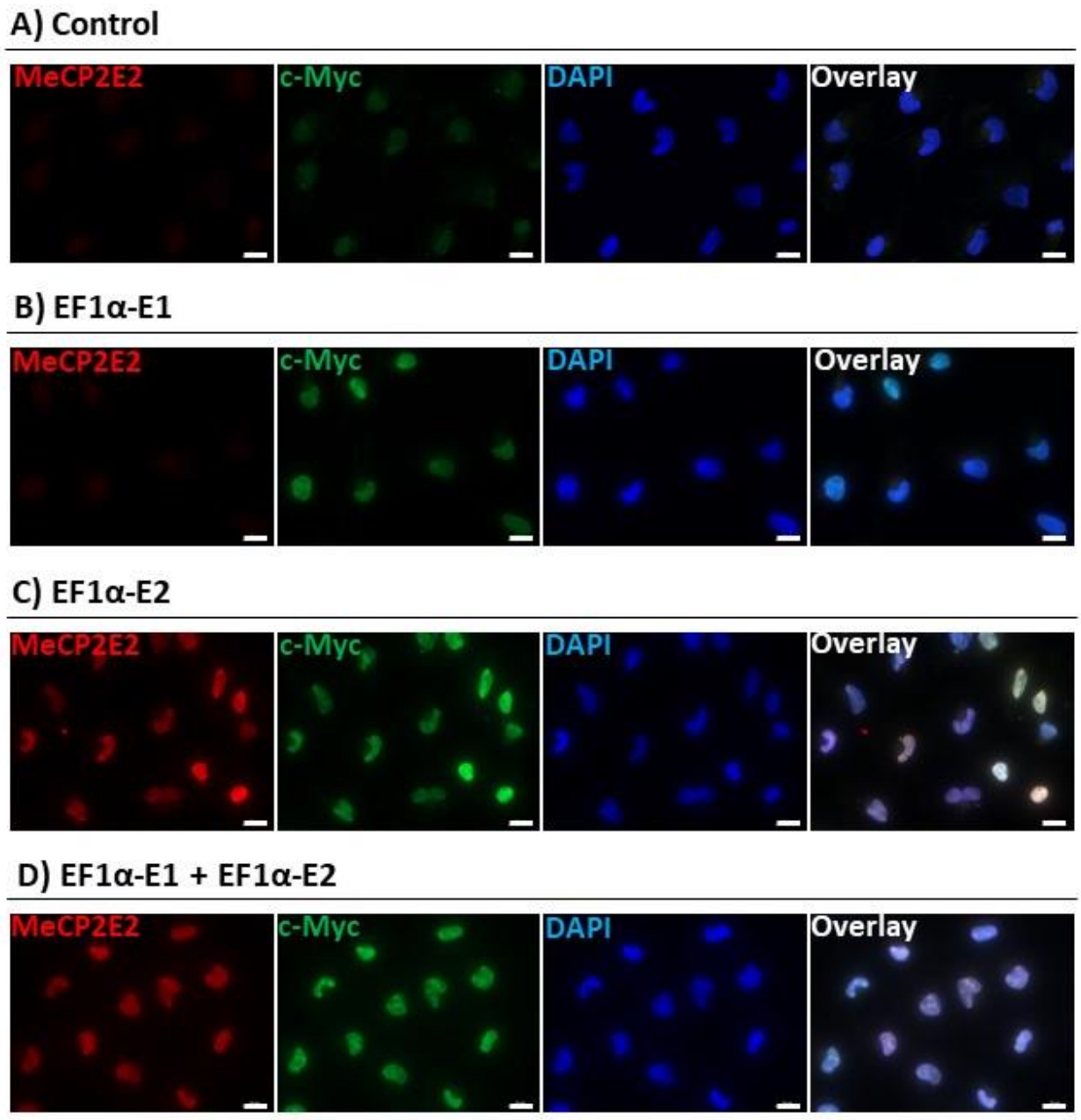

These immunofluorescence results confirmed that the transduced cells maintained stable long-term overexpression of MeCP2 isoforms. In the polybrene-treated control and transduced cells, MeCP2 was detected throughout the nucleus. Slight differences in the nuclei of E1+E2 cells was observed when stained with the total MeCP2 or c-Myc antibodies, which are both C-terminal binding antibodies (Figures 7D, 8D, and 9D). The source of this punctate staining and why it is only observed with C-terminal binding antibodies is unclear and requires further investigation.

The intensity of c-Myc staining in polybrene-treated control cells and MeCP2 overexpressing cells was quantified using ImageJ software. Total cell fluorescence can be measured and then corrected by subtracting the background signal. This showed that the intensity of c-Myc staining was significantly increased in E1-, E2-, and E1+E2-transduced cells compared to polybrene-treated control cells (Figure 10A) ($p<0.0001$). The difference in the intensity of c-Myc staining between E1-transduced cells with E2-transduced and E1+E2-transduced cells ($p<0.01$) may be due to a slight difference in transduction efficiency between the Lenti-EF1α-E1 and Lenti-EF1α-E2 vectors. The number of transduced cells having a greater corrected total cell fluorescence value than the average polybrene-treated control cell was divided by the total number of transduced cells to determine an approximate percentage of overexpressed cells which determined that approximately 95% of transduced cells were overexpressing in all three transduction events (Figure 10B).

Primary antibody omissions for the immunofluorescence experiment are shown in Figure 11. Two combinations of secondary antibodies were used for double staining. Primary omission with application of the goat-anti-mouse and goat-anti-chicken secondary antibodies confirmed the absence of non-specific staining (Figure 11A). Cell nuclei were stained with DAPI. Application of the goat-anti-mouse and goat-anti-rabbit secondary antibodies with primary omission showed no non-specific staining except for some staining observed in E2-transduced cells with the goat-anti-rabbit secondary antibody (Figure 11B). This staining is cytoplasmic as shown in the overlay image with DAPI staining and could be due to leakage of BDNF rabbit primary antibody from the adjacent well of the chamber slide. The wells of the chamber slide are formed by a removable plastic device on top of the microscope slide and the seal could have failed in this case.

Figure 10. Quantification of fluorescence intensity and percentage of overexpressing cells using c-Myc staining. A) Corrected total cell fluorescence (CTCF) was determined by measuring fluorescence intensity of c-Myc staining in ImageJ and subtracting background signal. B) Percentage of overexpressing cells was determined by counting cells with a higher CTCF than the average CTCF seen in polybrene-treated control cells to account for endogenous c-Myc expression. N=3 from cells seeded in 3 separate wells; n=7-9 representing different image fields. Data in A) were analyzed by one-way ANOVA followed by Tukey's multiple comparisons test (**p<0.01, ****p<0.0001).

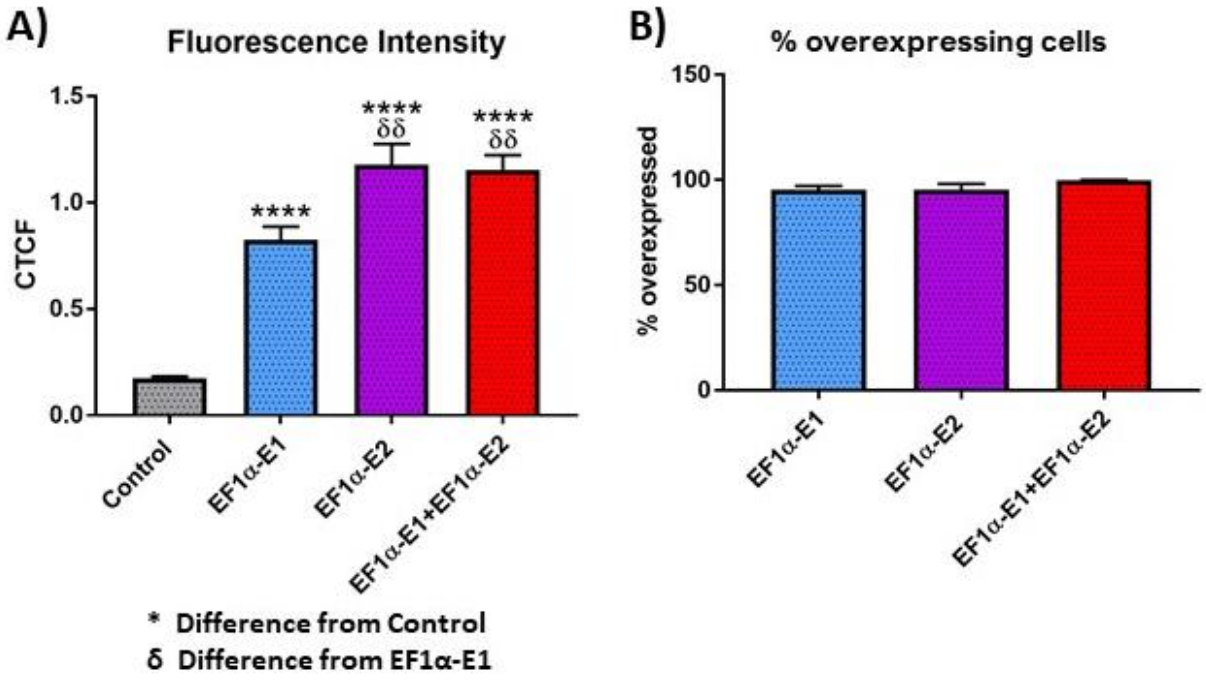

Figure 11. Immunofluorescence primary omissions. A) Cells were incubated with AlexaFluor 488 goat-anti-mouse and AlexaFluor 594 goat-anti-chicken secondary antibodies and stained with DAPI. B) Cells were incubated with AlexaFluor 488 goat-anti-mouse and AlexaFluor 594 goat-anti-rabbit secondary antibodies and stained with DAPI. Scale bars indicate 50 µm.

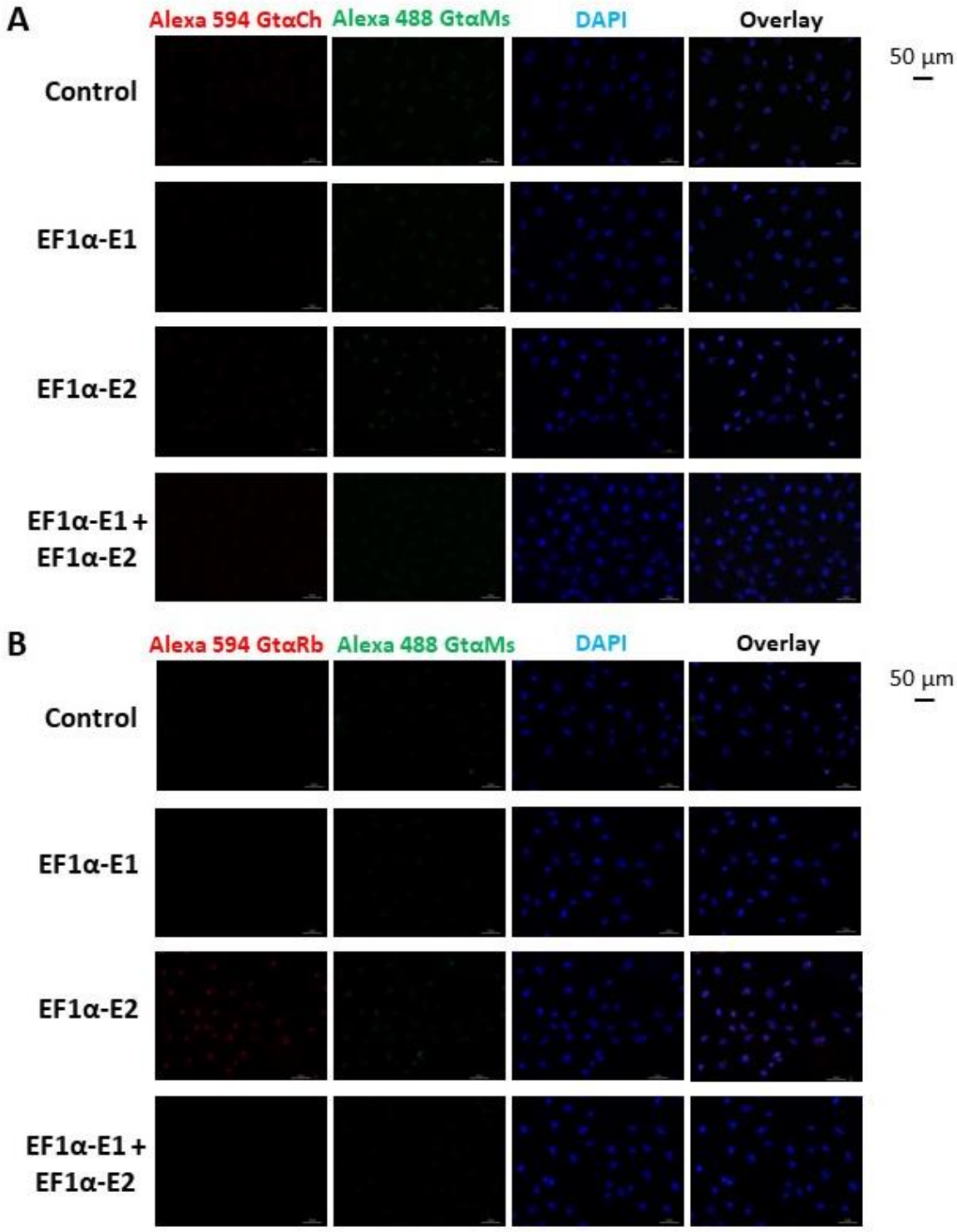

III.iii. MTT cell viability analysis of MeCP2E1 and E2 overexpressing cells

Previous studies have shown that MeCP2E1 overexpression reduces stem cell proliferation.[33] and overexpression of MeCP2E2 promotes apoptosis in cerebellar rat granule cells.[193] Cell viability of the MeCP2E1 and E2 overexpressing Daoy cells was tested by MTT assay. The MTT assay determines cell viability by adding methyl-thiazolyl-tetrazolium (MTT) to cultured cells and measuring the amount of MTT-formazan produced by spectrophotometry. MTT is reduced to MTT-formazan by reducing enzymes present in metabolically active cells.[269,270] The assay was performed after the cells had been passaged about 10 times since transduction, over a time period of about 5 weeks. Polybrene-treated, EGFP-transduced, E1-transduced, E2-transduced and E1+E2-transduced Daoy cells were seeded at equal densities in 96-well plates and MTT assay performed after 24, 48 and 72 hours in culture. The assay was performed for two sets of cells seeded in triplicate wells (N=2, n=6). At each time point the MTT reagent was added to the culture medium and incubated for 3 hours at 37^{o}C. Then the culture medium was removed, dimethyl-sulfoxide (DMSO) added and absorbance at 570 nm measured. The absorbance values of EGFP-, E1-, E2- and E1+E2-transduced cells were expressed relative to average absorbance value for polybrene-treated controls at each time point to determine percent cell viabilities. Analysis of the comparisons between the five cell groups at each time point is shown in Figure 12A. Statistical significance was assessed by one-way ANOVA. At the 24-hour time point percent viability of E2- and E1+E2-transduced cells was significantly reduced by approximately 30% ($p<0.01$) and 25% ($p<0.05$), respectively compared to polybrene-treated controls. EGFP- and E1-transduced cells showed slight decreases in percent viability of 10% and 20%, respectively but these were not statistically significant. There were no statistically significant differences between MeCP2 overexpressing cells and EGFP-transduced control cells at 24 hours and EGFP-transduced cells also showed a higher degree of variability which makes it more difficult to conclude whether the decreases in cell viability of E2- and E1+E2-transduced cells are due specifically to MeCP2E2 overexpression and not an effect of transduction.

Figure 12. MTT cell viability assay of Daoy cells transduced with lentiviral vectors expressing EGFP or overexpressing MeCP2E1/E2 isoforms. MTT assay was performed at 24, 48 and 72 hours following seeding and percent viability determined relative to polybrene-treated control cells. A) Differences in percent viability between the transduced cell types at each time point. B) Differences in percent viability between time points for each cell type. N=6; data were analyzed by one-way ANOVA followed by Tukey's multiple comparisons test (*p<0.05, **p<0.01, ***p<0.001, ****p<0.0001.)

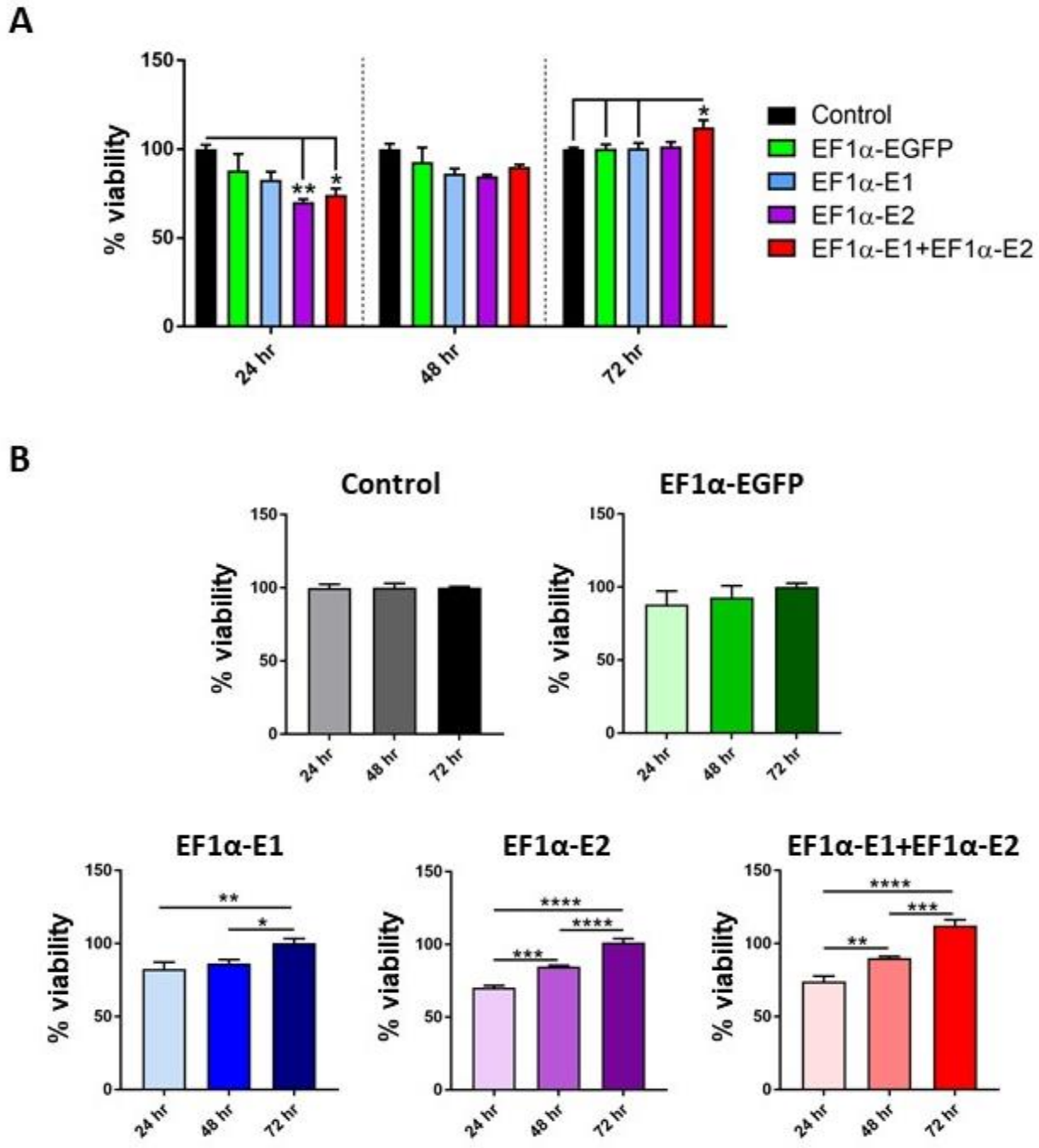

At the 48-hour time point there were no longer any statistically significant differences in percent viability, yet the transduced cells appeared slightly decreased relative to the polybrene-treated cells, with EGFP- and E1+E2-transduced cells showing approximately 10% decrease and E1- and E2-transduced cells showing approximately 15% decrease. At the 72-hour time point the only statistically significant change was that E1+E2-transduced cells showed a 10% increase in percent viability over polybrene-treated, EGFP-transduced and E1-transduced cells ($p<0.05$). EGFP-, E1-, and E2-transduced cells had similar percent viabilities as polybrene-treated controls at 72 hours. MTT assay data were also analyzed by one-way ANOVA for differences in percent viability between the three time points. This was performed separately for each of the five groups of cells (Figure 12B). Polybrene-treated control cell viabilities were expressed relative to the average polybrene-treated control value and therefore appear at about 100% cell viability at each time point. EGFP-transduced cells showed a slight trend of increased percent viability from 24 to 48 to 72 hours but these were not statistically significant. However, E1-, E2-, and E1+E2-transduced cells showed significant increases in percent viability over the time points. E1-transduced cells showed significant increases in percent survival from approximately 80% at 24-hours to 100% at 72-hours ($p<0.01$), and from approximately 85% at 48-hours to 100% at 72-hours ($p<0.05$). E2-transduced cells showed increases in percent survival from approximately 70% at 24 hours to 85% at 48 hours to 100% at 72 hours. The differences between all the time points were statistically significant, between 24 and 48 hours ($p<0.001$), between 24 and 72 hours as well as between 48 and 72 hours ($p<0.0001$). E1+E2-transduced cells also had increased percent survival between all the time points from approximately 75% at 24 hours to 90% at 48 hours and 110% at 72 hours. The differences between all time points were statistically significant, between 24 and 48 hours ($p<0.01$), 24 and 72 hours ($p<0.0001$) and 48 and 72 hours ($p<0.001$).

In summary, the MTT results indicated that despite seeding with identical cell densities at the start of the experiment, percent viabilities of E2- and E1+E2-transduced cells were significantly reduced compared to polybrene-treated control cells at 24 hours in culture. However, this reduction was not significant compared to EGFP-transduced cells and EGFP-transduced cells showed a slight but non-significant decrease in percent viability as well, indicating the change may not be specific to MeCP2-overexpressing cells. Differences in percent viability specific to the

MeCP2 overexpressing cells became clearer when making comparisons between different time points. EGFP-transduced cells showed slight but non-significant trend of increased percent viability of the time course of the experiment, but MeCP2-overexpressing cells displayed significant changes in percent viability over time. This indicated that the viability of MeCP2 overexpressing cells experiences significant change in the time following seeding, with fewer cells present 24 hours following seeding but cell numbers reaching a similar number by 72 hours. Greater more significant changes were seen in E2- and E1+E2-transduced cells indicating the MeCP2E2 isoform may have greater impact on the viability of these cells, since E1+E2-transduced also primarily overexpress the E2 isoform. Further studies are required to address whether increased cell death is occurring following seeding by apoptosis or other methods.

III.iv. Characterization of integration of lentiviral vectors in genomic DNA of Daoy cells

Stable overexpression of *MECP2E1 and MECP2E2* in Daoy cells was achieved through transduction with lentiviral vectors which are designed to integrate in the genome of the target cell and maintain overexpression over many cell divisions. Genomic DNA from E1-, E2-, and E1+E2 -overexpressing Daoy cells were analyzed by qPCR to confirm integration of the lentiviral vectors. This was done using isoform-specific forward primers which bind in exon 1 or exon 2 for *E1* and *E2*, respectively, and a common reverse primer which binds in exon 3. The vectors were constructed using only the cDNA sequence for *MECP2* isoforms and do not include the endogenous promoter or intronic regions. The coding sequence in the Lenti-EF1α-E1 vector is composed of exons 1, 3, and 4; while coding sequence in the Lenti-EF1α-E1 vector is composed of exons 2, 3, and 4. Genomic DNA from the transduced cells will also contain the endogenous *MECP2* gene, but it is not possible for the endogenous gene to be amplified as efficiently due to the presence of large introns. The structure of endogenous *MECP2* gene (Figure 13A) contains the four exons separated by three introns. Intron 2 is very large, 42.4 kilobases long, and lies between exons 2 and 3. The forward and reverse primers span intron 2 and therefore the amplicon size for the endogenous MECP2 gene is too long to be amplified in the qCPR method.

Figure 13. qPCR analysis of genomic DNA from Daoy cells transduced with lentiviral vectors expressing MeCP2 isoforms. A) Schematic of endogenous *MECP2* gene showing that no PCR product is expected since the forward and reverse primers span intron 2 which is 42.2 kb in size. The coding region of exon 1 is shown in blue and of exon 2 in purple. B) Schematic of the *MECP2* DNA sequences included in the Lenti-EF1α-E1 and Lenti-EF1α-E2 vectors which will produce PCR products, 65 bp for *E1* and 75-79 bp for *E2*. Approximate primer binding sites are shown. Two forward primers were tested for *MECP2E2*. qPCR results are shown for C) *MECP2E1*: N=2, n=3-4, and D) *MEPC2E2*: N=1-2, n=4-8. C_T values were normalized to *GAPDH* and expressed as $2^{-(\Delta CT)}$. Values were analyzed by one-way ANOVA followed by Tukey's multiple comparisons test (***p<0.001, ****p<0.0001).

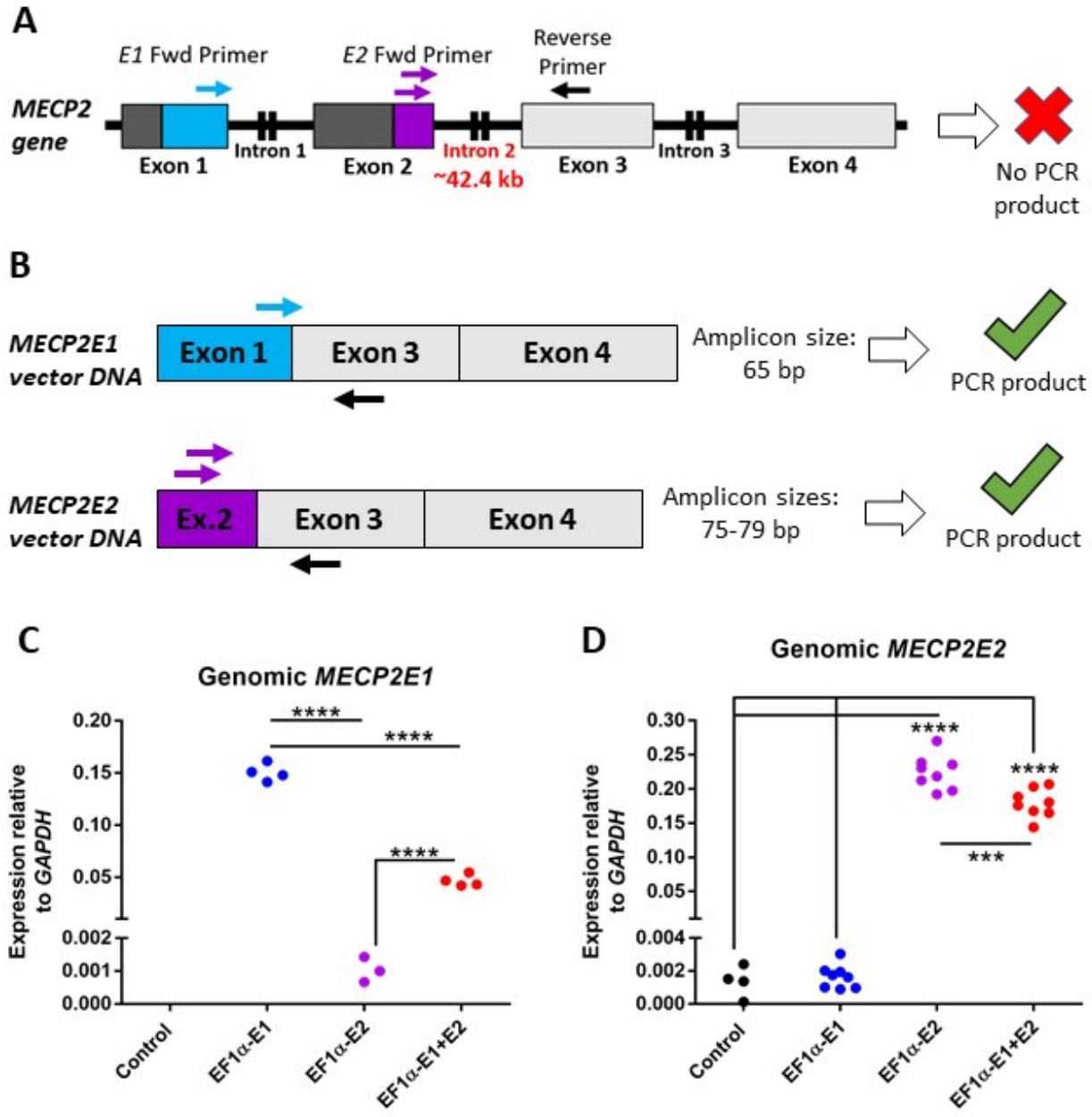

MECP2 lentiviral vectors do not include introns and will be amplified by qPCR of genomic DNA. As shown in Figure 13B the qPCR amplicon size from Lenti-EF1α-E1 DNA sequence is 65 base pairs (bp) and for Lenti-EF1α-E2 is 75 or 79 bp, depending on the forward primer used. The two forward primers used to analyze *E2* have similar binding sites in exon 2. The *GAPDH* gene was used as the housekeeping gene since the endogenous gene can be amplified as the amplicon size with the primers used is 206 bp.

As described earlier, at the protein level MeCP2E1 did not appear to be overexpressed in E1+E2-transduced cells, while MeCP2E2 was overexpressed. Analysis of genomic DNA could provide an explanation for this observation. One possible scenario is that the Lenti-EF1α-E1 vector was not integrated efficiently in E1+E2 cells, while the Lenti-EF1α-E2 vector was, leading to failure to overexpress MeCP2E1. Another possible scenario would be that both vectors did integrate into the Daoy cell genome, either at similar levels of efficiency or different levels, and that a post-transcriptional or post-translational mechanism led to reduced MeCP2E1 protein levels. Since the vector sequence does not contain known *MECP2* regulatory elements such as its endogenous promoter, intron sequences, and 3'UTR, and is under control of the ubiquitous EF1α promoter, it is unlikely that reductions would be transcriptional. The second scenario would require further experimental investigation.

Genomic DNA was extracted from polybrene-treated control, E1-transduced, E2-transduced and E1+E2-transduced cells and probed for the presence of the *E1* and *E2* vector DNA sequences by qPCR. All cells were analyzed with both *E1*- and *E2*-specific primers. Therefore polybrene-treated and E2 cells can both be considered controls in analysis with the *E1*-specific primers, and polybrene-treated and E1 cells can both be considered controls in analysis with *E2*-specific primers. The C_T values were normalized to *GAPDH* to determine the ΔC_T values which were then expressed as $2^{\wedge -\Delta CT}$. Comparison of the $2^{\wedge -\Delta CT}$ values was done to analyze the relative differences in detection of vector DNA sequences between the transduced cells. The copy number per cell couldn't be determine since absolute quantification wasn't performed. Analysis with *E1*-specific primers (Figure 13C) confirmed integration of the Lenti-EF1α-E1 vector in genomic DNA of E1 and E1+E2 cells. There was no amplification for *E1* in polybrene-treated control cells, but there was a low level of amplification in E2 cells which occurred late in the qPCR run, around 32-33 cycles.

This could have occurred due to contamination of the E2 DNA samples during extraction and preparation of the genomic DNA or during the setup of the qPCR experiment. However, amplification of *E1* in genomic DNA from E1 and E1+E2 cells was significantly higher than that detected in E2 cells, with 146-fold ($p<0.0001$) and 45-fold ($p<0.0001$) differences, respectively. Comparison of the E1 and E1+E2 cells showed that the relative level of *E1* vector DNA in genomic DNA of E1 cells was about 3-fold greater than E1+E2 cells, which was statistically significant ($p<0.0001$). Analysis of the genomic DNA samples with *E2*-specific primers (Figure 13D) confirmed integration of the Lenti-EF1α-E2 vector in genomic DNA of E2 and E1+E2 cells. Low levels of amplification of *E2* were observed in polybrene-treated and E1 cells between 33-34 PCR cycles which again could have occurred due to contamination. The amplification of *E2* in E2 and E1+E2 cells was significantly higher than amplification in controls, with fold differences ranging from 108 and 165 observed ($p<0.0001$). The relative level of *E2* vector DNA in E2 cells was 1.25-fold greater than that in E1+E2 cells which was also statistically significant ($p=0.0001$).

The lower level of detection of *E1* and *E2* vector DNA in genomic DNA of E1+E2 cells compared to E1 and E2 cells can be explained by the fact that E1+E2 cells were transduced with 2.5 μg of vector each of Lenti-EF1α-E1 and Lenti-EF1α-E2 while the E1 and E2 cells were transduced with 5 μg of Lenti-EF1α-E1 or Lenti-EF1α-E2, respectively. However, the level of *E1* vector DNA detected in E1+E2 cells was 3-fold lower than E1 cells while the level of *E2* vector DNA was 1.25-fold lower than E2 cells, indicating that Lenti-EF1α-E1 vector did not incorporate as efficiently as Lenti-EF1α-E2 vector in E1+E2 cells. Despite this there is significant levels of the Lenti-EF1α-E1 vector detected in E1+E2 cells but this was not evident at the protein level as seen earlier.

In conclusion, genomic DNA analysis of E1-transduced, E2-transduced and E1+E2-transduced Daoy cells confirmed integration of the Lenti-EF1α-E1 vector in genomic DNA of E1-transduced and E1+E2-transduced cells and integration of the Lenti-EF1α-E2 vector in genomic DNA of E2-transduced and E1+E2-transduced cells. E1+E2-transduced cells integrated lower levels of the Lenti-EF1α-E1 vector than the Lenti-EF1α-E2 vector, yet this does not fully explain why E1 protein was not overexpressed in these cells. Further molecular analyses of mRNA transcripts and protein are required to address this, of which only transcripts were analyzed as part of this thesis. The genomic DNA analysis confirms production of stably transduced cells which are expected to

maintain overexpression of MeCP2 and can be used to investigate downstream effects of MeCP2 overexpression.

III.v. Analysis of MECP2E1 and E2 gene expression in MECP2E1 and E2 transduced Daoy cells

Expression of *MECP2E1* and *E2* mRNA transcripts was analyzed by extracting total RNA from five sets of polybrene-treated, EGFP-, E1-, E2-, and E1+E2-transduced cells, converting to cDNA and performing real-time qRT-PCR. This analysis detects gene expression from both the endogenous *MECP2* gene and the isoform-specific lentiviral vectors. Transcript levels of *MECP2E1* were increased by approximately 50-fold in E1 cells relative to endogenous transcript levels in polybrene-treated controls, and was significantly greater than polybrene-treated, EGFP, E2 and E1+E2 cells ($p<0.0001$) (Figure 14A). E1+E2 cells showed an approximately 4-fold increase in *E1* transcripts relative to the polybrene-treated cells but the difference was not statistically significant compared to polybrene-treated, EGFP or E2 cells. Transcript levels of *MECP2E2* were increased by approximately 30-fold in E2 cells relative to endogenous transcript levels in polybrene-treated controls, a statistically significant increase compared to polybrene-treated, EGFP, and E1 cells ($p<0.0001$) (Figure 14B). E1+E2 cells showed an approximately 48-fold increase in *MECP2E2* transcripts relative to the polybrene-treated cells, an increase which was statistically significant compared to polybrene-treated, EGFP and E1 cells. ($p<0.0001$). The difference in *MECP2E2* transcripts between E2 and E1+E2 cells was 1.6-fold ($p=0.0063$).

In conclusion, *MECP2E1* transcripts were significantly overexpressed in E1-transduced cells but not E1+E2-transduced cells, while *MECP2E2* transcripts were significantly overexpressed in E2-transduced and E1+E2-transduced cells. Transcripts expressed from the lentiviral vectors lack the 3'UTR of *MECP2,* which is known to be post-transcriptionally regulated for example by microRNAs. Expression of nascent transcripts in these cells was included in this study, this could be further addressed by studying the transcript stabilities in future studies.

Figure 14. RT-PCR analysis of *MECP2E1/E2* isoforms in Daoy cells transduced with lentiviral vectors expressing MeCP2 isoforms**.** C_T values for A) *MECP2E1* and B) *MECP2E2* were normalized to the housekeeping gene *GAPDH*. Fold changes were determined relative to average polybrene-treated control. Fold change values were analyzed by one-way ANOVA followed by Tukey's multiple comparisons test. N=5±SEM; **p<0.01; ****p<0.0001.

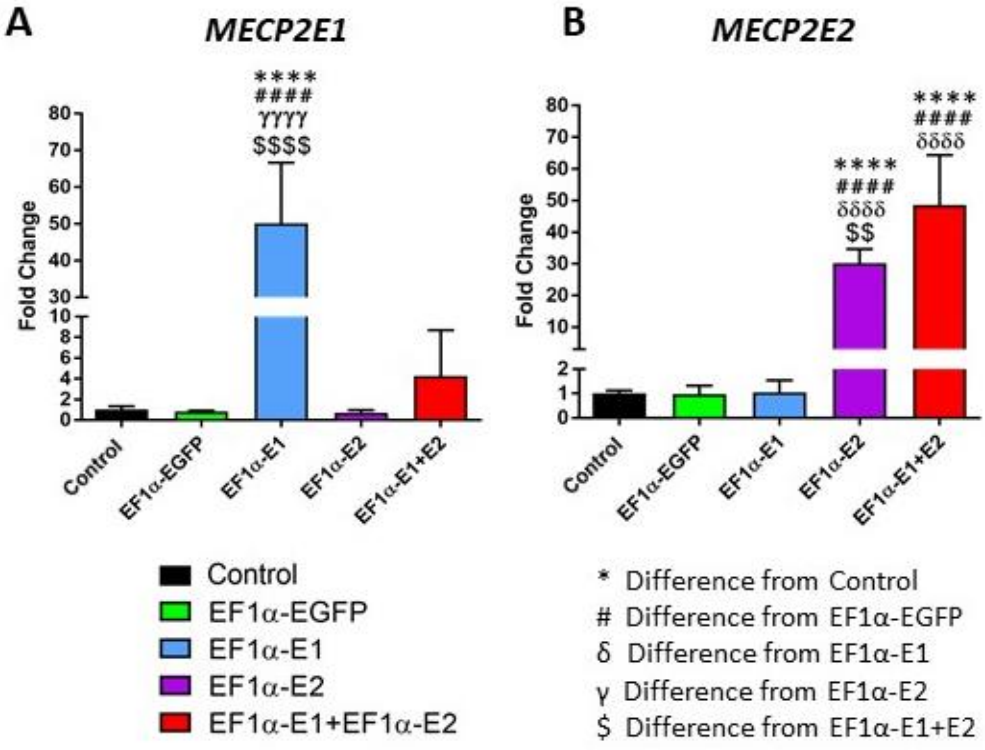

III.vi. Characterization of gene expression changes of select targets in MeCP2E1 and E2 overexpressing Daoy cells

The previous sections outlined how EGFP-expressing and MeCP2-overexpressing Daoy cells were established and validated. Following this, cells were analyzed for changes in gene expression of a number of selected target genes. The selected targets were *BDNF, miR-132, Nucleolin, 45S pre-ribosomal RNA,* as well as *28S* and *18S ribosomal RNAs*. The *45S pre-rRNA* transcript is processed and cleaved to form the *28S* and *18S rRNA* transcripts. Expression of these target genes were chosen based on results of previous studies which indicate they may be targeted by MeCP2 regulation at the level of transcription and are implicated in the pathogenesis of Rett Syndrome,

but it is unknown whether the two MeCP2 isoforms E1 and E2 have unique or similar roles in regulating their transcription.

Gene expression was analyzed by real-time qRT-PCR of both steady-state total RNA and nascent RNA transcripts. Nascent RNA transcripts were analyzed to determine whether changes in transcript levels were direct transcriptional effects. If a change in the level of a transcript is observed between two total RNA samples, the change could be due to a direct transcriptional effect impacting the activity of the gene but could also be attributed to a post-transcriptional change such as a change in the transcript stability.

Initially, total RNA was extracted from two sets of samples, each set consisting of polybrene-treated, EGFP-, E1-, E2-, and E1+E2-trasnduced Daoy cells. Total RNA was prepared using TRIzol reagent. Total RNA was converted to cDNA using Superscript III Reverse Transcriptase and analyzed by real-time qRT-PCR for expression of *BDNF, 45S pre-rRNA, 28S rRNA,* and *18S rRNA* (Figure 15A). C_T values were normalized to the housekeeping gene *GAPDH* and expressed as fold changes relative to the average polybrene-treated control by the $2^{-\Delta\Delta CT}$ method. *BDNF* transcripts were 1.9-fold higher in E2-transduced cells compared to both polybrene-treated and EGFP-transduced controls, but this was not statistically significant. *BDNF* transcripts were not significantly altered in E1- or E1+E2-transduced cells. There were no significant differences observed in ribosomal RNA transcripts, with only small subtle changes in some samples and high variation in some samples. To analyze *miR-132* expression, total RNA was reverse transcribed and analyzed by real-time qRT-PCR using MultiScribe Reverse Transcriptase and TaqMan microRNA assays. The *snRNA U6* was used as the endogenous control. Expression of both strands of *miR-132,* the *3p* and *5p* strands were analyzed. They are generated following cleavage of the pre-miRNA hairpin, with one strand retaining the original 3-primed end and the other the original 5-primed end. To compare expression of the two strands in polybrene-treated control and transduced Daoy cells, the C_T values for each strand were normalized to *U6* and then expressed as $2^{-\Delta CT}$ (Figure 15B). This indicated that the *3p* strand is the dominant strand expressed in Daoy cells, at levels about 300-fold higher than the *5p* strand. In polybrene-treated control and E1-transduced cells only one of the four technical replicates amplified *5p.*

Figure 15. Preliminary RT-PCR analysis of steady-state total RNA expression in Daoy cells transduced with lentiviral vectors expressing MeCP2 isoforms. A) Analysis of BDNF, 45S pre-rRNA, 28S rRNA and 18S rRNA. C_T values were normalized to the housekeeping gene GAPDH and fold changes determined relative to average polybrene-treated control. N=2±SEM, fold change values were analyzed by one-way ANOVA followed by Tukey's multiple comparisons test. B) Analysis of miR-132 showing that expression of the 3p transcript is significantly greater than the 5p transcript. C_T values were normalized to U6 and expressed as $2^{-\Delta CT}$. N=1-2±SEM, n=1-4. Statistical significance is shown for data sets analyzed by unpaired t-test with Welch's correction,*p<0.05. C) Fold change analysis of miR-132-3p in the transduced cell types. C_T values were normalized to the housekeeping gene U6 and fold changes determined relative to average polybrene-treated control. N=2±SEM, fold change values were analyzed by one-way ANOVA followed by Tukey's multiple comparisons test.

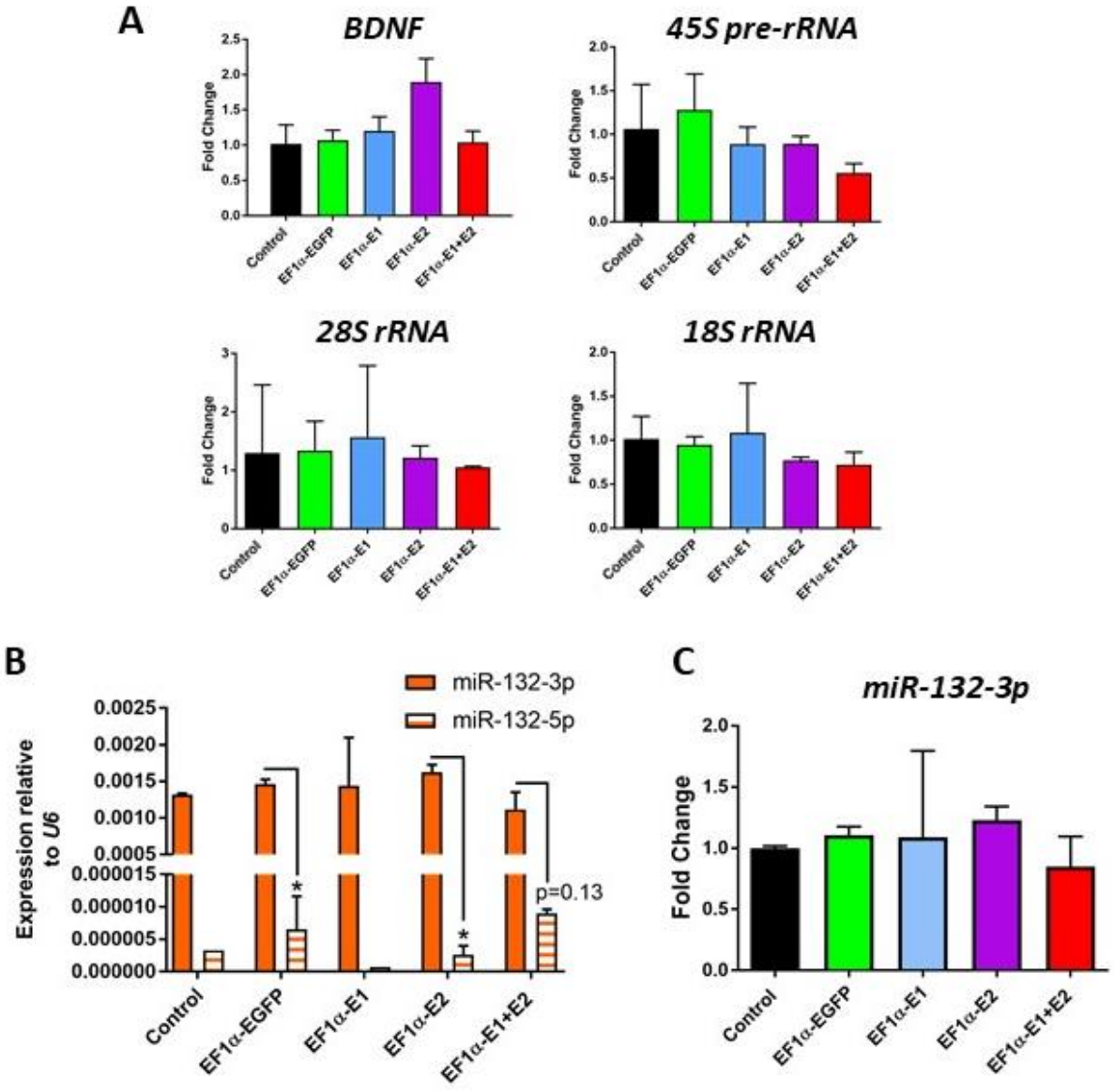

The difference between expression of *3p* and *5p* was statistically significant in EGPF-transduced and E2-transduced cells ($p<0.05$). The p-value for the comparison of *5p* and *3p* transcripts in E1+E2-transduced cells was 0.13. These results agree with published findings on levels of *miR-132-3p* and *-5p* strands in the human brain which indicated *3p* is the predominant strand.[56] When the fold changes in *3p* transcripts were determined relative to polybrene-treated control cells there were no significant differences in any of the transduced cells (Figure 15C). This preliminary analysis indicated *BDNF* transcripts may be increased in E2-transduced cells, and there could be small subtle changes in the other genes. In some samples a high level of variation was also observed between the samples. Subtle changes may become more significant if the level of nascent RNA is specifically measured. Subsequently, new samples were collected for nascent and total steady-state RNA, with uniform seeding and collection time points between samples to allow more confidence in the uniformity of the samples.

Polybrene-treated control, EGFP-, E1-, E2-, and E1+E2-transduced cells were seeded at 50,000 cells per well of 6-well plates. The following day, or approximately 16 hours later, 0.1 mM ethynyl-uridine (EU) was added to cells to label nascent RNA for 1, 6 and 24 hours. One group of samples was labelled with EU, and a second group left unlabeled for collection of total steady-state RNA. At each time point, three sets of EU-labelled and three sets of unlabeled cells were collected for analysis. Total RNA was extracted from all the samples using the MagMax *miR*Vana kit. Nascent RNA was purified from EU-labeled cells and converted to cDNA using the Click-iT Nascent RNA Capture kit and Superscript III Reverse Transcriptase. Total steady-state RNA from unlabeled cells was converted to cDNA by the standard protocol using Superscript III Reverse Transcriptase. The nascent and steady-state samples were analyzed using gene-specific primers for the targets of interest by real-time qRT-PCR and analyzed by the $2^{-\Delta\Delta CT}$ method.

The levels of nascent and steady-state *MECP2E1/E2* transcripts were analyzed to determine the level of overexpression of the *MECP2* transcripts in these samples (Figure 16). *MECP2E1* nascent and steady-state transcripts in E1-transduced cells were significantly increased compared to polybrene-treated and EGFP-transduced control cells (Figure 16A).

Figure 16. Expression of nascent and steady-state *MECP2E1* and *MECP2E2* transcripts in Daoy cells transduced with lentiviral vectors expressing MeCP2 isoforms. Nascent RNA was prepared from cells labelled with EU for 1, 6 and 24 hours. Total RNA was prepared from unlabeled cells collected at the same time points. Gene expression was analyzed by RT-PCR for A) *MECP2E1* transcripts and B) *MECP2E2* transcripts. C_T values were normalized to the housekeeping gene *GAPDH* and fold change determined relative to average Polybrene control N=3±SEM. Fold change values were analyzed by one-way ANOVA followed by Tukey's multiple comparisons test. The levels of significance are *p<0.05, **p<0.01, ***p<0.001, ****p<0.0001.

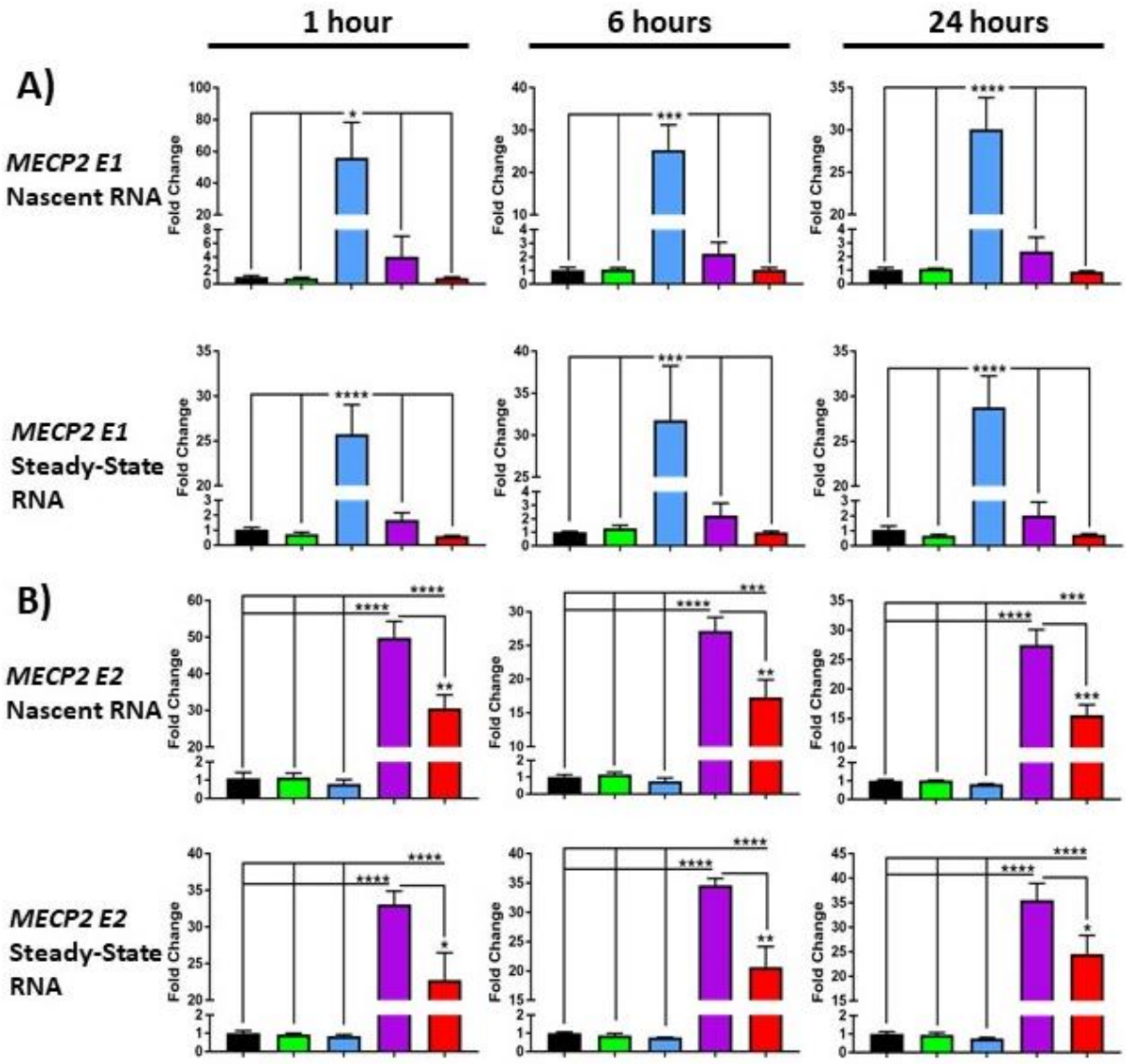

MECP2E1 nascent transcripts were increased compared to controls by approximately 55-fold at 1 hour ($p<0.05$), 25-fold at 6 hours ($p<0.001$), and 30-fold at 24 hours ($p<0.0001$). *MECP2E1* steady-state transcripts were increased compared to controls by approximately 25-fold at 1 hour ($p<0.0001$), 30-fold at 6 hours ($p<0.001$), and 30-fold at 24 hours ($p<0.0001$). Interestingly, *MECP2E1* nascent and steady-state transcripts were slightly increased in E2-transduced cells compared to controls, ranging from approximately 2-fold to 4-fold at different time point, however this was not statistically significant. This slight change was not observed in E1+E2-transduced cells. The levels of *MECP2E1* in E2- and E1+E2-transduced cells were statistically significant from E1-transduced cells, with identical p-values seen in comparison to controls.

MECP2E2 nascent and steady-state transcripts were significantly increased in E2- and E1+E2-transduced cells compared to the controls (Figure 16B). *MECP2E2* nascent transcripts were increased in E2-transduced cells compared to controls by approximately 50-fold at 1 hour ($p<0.0001$), 27-fold at 6 hours ($p<0.0001$), and 27-fold at 24 hours ($p<0.0001$). *MECP2E2* nascent transcripts were increased in E1+E2-transduced cells compared to controls by approximately 30-fold at 1 hour ($p<0.0001$), 17-fold at 6 hours ($p<0.001$), and 15-fold at 24 hours ($p<0.001$). The level of *MECP2E2* nascent transcripts in E2-transduced cells was approximately 1.5-fold greater than E1+E2-transduced cells at all time points which was statistically significant ($p<0.01$ at 1 and 6 hours; $p<0.001$ at 24 hours). *MECP2E2* steady-state transcripts were increased in E2-transduced cells compared to controls by approximately 33-fold at 1 hour ($p<0.0001$), 35-fold at 6 hours ($p<0.0001$), and 35-fold at 24 hours ($p<0.0001$). *MECP2E2* steady-state transcripts were increased in E1+E2-transduced cells compared to controls by approximately 23-fold at 1 hour ($p<0.0001$), 20-fold at 6 hours ($p<0.0001$), and 25-fold at 24 hours ($p<0.0001$). The level of *MECP2E2* steady-state transcripts in E2-transduced cells was approximately 1.5-fold greater than E1+E2-transduced cells at all time points which was statistically significant ($p<0.05$ at 1 and 24 hours; $p<0.01$ at 6 hours). Therefore, *MECP2E1* transcripts are significantly increased in E1-transduced cells, and *MEPC2E2* transcripts are significantly increased in E2- and E1+E2-transduced cells, to a greater degree in E2-transduced cells.

The nascent and steady-state transcript levels of the selected gene targets *BDNF, miR-132, Nucleolin,* and *ribosomal RNAs* were evaluated next. Significant increases in *BDNF* nascent and

steady-state transcripts were observed (Figure 17A). After 1 hour of EU labeling nascent *BDNF* transcripts were increased by approximately 1.9-fold in E1-transduced cells ($p<0.05$), 2.3-fold in E2-transduced cells ($p<0.01$) and 2.2-fold in E1+E2-transduced cells ($p<0.01$) compared to polybrene-treated controls. E2- and E1+E2-transduced cells were also significantly increased compared to EGFP-transduced control cells ($p<0.01$ and $p<0.05$, respectively) but E1-transduced cells were not. After 6 hours of EU labeling the fold change in nascent *BDNF* transcripts in E1-transduced cells was unchanged but was no longer statistically significant compared to control, while in E2- and E1+E2-transduced cells the fold changes were increased to 2.6-fold and 2.5-fold, respectively, however only the change observed in E2-transduced cells was statistically significant compared to polybrene-treated cells ($p<0.05$). Following 24 hours of EU labeling nascent *BDNF* transcripts were increased by about 1.5-fold in E1- and E2-transduced cells but this wasn't statistically significant while E1+E2-transduced cells showed approximately 1.9-fold increase which was significant compared to polybrene-treated cells ($p<0.01$) and compared to EGFP-transduced cells ($p<0.05$).

Steady-state *BDNF* transcripts were also significantly increased in E1-, E2-, and E1+E2-transduced cells at 1, 6 and 24 hours compared to both polybrene-treated and EGFP-transduced controls. At the 1-hour time point, *BDNF* transcripts were increased relative to polybrene-treated controls in E1-, E2-, and E1+E2-transduced cells by approximately 2-fold ($p<0.01$), 3-fold ($p<0.0001$) and 2.4-fold ($p<0.001$), respectively. The differences were also statistically significant compared to EGFP-transduced controls ($p<0.05$, $p<0.0001$ and $p<0.001$ respectively). At the 6-hour time point, *BDNF* *t*ranscripts were increased relative to polybrene-treated controls in E1-, E2-, and E1+E2-transduced cells by approximately 2.3-fold ($p<0.001$), 3-fold ($p<0.0001$) and 3-fold ($p<0.0001$), respectively.

The differences were also statistically significant compared to EGFP-transduced controls ($p<0.01$, $p<0.0001$, and $p<0.0001$ respectively). At the 24-hour time point the fold changes were slightly lower but *BDNF* transcripts were still increased relative to polybrene-treated controls in E1-, E2, and E1+E2-transduced cells by approximately 1.6-fold ($p<0.05$), 1.9-fold ($p<0.01$) and 1.9-fold ($p<0.01$), respectively. The differences were still statistically significant compared to EGFP-transduced controls ($p<0.05$, $p<0.01$ and $p<0.01$ respectively).

Figure 17. Expression of nascent and steady-state *BDNF* and *miR-132-3p* transcripts in Daoy cells transduced with lentiviral vectors expressing MeCP2 isoforms. Nascent RNA was prepared from cells labelled with EU for 1, 6 and 24 hours. Total RNA was prepared from unlabeled cells collected at the same time points. Gene expression was analyzed by RT-PCR for A) *BDNF* transcripts and B) *miR-132-3p* transcripts. *BDNF* and *miR-132-3p* C_T values were normalized to the housekeeping genes *GAPDH* and U6, respectively, and fold change determined relative to average polybrene-treated control. N=3±SEM. Fold change values were analyzed by one-way ANOVA followed by Tukey's multiple comparisons test, *p<0.05, **p<0.01, ***p<0.001, ****p<0.0001.

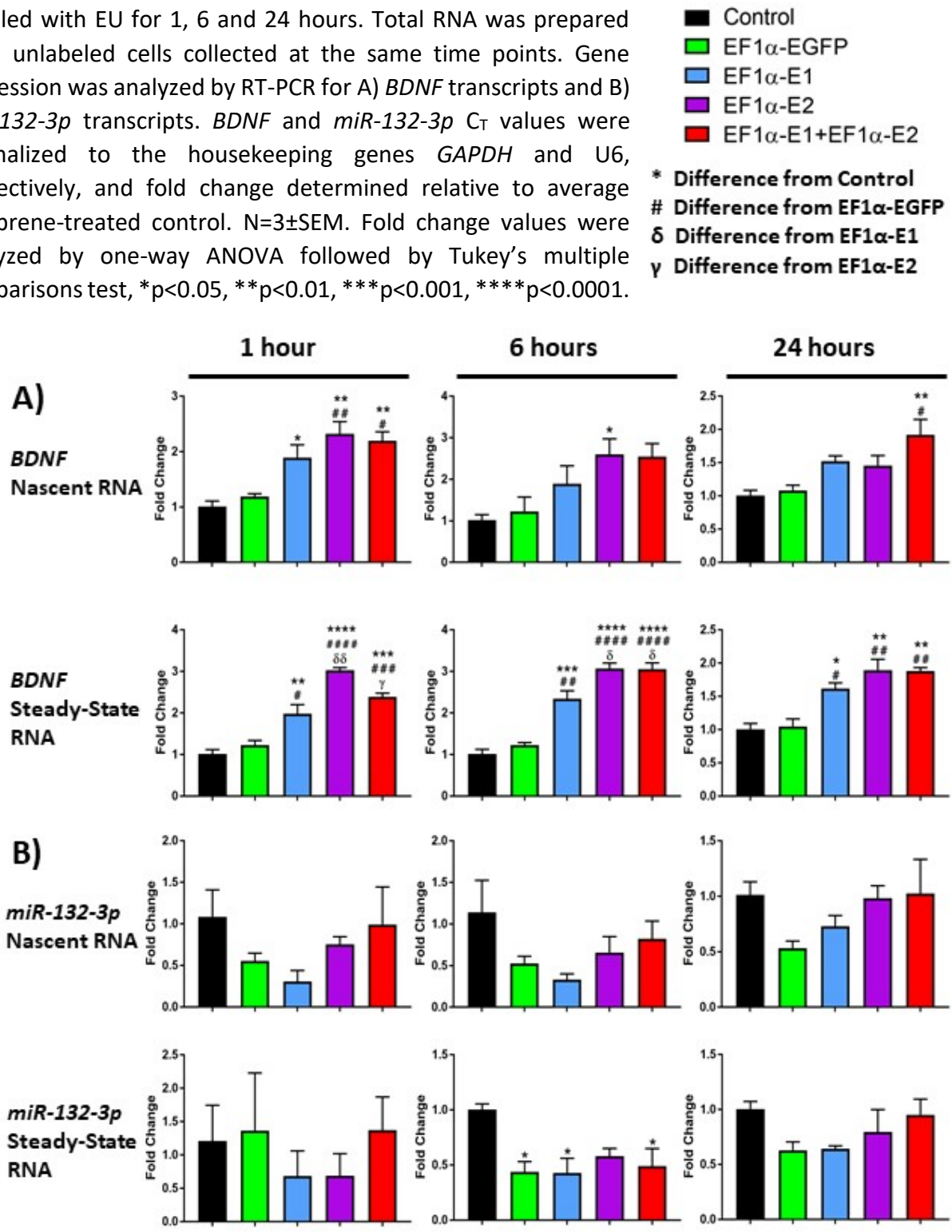

There were also statistically significant differences in steady-state *BDNF* transcripts between the E1-, E2-, and E1+E2-transduced cells at 1- and 6-hour time points. At the 1-hour time point E2-transduced cells were significantly higher than E1-transduced cells by about 1.5-fold ($p<0.01$) and E1+E2-transduced cells by about 1.25-fold ($p<0.05$). At the 6-hour time point E2- and E1+E2-transduced cells were both significantly higher compared to E1-transduced cells by about 1.3-fold ($p<0.05$).

The greater degree of fold-changes and statistical significance in steady-state *BDNF* compared to nascent *BDNF* may be due to the fact that the nascent RNA samples represent a smaller fraction of transcript, being only those newly synthesized transcripts produced during the time frame of labeling. The steady-state samples contain a greater number of transcripts, also representing transcripts present before the EU-labeling was begun. The gene expression results indicated that overexpression of either MeCP2E1 or E2 isoforms resulted in increases in nascent *BDNF* transcription.

The microRNA *miR-132* has been observed to negatively regulate MeCP2 levels in primary cortical and hippocampal rat neurons, and that decreasing MeCP2 leads to an increase in *miR-132* levels in primary hippocampal neurons.[68,158] The effect of MeCP2 overexpression on nascent *miR-132* expression has not been analyzed. Nascent and steady-state *miRNA* samples were prepared similarly to the other gene targets except TaqMan microRNA assays were used to generate cDNA and perform real-time qRT-PCR. The *miR-132-3p* strand was analyzed as it was determined to be the predominant strand expressed in Daoy cells as described previously. Nascent *miR-132-3p* transcripts showed no statistically significant changes (Figure 17B) but some variation was observed in the transduced cells compared to polybrene-treated controls, including in EGFP-transduced cells in which *miR-132-3p* was reduced about 0.5-fold at every time point. This indicates an off-target effect of transduction may be impacting *miR-132-3p* levels. This was also observed for steady-state *miR-132-3p* transcripts which were decreased by about 0.5-fold at 6 hours in EGFP-, E1-, and E1+E2-transduced cells ($p<0.05$). Though not statistically significant, E2-transduced cells were also decreased by about 0.6-fold. Therefore, it appeared that MeCP2 overexpression in Daoy cells did not have effects on *miR-132* specific to MeCP2. This could be attributed to the fact that Daoy cells are of cerebellar origin, and a recently published study from

our lab indicated *miR-132-3p* transcripts weren't significantly impacted in Rett syndrome post-mortem cerebellar brain tissue.[56]

Analysis of *Nucleolin* and the *45S pre-ribosomal RNA* transcripts is shown in Figure 18. *Nucleolin* transcripts were unchanged at the nascent and steady-state levels (Figure 18A). *Nucleolin* steady-state transcripts appeared slightly decreased by 0.75-fold at the 24-hour time point but this wasn't statistically significant. These results indicate *Nucleolin* nascent transcription is not impacted by MeCP2 overexpression. This has also been seen previously where nucleolin protein localization and nucleoli structure have been impacted by *Mecp2*/MeCP2 mutation but not transcript levels.[137,167]

Analysis of *45S pre-rRNA* transcripts resulted in quite high variability between replicates in some samples (Figure 18B). At the 1-hour time point E2-transduced cells had approximately 0.25-fold lower steady-state *45S* levels, which was only statistically significant compared to polybrene-treated controls ($p<0.05$). EGFP-transduced cells also had reduced *45S* by approximately 0.6-fold, though not statistically significant. The changes that were also observed in EGFP-transduced cells result in difficulties interpreting whether any changes could be specifically due to MeCP2 overexpression.

The results for *28S rRNA* and *18S rRNA* are shown in Figure 19. The *28S rRNA* nascent transcripts were decreased by approximately 0.65-fold in E2- and E1+E2-transduced cells relative to polybrene-treated controls which was statistically significant ($p<0.05$) (Figure 19A). EGFP-and E1-transduced cells also showed slight but non-significant decreases of about 0.8-fold at this time point. *28S rRNA* steady-state transcripts were decreased by about 0.6-fold in E1-transduced cells ($p<0.05$) and 0.4-fold in E2-transduced cells. The *18S rRNA* nascent transcripts were significantly reduced in E2- and E1+E2-transduced cells by approximately 0.6-fold and 0.7-fold, respectively, which were both statistically significant compared to both polybrene-treated and EGFP-transduced controls ($p<0.05$) (Figure 19B).

Figure 18. Expression of nascent and steady-state *nucleolin* and *45S pre-rRNA* transcripts in Daoy cells transduced with lentiviral vectors expressing MeCP2 isoforms. Nascent RNA was prepared from cells labelled with EU for 1, 6 and 24 hours. Total RNA was prepared from unlabeled cells collected at the same time points. Gene expression was analyzed by RT-PCR for A) *Nucleolin* transcripts and B) *45S pre-rRNA* transcripts. C_T values were normalized to the housekeeping gene *GAPDH* and fold change determined relative to average polybrene-treated control N=3±SEM. Fold change values were analyzed by one-way ANOVA followed by Tukey's multiple comparisons, *p<0.05.

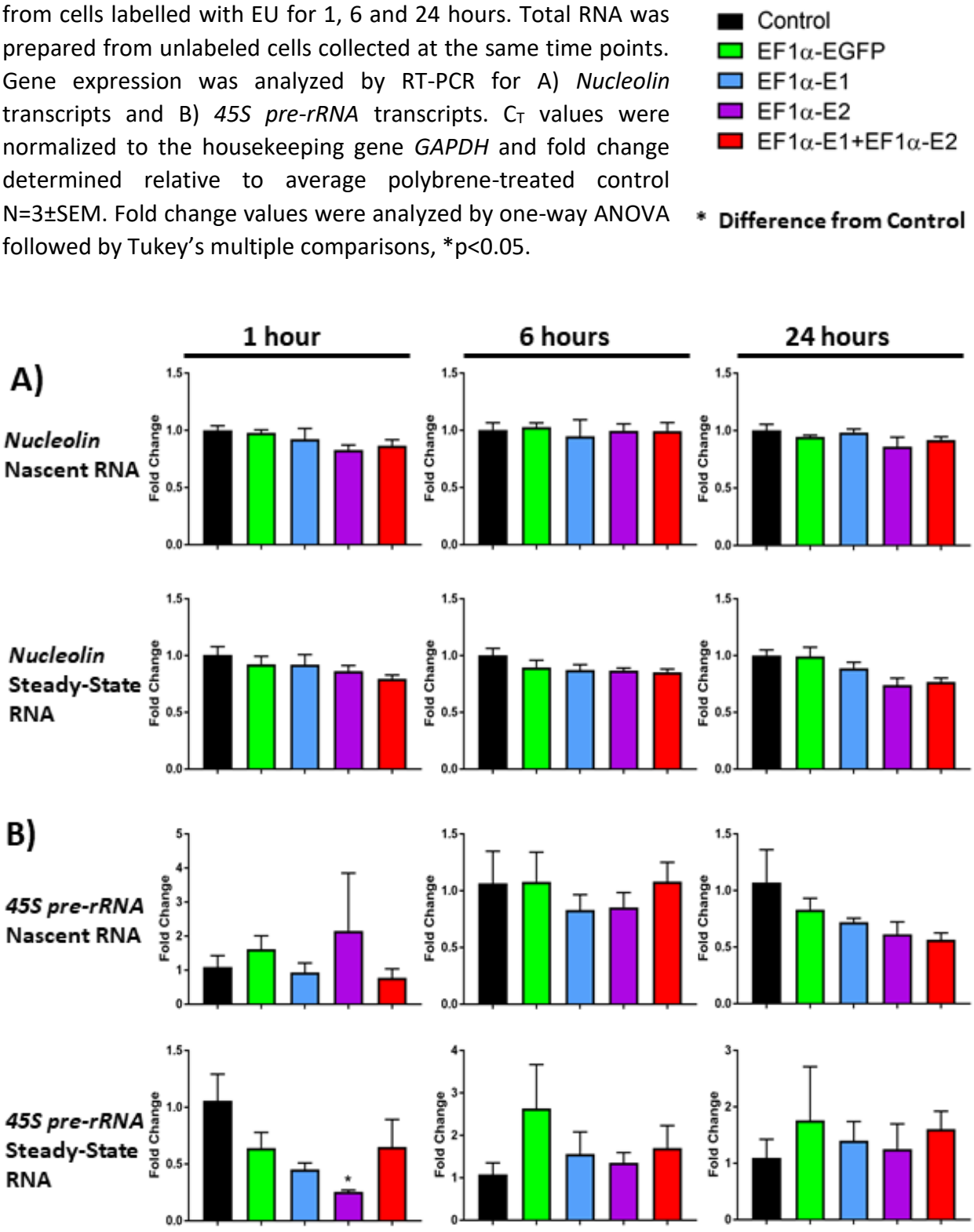

Figure 19. Expression of nascent and steady-state *28S* and *18S rRNA* transcripts in Daoy cells transduced with lentiviral vectors expressing MeCP2 isoforms. Nascent RNA was prepared from cells labelled with EU for 1, 6 and 24 hours. Total RNA was prepared from unlabeled cells collected at the same time points. Gene expression was analyzed by RT-PCR for A) *28S rRNA* transcripts and B) 18S *rRNA* transcripts. C_T values were normalized to the housekeeping gene *GAPDH* and fold change determined relative to average Polybrene control N=3±SEM. Fold change values were analyzed by one-way ANOVA followed by Tukey's multiple comparisons test, *p<0.05.

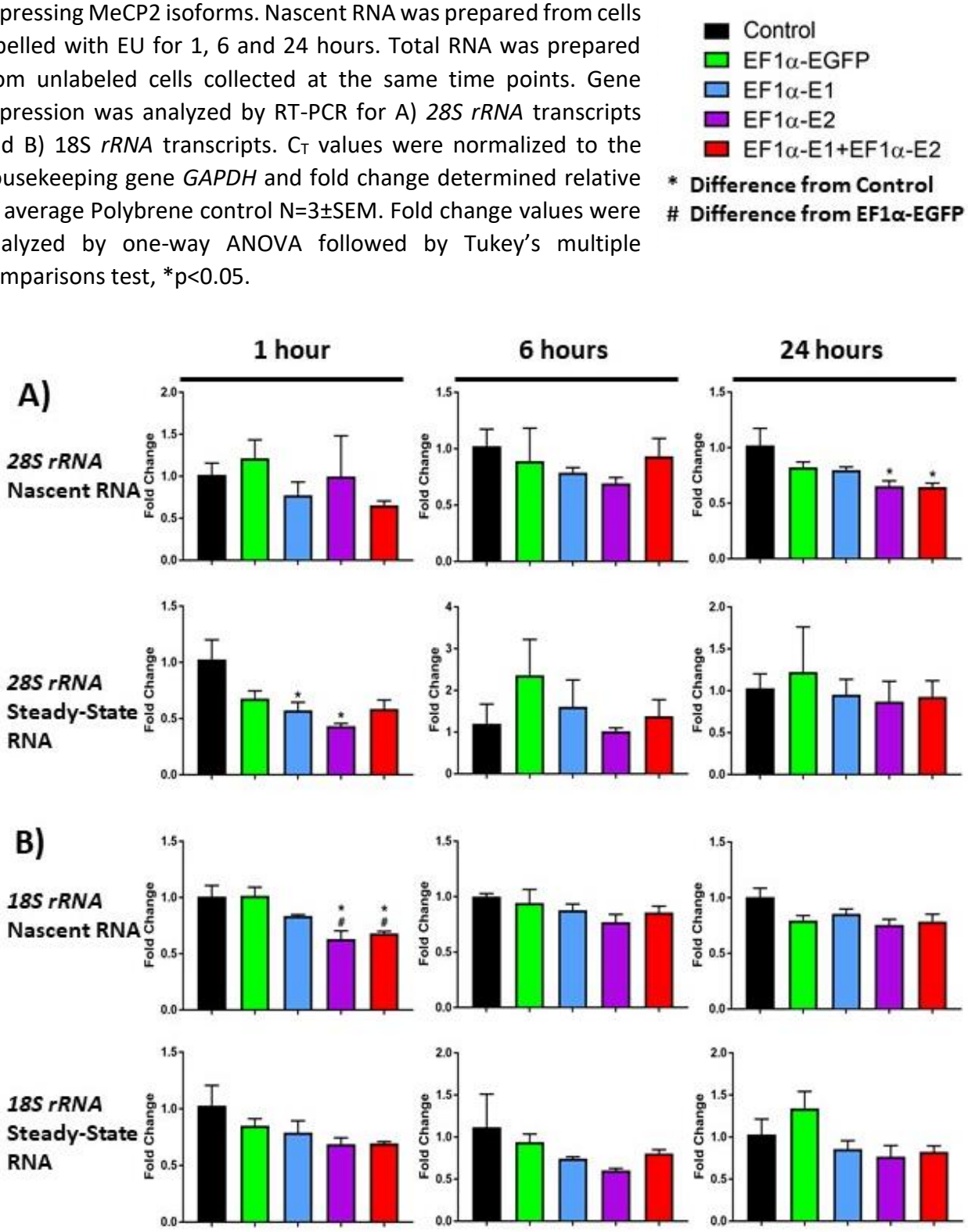

In describing the results shown in Figures 16-19, the fold changes relative to polybrene-treated control cells showed alterations between the analyzed time points. Statistical differences evaluated shown in those figures was for differences between the groups of cells at the particular time point. To evaluate whether there were also statistically significant differences between time points, the fold changes for each cell type at the three time points were compared. In Figures 20 and 21 the data is displayed to focus on the differences in fold changes between time points. Note that the fold changes of EGFP-, E1-, E2-, and E1+E2-transduced cells are expressed relative to polybrene controls.

The fold change of nascent *MECP2E1* in E1-transduced cells decreased from approximately 55-fold at 1 hour to 25-fold and 30-fold at 6 and 24 hours, but this was not statistically significant (Figure 20A). Steady-state *MECP2E1* was slightly increased from 0.6-fold to 1-fold between 1 hour and 6-hour time points in E1+E2 cells ($p<0.05$) but was otherwise not significantly changed between time points. The fold change of nascent *MECP2E2* transcripts in E2-transduced cells decreased from approximately 50-fold at 1 hour to 27-fold at 6 and 24 hours ($p<0.01$) and in E1+E2-transduced cells decreased from approximately 30-fold at 1 hour to 15-fold at 6 and 24 hours ($p<0.05$) (Figure 20B). *MECP2E2* steady-state transcripts remained consistent over the time points. The fold changes in *BDNF* nascent transcripts in E1-, E2-, and E1+E2-transduced cells showed similar trends of no change or slight increase between 1 and 6 hours and then a decrease at 24 hours, though these were not statistically significant (Figure 20C). At the steady-state level this trend was also observed. In E1-transduced cells the changes weren't statistically significant. In E2-transduced cells *BDNF* levels were approximately 3-fold at 1 and 6 hours and decreased to 2-fold at 24-hours ($p<0.01$). In E1+E2-transduced cells *BDNF* levels increased from approximately 2.4-fold at 1 hour to 3-fold at 6 hours ($p<0.01$) and decreased to 2-fold at 24 hours. The fold change at 24 hours was statistically significant compared to both 1 hour ($p<0.05$) and 6 hours ($p<0.001$).

Figure 20. Expression of nascent and steady-state *MECP2E1, MECP2E2, BDNF* and *miR-132-3p* transcripts over time in Daoy cells transduced with lentiviral vectors expressing MeCP2 isoforms. Differences in the expression of each gene between 1, 6 and 24 hours. N=3±SEM. Fold change values for the three time points were analyzed for each cell type by one-way ANOVA followed by Tukey's multiple comparisons test. The levels of significance are *p<0.05, **p<0.01, ***p<0.001.

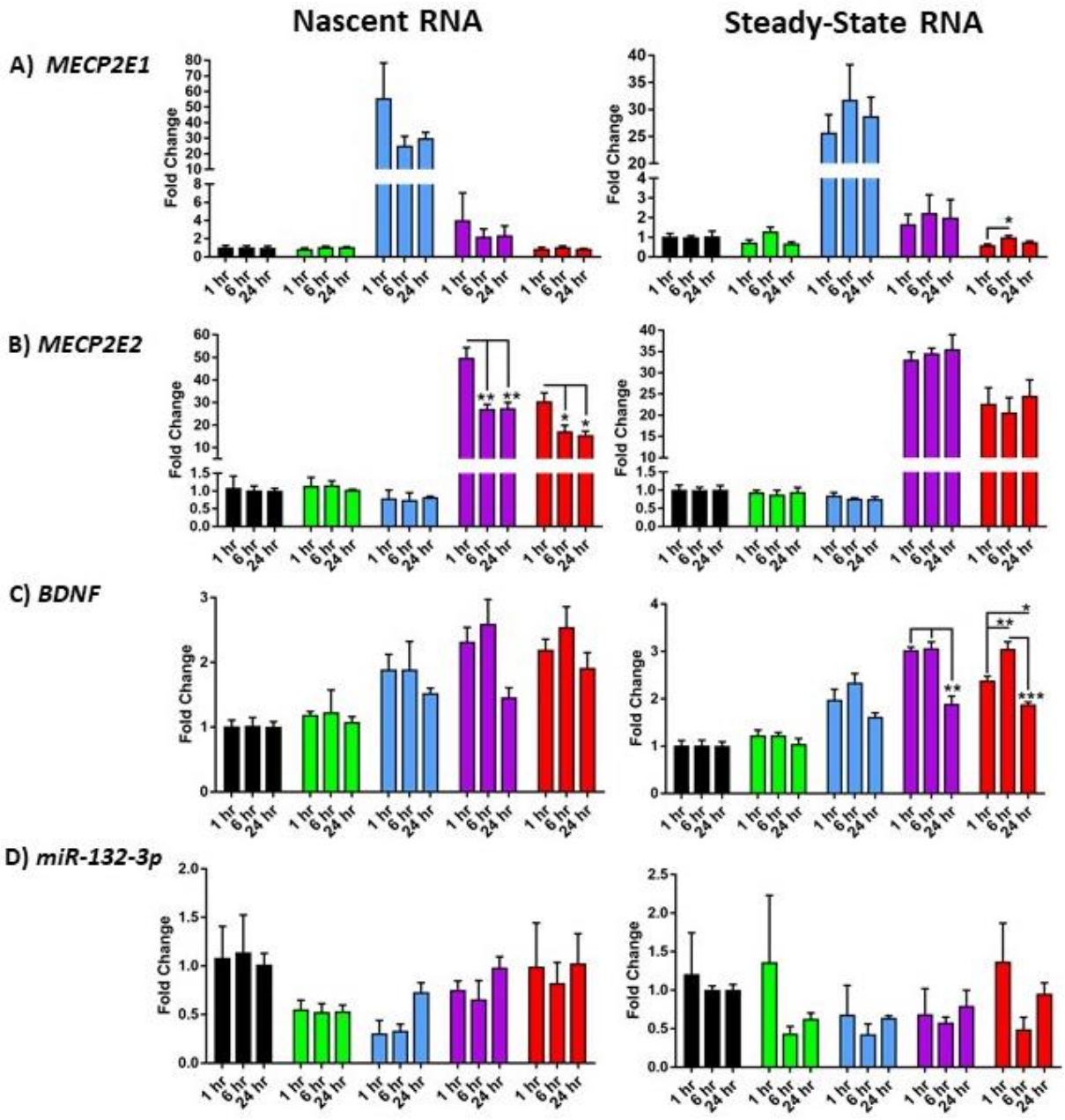

There were no statistically significant differences in *miR-132-3p* nascent or steady-state transcripts between the time points (Figure 20D). The steady state *miR-132-3p* transcripts appear to show a similar pattern of variation between the time points in EGFP-transduced cells as well as E1-, E2- and E1+E2-transduced cells indicating that changes are likely an off-target effect of transduction. *Nucleolin* nascent and steady-state transcripts didn't show significant changes over time (Figure 21A). The fold changes of *45S pre-rRNA, 28S rRNA,* and *18S rRNA* did show any statistically significant changes over time (Figure 21 B-D).

III.vii. Conclusion

In conclusion, Daoy cells which overexpress MeCP2E1 or E2 isoforms were successfully established by stable lentiviral transduction and validated by confirmational studies at the level of genomic DNA, mRNA transcripts, and protein. Daoy cells transduced with Lenti-EF1α-E1 or Lenti-EF1α-E2 vectors alone to overexpress each isoform individually were successfully established. Daoy cells transduced with both vectors in combination were seen to predominantly overexpress the E2 isoform, despite detection of integration of the Lenti-EF1α-E1 vector in these cells. Future studies could be done to investigate the mechanisms occurring in cells transduced with a combination of the two vectors, such as whether there is selection over time of cells expressing one vector, or whether there are post-transcriptional and/or translational regulatory mechanisms occurring between the two isoforms.

Immunofluorescence analysis indicated that endogenous and overexpressed MeCP2 is localized to nuclei of the cells. Further co-labeling studies by immunofluorescence could analyze whether MeCP2 localizes primarily at heterochromatic or euchromatic regions and whether this is altered by isoform-specific overexpression.

Cell viability of MeCP2 overexpressing cells was assessed at one time five weeks after transduction. E2 overexpressing cells showed significant reductions in cell viability 24 hours following seeding but this effect was gone 72 hours after seeding. MeCP2 overexpression has been shown to impact cell viability and proliferation in previous studies.[33,193]

Figure 21. Expression of nascent and steady-state *nucleolin, 45S pre-rRNA, 28S rRNA* and *18S rRNA* transcripts over time in Daoy cells transduced with lentiviral vectors expressing MeCP2 isoforms. Data shown in Figures 9 and 10 are shown in a different arrangement to display differences in the expression of each gene between 1, 6 and 24 hours. N=3±SEM. Fold change values for the three time points were analyzed for each cell type by one-way ANOVA followed by Tukey's multiple comparisons test.

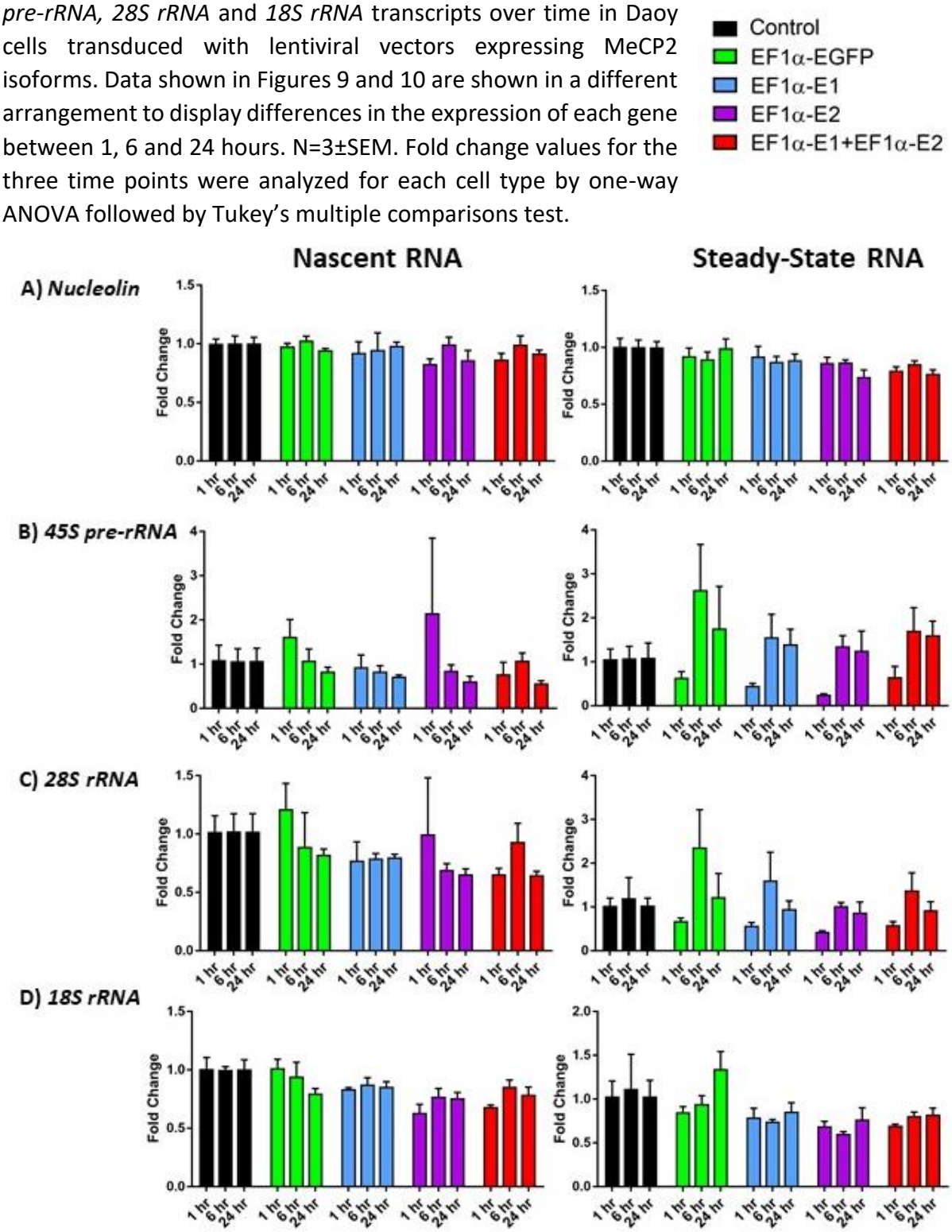

This aspect was not pursued further as part of this study but could be a focus of further in-depth study on the mechanisms by which MeCP2 influences cell viability and whether this effect is consistently seen following repeated passages of the cells.

The transcriptional effects of MeCP2 overexpression on its target genes by nascent RNA analysis were the primary effect studied for the first aim of this thesis. No significant differences in endogenous *E1* expression were seen in E2-transduced cells, and *vice versa*, indicating overexpression of one isoform does not increase transcription of the other.

Significant increases in *BDNF* transcription were observed in E1- and E2-overexpressing cells. This is in agreement with gene expression studies performed in the brain of mice with a duplication of the *Mecp2* gene[80,139,140] and shows that *Bdnf/BDNF* is a transcriptional target of both isoforms. This effect was seen more strongly in the steady-state transcripts, though also observed in nascent transcripts. This could be due to the fact that nascent transcripts are only produced during the time period of the experiment while steady-state transcripts also contain transcripts produced in the time period before labeling was begun. The *miR-132-3p* strand was determined to be the predominant strand expressed in Daoy cells which agrees with studies of *miR-132* in post-mortem human brain tissue.[56] There were no significant changes in *miR-132-3p* in the MeCP2 overexpressing Daoy cells, which could indicate the MeCP2/BDNF/*miR-132* network is not present in cells of the cerebellum which was also observed *in vivo.*[56] However, a more complete analysis of this network involving knockdown or overexpression of each of the components of this network in Daoy cells would be required to make a firm conclusion.

There were no significant changes in *Nucleolin* transcripts in MeCP2 overexpressing Daoy cells. A previous study indicated Nucleolin protein localization was impacted in post-mortem cerebellar tissue of Rett Syndrome patients, while transcripts were unaffected. Future studies using the MeCP2 overexpressing cells generated here could address whether Nucleolin protein levels are affected. *Ribosomal RNA* transcript results were more difficult to interpret due to instances of variability between replicates and the time points. The only samples which showed a significant change from both polybrene and EGFP-transduced control was a decrease in *18S rRNA* nascent transcripts in E2- and E1+E2-transduced cells at the 1-hour time point. There appeared to be overall a trend of decreased or unchanged *ribosomal RNA* levels. Ribosomal protein and RNA

genes were found to be downregulated in *MECP2* knockout hESCs.[84] In mice, *Mecp2* loss- and gain-of-function mutations lead to inverse gene expression changes but also gene expression changes in the same direction.[140] Gene expression changes can also be subtle. This highlights the complex role of MeCP2 in gene expression regulation.

It is important to perform further studies on the impacts of MeCP2 isoform overexpression on protein levels of BDNF and Nucleolin as well as additional potential downstream targets to further characterize the functional outcomes of MeCP2 overexpression.

Chapter IV: Results Aim 2: Investigate the effect of metformin and simvastatin treatment of Daoy cells on *de novo* transcription of *MECP2* and *BDNF* by nascent RNA analysis.

The first aim of the thesis, described in Chapter III, was to investigate MeCP2 isoform-specific effects on gene expression of selected target genes by overexpressing the E1 and E2 isoforms in Daoy cells. Gaining insight into the gene expression changes that result from alterations in MeCP2, could assist in evaluating potential therapies for disorders resulting from *MECP2* mutations. *MECP2* mutations cause Rett Syndrome and *MECP2* Duplication Syndrome and currently there are no effective therapies for these severe neurodevelopmental disorders. Metformin and simvastatin are commonly used FDA-approved drugs currently being studied in our lab as potential therapies for Rett Syndrome, by both *in vitro* and *in vivo* studies. These drugs were selected because of their ability to cross the blood-brain barrier,[207,237] their neuroprotective potential in diseases such as Alzheimer's and Parkinson's, and their potential to correct defects in carbohydrate and cholesterol metabolism that have been observed in Rett Syndrome patients.[4] The focus of the second aim of this thesis was to investigate the effects of metformin and simvastatin treatment on *MECP2E1, MECP2E2, BDNF, 45S rRNA, 28S rRNA,* and *18S rRNA* transcription in Daoy cells. Drugs which induce *MECP2* expression are of interest for Rett Syndrome therapies since increasing expression of the mutated form of the protein in a mouse model of *Mecp2*-T158M mutant mice ameliorated symptoms.[197] Induction of *BDNF* is also a desired effect of drug treatment since BDNF is a critical factor in neurodevelopment and has been observed to be reduced in Rett Syndrome.[152]

The drug metformin is commonly used for treatment of type 2 diabetes patients. Metformin was not specifically designed for treatment of type 2 diabetes, and the benefits of the drug were known before the mechanism of action in the liver was understood.[231] Clinical studies have shown that metformin treatment also reduces the risk of Parkinson's disease in type 2 diabetes patients.[271] The neuroprotective effects of metformin were also seen in mouse models of Parkinson's disease with increased BDNF protein levels observed in metformin-treated mice.[232,240] Metformin was also found to enhance neurogenesis and spatial memory formation in mice.[239] The mechanisms of metformin action in the brain still require further investigation, including whether increases in *MECP2* and/or *BDNF* transcription may be involved.

Simvastatin is a member of the statin family of drugs used to treat dyslipidemia in patients with elevated cholesterol through inhibition of HMG-CoA reductase, the rate-limiting step in cholesterol biosynthesis.[206] Elevated cholesterol is also observed in Rett Syndrome patients and mouse models.[4,176] Statins have been implicated in providing neuroprotection for various cognitive and neurological disorders.[207] Upregulation of BDNF has been observed in mouse models treated with simvastatin following brain injury and spinal cord injury.[224]

The effects of metformin and simvastatin treatment on *MECP2E1, MECP2E2, BDNF, 45S rRNA, 28S rRNA,* and *18S rRNA* transcription were tested in the Daoy cell model using nascent RNA analysis. Daoy cells were seeded at 50,000 cells per well in 6-well plates. Approximately 16 hours later the cells were synchronized by serum starvation by incubating in serum-free media for 24 hours. Once serum starvation was completed, drug treatments were applied in media containing serum. One set of drug-treated cells were labeled with 1 mM EU to label nascent RNA produced during drug treatment, and a second set of cells was left unlabeled for analysis of steady-state RNA levels.

Based on the recommendations of the Click iT Nascent RNA capture kit, two time points of 6 and 24 hours were initially selected for collection and analysis of RNA levels. Two concentrations of simvastatin were already assessed, 2.5 and 5.0 µM, by cell viability analysis performed in Daoy cells by our lab.[250] Two concentrations of metformin were assessed, 250 and 1000 µM, based on previous reports and our unpublished data. A combination of 250 µM metformin and 2.5 µM simvastatin was also tested for possible synergistic effects of the two drugs.

Additional conditions were collected for metformin treatment based on previous lab data. Cells treated with 1000 µM and 2000 µM metformin for 6 and 48 hours were collected and analyzed.

In order to assess the impact of serum starvation, applied prior to drug treatment to synchronize the cells, since metformin and simvastatin are both drugs which modulate the metabolic state of cells. Review of the literature also indicated serum starvation prior to drug treatment is included in some studies and not others. The genes *MECP2E1, MECP2E2,* and *BDNF* were assessed for non-serum starved conditions.

RNA extraction from the samples was performed using the RNeasy Plus Mini kit. Nascent RNA was purified from EU-labeled cells and converted to cDNA using the Click-iT Nascent RNA Capture

kit and Superscript III Reverse Transcriptase. Total steady-state RNA from unlabeled cells was converted to cDNA by the standard protocol using Superscript III Reverse Transcriptase. The nascent and steady-state samples were analyzed using gene-specific primers for the targets of interest by real-time qRT-PCR and analyzed by the $2^{-\Delta\Delta CT}$ method.

IV.i. Simvastatin treatment does not impact MECP2E1 or MECP2E2 expression but reduces BDNF transcription in Daoy cells

Daoy cells were treated with two concentrations of simvastatin, 2.5 µM and 5.0 µM, selected based on cell viability analysis performed in Daoy cells by our lab.[250] Nascent and steady-state *MECP2E1, MECP2E2,* and *BDNF* are shown in Figure 22. *MECP2E1* and *MECP2E2* transcript levels did not show any statistically significant changes following simvastatin treatments at 6 or 24 hours (Figure 22A,B). Nascent and steady-state *BDNF* transcripts were not significantly changed at 6 hours (Figure 22C) However, at 24 hours nascent *BDNF* transcripts were significantly decreased in 5.0 µM simvastatin treated cells by approximately 0.2-fold ($p<0.05$). Steady-state *BDNF* transcripts were significantly decreased at 24 hours in both 2.5 µM and 5.0 µM simvastatin treated cells by approximately 0.4-fold and 0.3-fold, respectively ($p<0.01$) (Figure 22C). Therefore, 5.0 µM simvastatin treatment resulted in reduced *BDNF* transcription after 24 hours. Though steady-state *BDNF* was decreased to similar levels by both simvastatin concentrations, nascent *BDNF* only showed statistically significant decreases by the 5.0 µM treatment. Simvastatin at 2.5 µM treatment appeared to result in a slight decrease in nascent *BDNF* as well but this was not statistically significant. This may indicate that *BDNF* is also being reduced by post-transcriptional mechanisms, but this would need to be tested experimentally. These results indicate that simvastatin treatment reduces expression of *BDNF* in Daoy cells which appears to contradict what has been seen by *in vivo* studies in mice. This may be due to differences between the *in vitro* and *in vivo* contexts, or different regulation of murine *Bdnf* and human *BDNF* genes. The concentrations of simvastatin used here may not be favorable in the Daoy cell line, and future studies could evaluate lower simvastatin concentrations. This should be evaluated carefully in potential future *in vivo* studies since elevation of BDNF is an important target in the treatment of Rett Syndrome. This also indicates thorough testing of simvastatin concentrations is required.

Figure 22. Expression of nascent and steady-state *MECP2E1, MECP2E1* and *BDNF* transcripts in Daoy cells treated with simvastatin. Daoy cells were serum-starved for 24 hours prior to drug treatment with 2.5 and 5.0 µM simvastatin. Samples were collected at 6 and 24 hours and gene expression was analyzed by RT-PCR for A) *MECP2E1,* B) *MECP2E2* and C) *BDNF* transcripts. C_T values were normalized to the housekeeping gene *GAPDH* and fold change determined relative to average control. N=3±SEM. Fold change values were analyzed by one-way ANOVA followed by Tukey's multiple comparisons test, *p<0.05, **p<0.01.

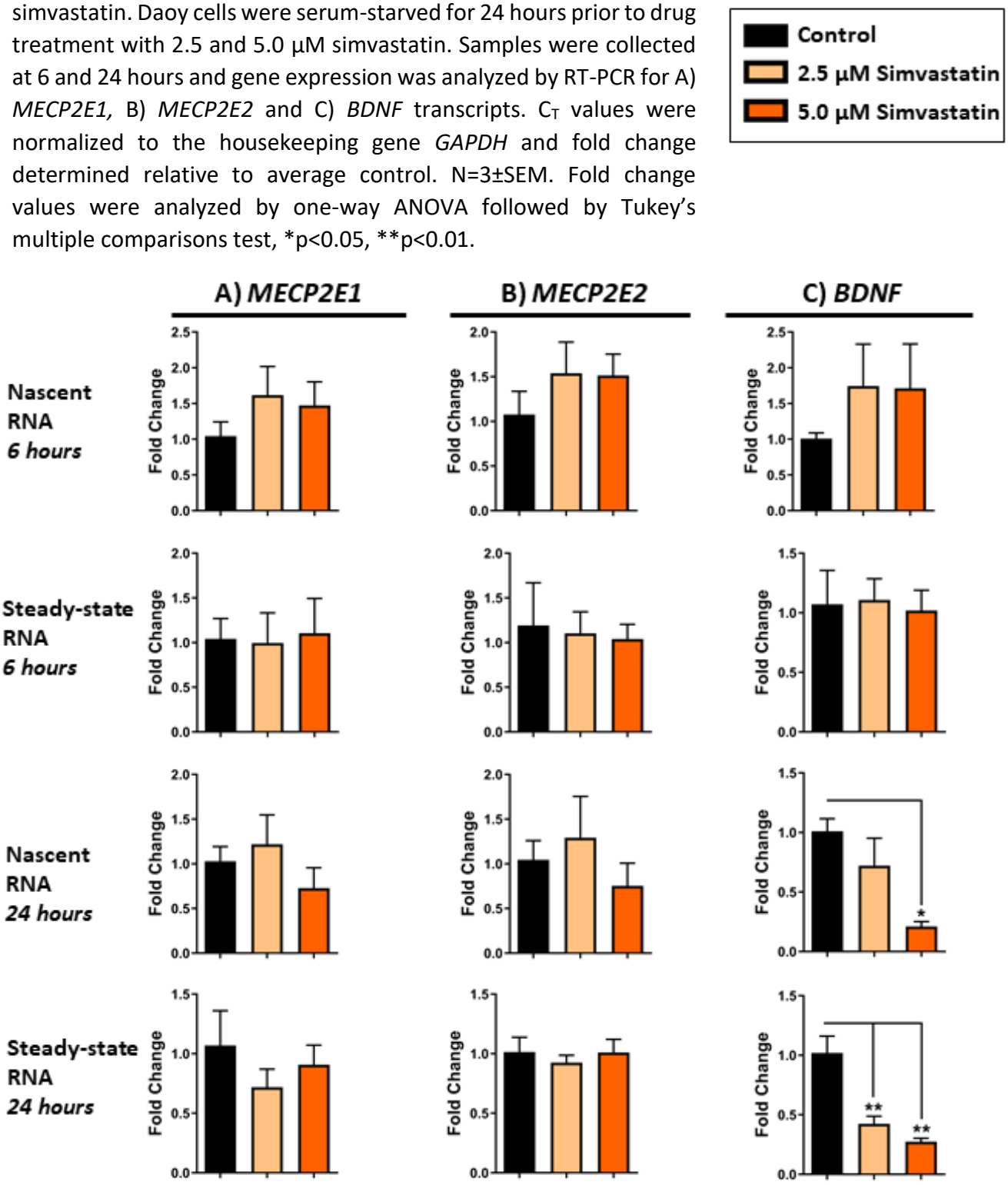

IV.ii. Metformin affects MECP2 and BDNF transcripts in a time- and dose-dependent manner

Concentrations of metformin were selected based on unpublished cell viability and steady-state gene expression analysis performed in our lab. Daoy cells treated with 250 μM or 1000 μM metformin for 6 and 24 hours displayed no significant changes in nascent or steady-state *MECP2E1, MECP2E2* and *BDNF* transcripts (Figure 23).

In order to investigate whether increased metformin concentration and/or length of time of treatment would result in changes in gene expression, additional samples were collected and analyzed. Daoy cells were treated with 1000 μM and 2000 μM metformin for 6 hours and 48 hours (Figure 24). In this set of samples nascent and steady-state *MECP2E1* transcripts were not significantly changed (Figure 24A). Nascent *MECP2E2* transcripts were unchanged at 6 hours but steady-state *MECP2E2* transcripts were slightly yet significantly decreased by approximately 0.8-fold in 6-hour 2000 μM treated cells ($p<0.05$) (Figure 24B). After 48 hours *MECP2E2* transcripts showed more significant decreases. Nascent *MECP2E2* transcripts were reduced approximately 0.75-fold by 1000 μM ($p<0.01$) and approximately 0.6-fold by 2000 μM treatment ($p<0.001$). The decrease in nascent *MECP2E2* in 2000 μM treated cells was also significantly lower compared to 1000 μM treated cells ($p<0.05$) indicating a dose-dependent effect. Steady-state *MECP2E2* transcripts were decreased approximately 0.7-fold by 1000 μM ($p<0.001$) and approximately 0.5-fold by 2000 μM treatment ($p<0.0001$). The difference between 1000 μM and 2000 μM treatment was also statistically significant ($p<0.01$). The decrease in *MECP2E2* transcripts at both nascent and steady-state levels indicates that metformin treatment reduces *MECP2E2* at the transcriptional level. Nascent and steady-state *BDNF* transcripts were unchanged at 6 hours (Figure 24C). Nascent *BDNF* transcripts remained unchanged after 48 hours but steady-state *BDNF* transcripts were significantly increased by about 2-fold compared to controls in cells treated with 2000 μM ($p<0.001$), which was also significantly greater compared to cells treated with 1000 μM metformin ($p<0.01$). The increase in *BDNF* transcripts at only the steady-state level indicates that metformin treatment may impact *BDNF* at the post-transcriptional level, but this would require further experimental analysis of transcript stability.

Figure 23. Expression of nascent and steady-state *MECP2E1, MECP2E1* and *BDNF* transcripts in Daoy cells treated with metformin. Daoy cells were serum-starved for 24 hours prior to drug treatment with 250 and 1000 µM metformin. Samples were collected at 6 and 24 hours and gene expression was analyzed by RT-PCR for A) *MECP2E1,* B) *MECP2E2* and C) *BDNF* transcripts. C_T values were normalized to the housekeeping gene *GAPDH* and fold change determined relative to average control. N=3±SEM. Fold change values were analyzed by one-way ANOVA followed by Tukey's multiple comparisons test.

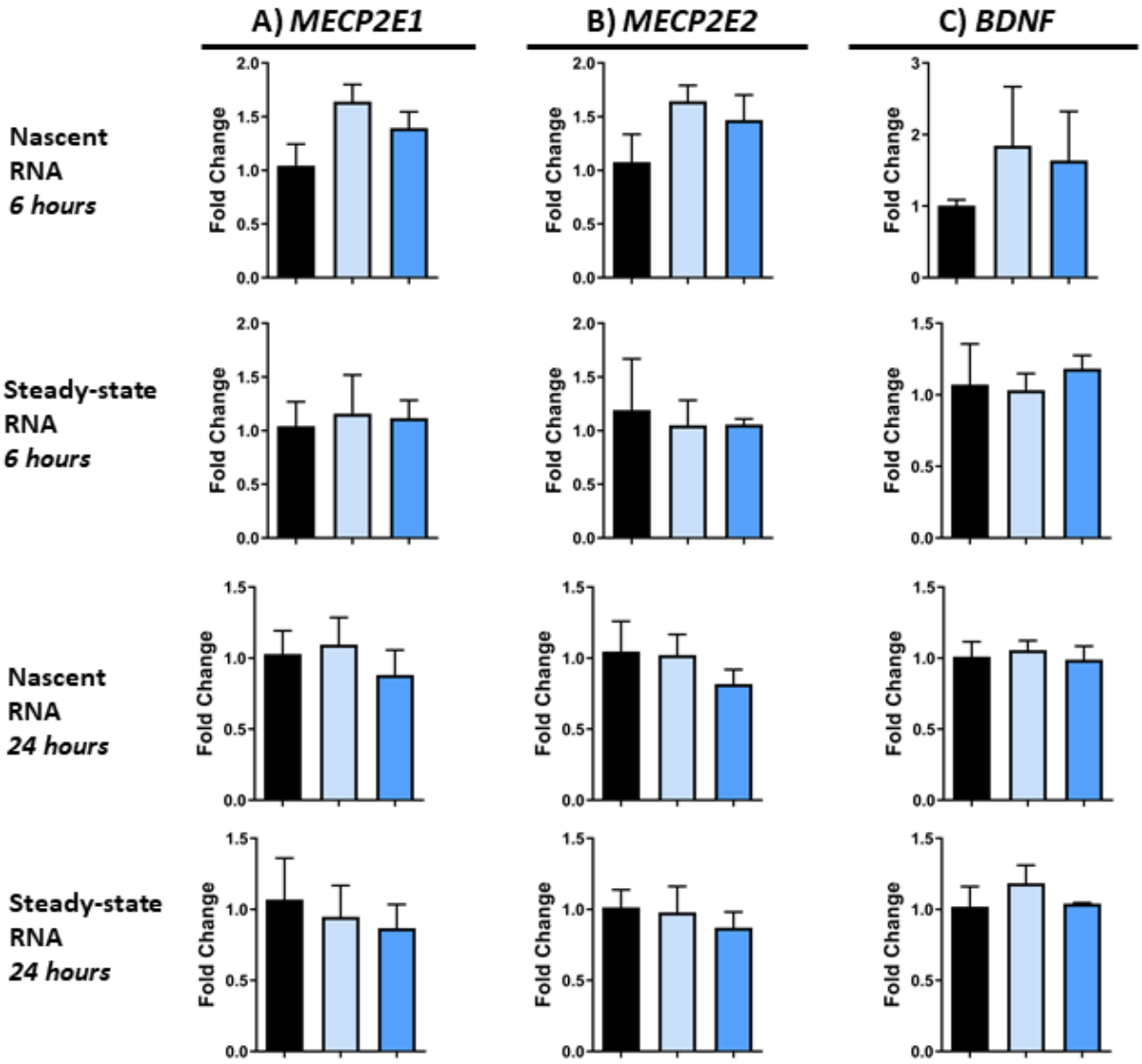

Figure 24. Expression of nascent and steady-state *MECP2E1, MECP2E1* and *BDNF* transcripts in Daoy cells treated with metformin. Daoy cells were serum-starved for 24 hours prior to drug treatment with 1000 and 2000 µM metformin. Samples were collected at 6 and 48 hours and gene expression was analyzed by RT-PCR for A) *MECP2E1,* B) *MECP2E2* and C) *BDNF* transcripts. C_T values were normalized to the housekeeping gene *GAPDH* and fold change determined relative to average control. N=3±SEM. Fold change values were analyzed by one-way ANOVA followed by Tukey's multiple comparisons test, *p<0.05, **p<0.01, ***p<0.001, ****p<0.0001.

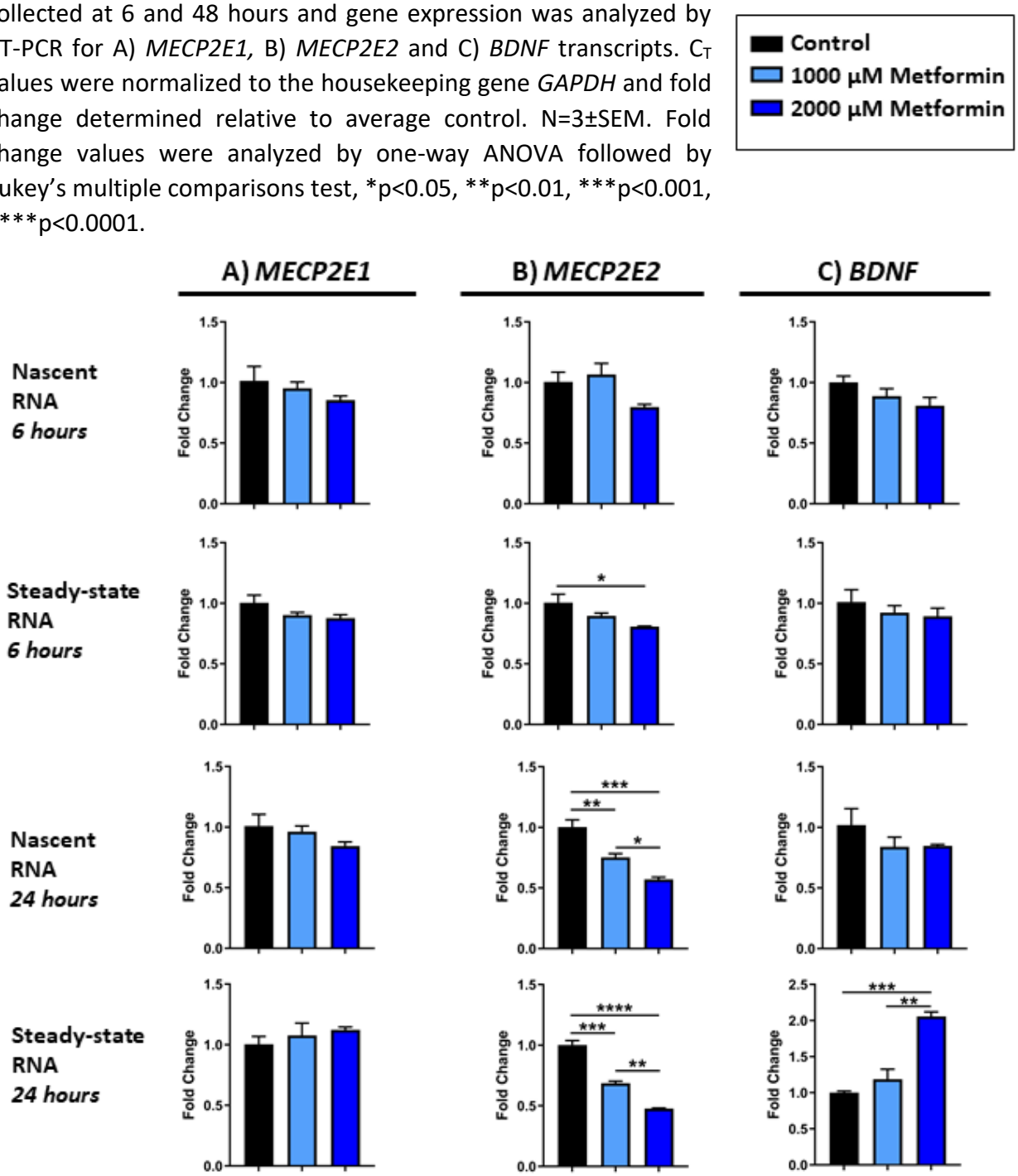

In order to assess the reproducibility of these results Daoy cells were treated with metformin of the same catalogue number used above but from a different lot number, referred to as Lot B, at concentrations of 1000 μM and 2000 μM for 6 and 48 hours (Figure 25). Some differences were observed with this specific lot of metformin. The levels of nascent and steady-state *MECP2E1* transcripts at 6 hours and of nascent *MECP2E1* transcripts at 48 hours were again unchanged, however, steady-state *MECP2E1* transcripts were increased by 1.4-fold in cells treated with 2000 μM metformin for 48 hours which was significant compared to both control and 1000 μM treated cells ($p<0.05$) (Figure 25A). Nascent *MECP2E2* transcripts were again unchanged at 6 hours and steady-state *MECP2E2* were also unchanged using this lot number (Figure 25B). After 48 hours nascent and steady-state *MECP2E2* transcripts showed similar results to that of the previous lot number. Nascent *MECP2E2* transcripts were decreased approximately 0.7-fold by 1000 μM metformin ($p<0.05$) and approximately 0.6-fold by 2000 μM treatment ($p<0.01$). Steady-state *MECP2E2* transcripts were reduced by approximately 0.7-fold by 1000 μM ($p<0.001$) and approximately 0.5-fold by 2000 μM treatment ($p<0.0001$). The decrease in steady-state *MECP2E2* in 2000 μM treated cells was again significantly lower compared to 1000 μM treated cells ($p<0.01$). Nascent and steady-state *BDNF* transcripts were again unchanged at 6 hours (Figure 25C). Nascent *BDNF* transcripts remained unchanged after 48 hours but steady-state *BDNF* transcripts were significantly increased by about 1.3-fold in cells treated with 1000 μM metformin ($p<0.01$), a result unique to this specific lot of metformin. Steady-state *BDNF* transcripts were again significantly increased in cells treated with 2000 μM metformin, by approximately 2.25-fold which was statistically significant compared to both control and cells treated with 1000 μM metformin ($p<0.0001$). Taken together, the results for 1000 and 2000 μM metformin were shown to be largely reproducible with two lot numbers of metformin. The reduction of *MECP2E2* transcripts at the transcriptional level was reproduced as well as the increase in *BDNF* transcripts at the steady-state level. The mechanism by which metformin results in increases in *MECP2E1* and *BDNF* steady-state transcripts could be assessed in future studies of transcript stability.

Figure 25. Expression of nascent and steady-state *MECP2E1, MECP2E1* and *BDNF* transcripts in Daoy cells treated with a different lot number of metformin. Daoy cells were serum-starved for 24 hours prior to drug treatment with 1000 and 2000 µM metformin (Met) (Lot B). Samples were collected at 6 and 48 hours and gene expression was analyzed by RT-PCR for A) *MECP2E1,* B) *MECP2E2* and C) *BDNF* transcripts. C_T values were normalized to the housekeeping gene *GAPDH* and fold change determined relative to average control. N=3±SEM. Fold change values were analyzed by one-way ANOVA followed by Tukey's multiple comparisons test, *p<0.05, **p<0.01, ***p<0.001, ****p<0.0001.

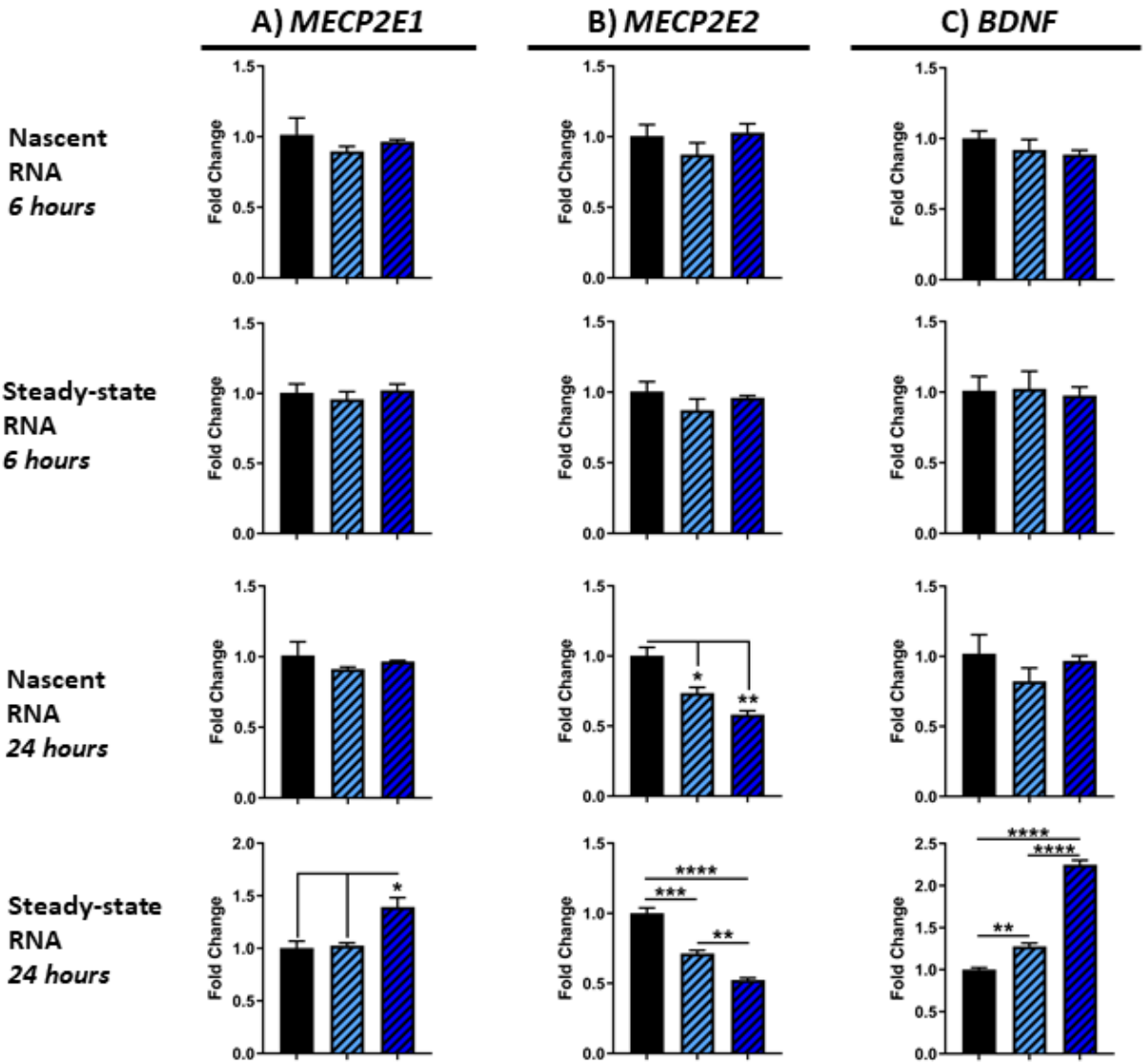

IV.iii. Effects of combination treatment of metformin and simvastatin on MECP2E1, MECP2E2, and BDNF

Combination treatments may be required for MeCP2-related disorders due to the broad impact of *MECP2* mutations. Combining metformin and simvastatin may be of interest in correcting both the glucose and cholesterol metabolism abnormalities seen in RTT patients. The scope of this study was to assess changes in gene expression resulting from treatment with these drugs and this was also tested for one combination condition. Daoy cells were treated with a combination of 2.5 µM simvastatin and 250 µM metformin for 6 and 24 hours followed by testing of nascent and steady-state levels of *MECP2E1, MECP2E2,* and *BDNF* transcripts by RT-PCR (Figure 26). The results for the individual treatments of 2.5 µM simvastatin and 250 µM metformin shown previously have also been included to allow comparison to the combination treatment.

MECP2E1 and *MECP2E2* transcript levels did not show any statistically significant changes in Daoy cells treated with the combination, similar to the individual treatments (Figure 26A,B). The effect of the combination treatment on *BDNF* transcripts was similar to the effect of simvastatin treatment alone. Nascent and steady-state *BDNF* transcripts were not significantly changed at 6 hours (Figure 26C). Nascent *BDNF* transcripts were reduced at 24 hours in cells treated with the combination by approximately 0.4-fold which was statistically significant compared to 250 µM metformin ($p<0.05$) but not compared to the control. Steady-state *BDNF* transcripts were reduced by about 0.4-fold in cells treated with 2.5 µM simvastatin alone as well as the combination and these decreases were both statistically significant compared to control ($p<0.05$) and cells treated with 250 µM metformin ($p<0.01$). The effect of 2.5 µM simvastatin on steady-state *BDNF* transcripts appeared to predominate in the combination treatment.

Future studies could expand the results to include additional combination treatments of metformin and simvastatin.

Figure 26. Expression of nascent and steady-state *MECP2E1, MECP2E1* and *BDNF* transcripts in Daoy cells treated with a combination of simvastatin and metformin. Daoy cells were serum-starved for 24 hours prior to drug treatment with 2.5 µM simvastatin (Stat), 250 µM metformin (Met) and a combination of 2.5 µM Stat + 250 µM metformin. Samples were collected at 6 and 24 hours and gene expression was analyzed by RT-PCR for A) *MECP2E1,* B) *MECP2E2* and C) *BDNF* transcripts. C_T values were normalized to the housekeeping gene *GAPDH* and fold change determined relative to average control. N=3±SEM. Fold change values were analyzed by one-way ANOVA followed by Tukey's multiple comparisons test, *p<0.05, **p<0.01.

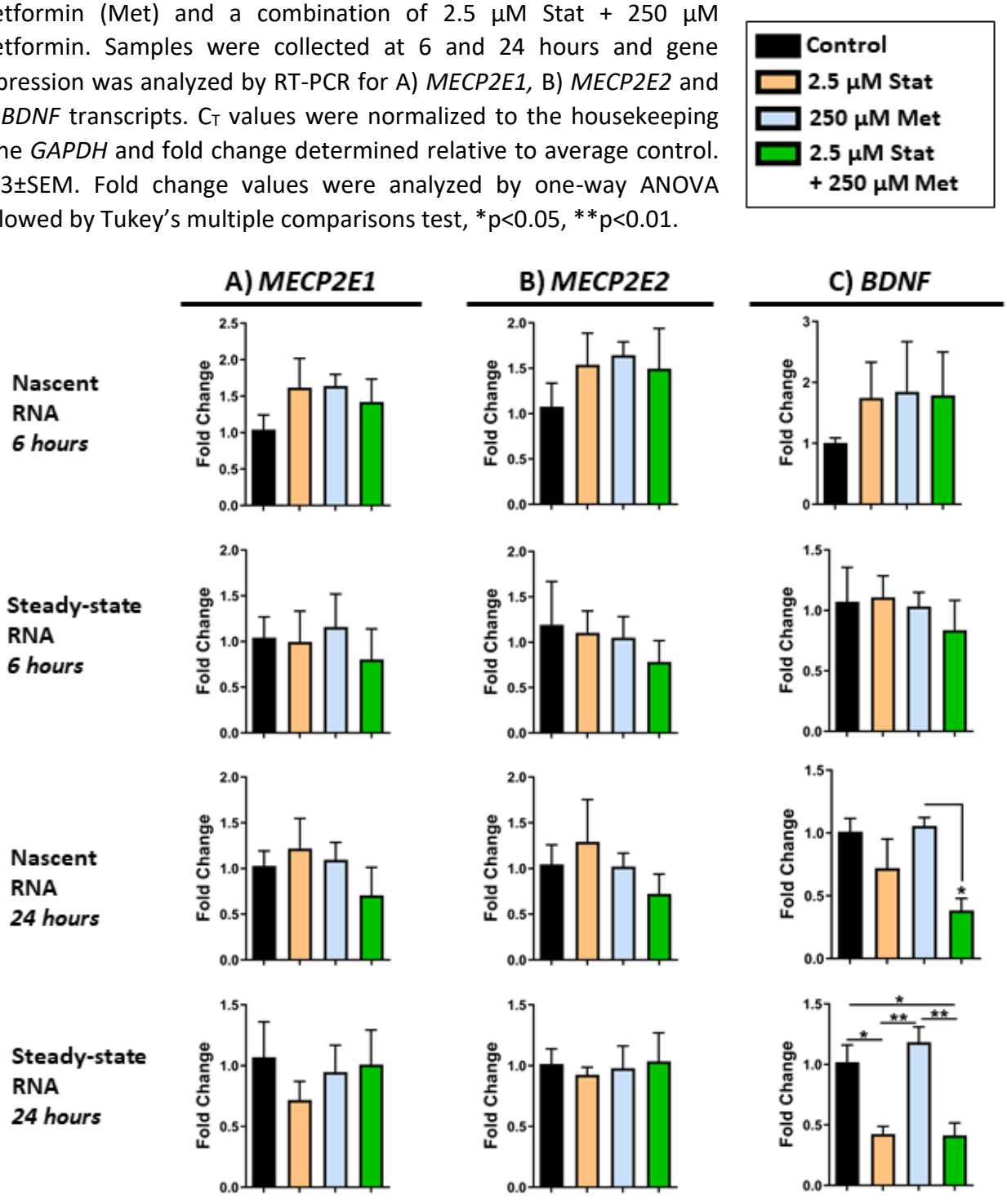

IV.iv. Simvastatin and metformin treatments do not significantly impact ribosomal RNA expression

Ribosomal RNA expression was also evaluated in metformin and simvastatin treated Daoy cells. Nascent and steady state *45S pre-rRNA, 28S rRNA,* and *18S rRNA* transcripts were evaluated in Daoy cells treated with 2.5 µM and 5.0 µM simvastatin, 250 µM and 1000 µM metformin and the combination treatment of 2.5 µM simvastatin + 250 µM metformin. Two time points of 6 and 24 hours were evaluated. No statistically significant differences in *rRNA* transcripts were observed as a result of simvastatin treatment (Figure 27). Though a trend of slight decrease was observed in levels of steady state *rRNA* transcripts at 6 hours, these were not statistically significant, and levels appeared similar to controls by 24 hours. There were also no statistically significant differences in *rRNA* transcript levels in Daoy cells treated with 250 µM and 1000 µM metformin (Figure 28) or in Daoy cells treated with a combination of 2.5 µM simvastatin + 250 µM metformin (Figure 29).

In evaluating *rRNA* transcripts, there were a number of conditions, where a high level of variation was observed between replicates, which along with lack of statistical significance makes it difficult to evaluate trends that may be occurring. This could reflect high levels of variation in these transcripts in Daoy cells. Overall, these results indicated that these concentrations of simvastatin and metformin treatment at the time points evaluated do not significantly impact expression of the *45S rRNA* precursor or levels of processed *28S* and *18S* transcripts.

Figure 27. Expression of nascent and steady-state *ribosomal RNA* transcripts in Daoy cells treated with simvastatin. Daoy cells were serum-starved for 24 hours prior to drug treatment with 2.5 and 5.0 µM simvastatin. Samples were collected at 6 and 24 hours and gene expression was analyzed by RT-PCR for A) *45S pre-rRNA,* B) *28S rRNA* and C) *18S rRNA* transcripts. C_T values were normalized to the housekeeping gene *GAPDH* and fold change determined relative to average control. N=3±SEM. Fold change values were analyzed by one-way ANOVA followed by Tukey's multiple comparisons test.

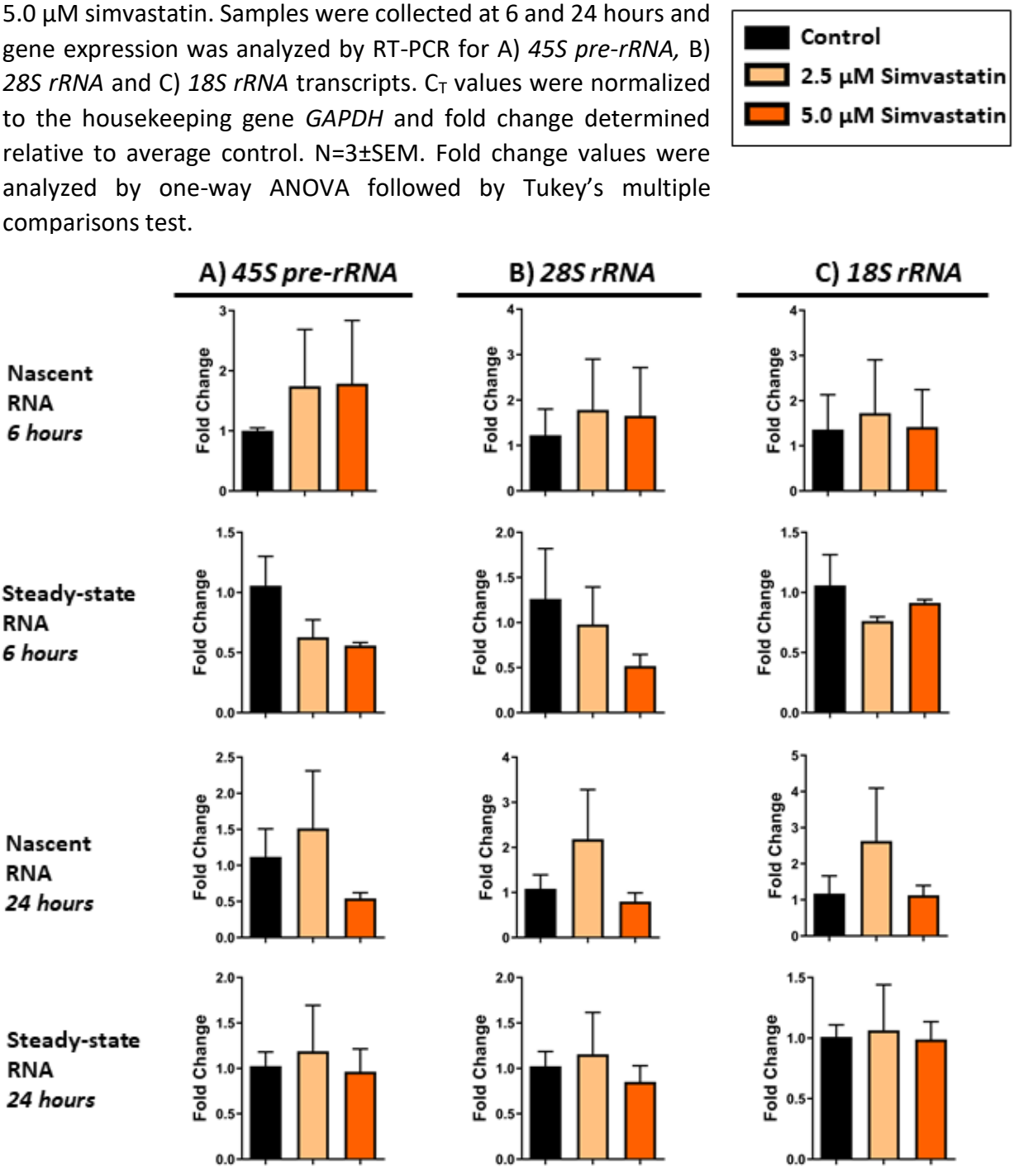

Figure 28. Expression of nascent and steady-state *ribosomal RNA* transcripts in Daoy cells treated with metformin. Daoy cells were serum-starved for 24 hours prior to drug treatment with 250 and 1000 µM metformin. Samples were collected at 6 and 24 hours and gene expression was analyzed by RT-PCR for A) *45S pre-rRNA,* B) *28S rRNA* and C) *18S rRNA* transcripts. C_T values were normalized to the housekeeping gene *GAPDH* and fold change determined relative to average control. N=3±SEM. Fold change values were analyzed by one-way ANOVA followed by Tukey's multiple comparisons test.

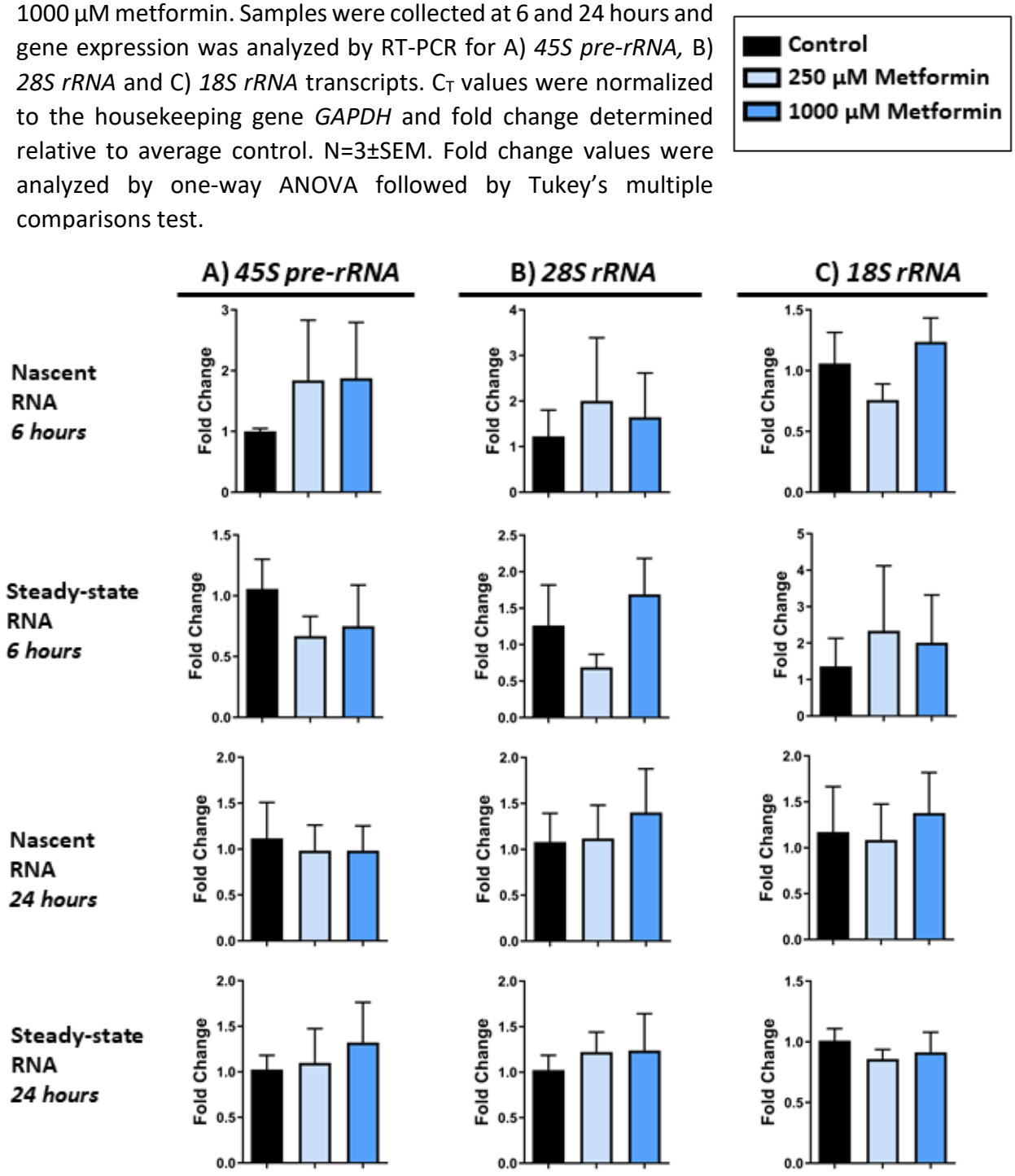

Figure 29. Expression of nascent and steady-state *ribosomal RNA* transcripts in Daoy cells treated with a combination of simvastatin and metformin. Daoy cells were serum-starved for 24 hours prior to drug treatment with 2.5 µM simvastatin (Stat), 250 µM metformin (Met) and a combination of 2.5 µM Stat + 250 µM metformin. Samples were collected at 6 and 24 hours and gene expression was analyzed by RT-PCR for A) *45S pre-rRNA,* B) *28S rRNA* and C) *18S rRNA* transcripts. C_T values were normalized to the housekeeping gene *GAPDH* and fold change determined relative to average control. N=3±SEM. Fold change values were analyzed by one-way ANOVA followed by Tukey's multiple comparisons test.

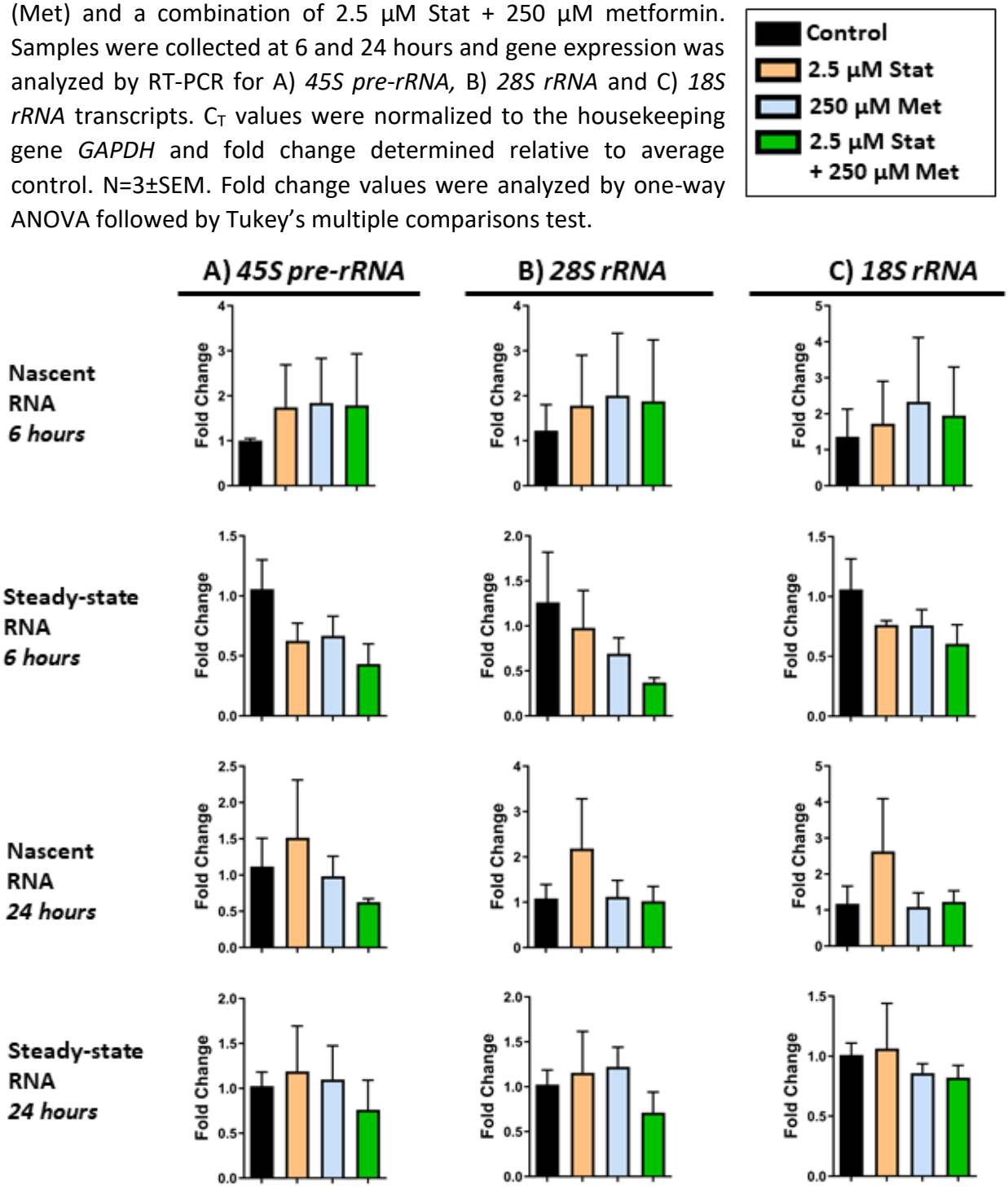

IV.v. Comparison of transcript analysis with non-serum starvation conditions

Metformin and simvastatin drugs are well characterized for their effects on metabolism. The results described in previous sections were in experimental conditions where cells were serum starved to synchronize them prior to drug treatment. This method is intended to bring the entire cell population to a similar metabolic state in the same stage of the cell cycle so that the effects of the drug treatments will be consistent among the cells. The transcript levels observed in cells which did not undergo serum starvation prior to drug treatment showed some differences with those that were serum starved.

Nascent *MECP2E1* transcript levels were unchanged in Daoy cells treated with simvastatin in non-serum starved condition (Figure 30A), similar to serum starved condition. However, decreases in steady-state *MECP2E1* transcripts were observed in non-serum starved condition which had not been observed in serum starved condition. At 6 hours, steady state *MECP2E1* was reduced by approximately 0.6-fold compared to controls in Daoy cells treated with either 2.5 µM or 5.0 µM simvastatin ($p<0.05$). At 24 hours, steady-state *MECP2E1* was reduced by approximately 0.7-fold compared to controls in Daoy cells treated with 2.5 µM simvastatin, which was not statistically significant, but remained reduced by approximately 0.6-fold by 5.0 µM simvastatin ($p<0.05$). Nascent and steady-state *MECP2E2* transcripts were not significantly altered by simvastatin treatment in the non-serum starved condition (Figure 30B). Similar to the results seen in the serum starved condition, nascent *BDNF* transcripts were significantly reduced at 24 hours in cells treated with 2.5 µM simvastatin by approximately fold changes of 0.2-0.3 for both nascent ($p<0.01$) and steady state ($p<0.001$) transcripts (Figure 30C).

MECP2E1 steady-state transcripts were slightly lowered by about 0.7-fold in 1000 µM metformin treated cells at 24 hours ($p<0.05$) (Figure 31A). There were no other statistically significant changes in *MECP2E2, MECP2E2* or *BDNF* transcripts in metformin treated cells (Figure 31A,B,C) indicating similar trends to metformin treated in the serum starved condition. A similar pattern of decreased *MECP2E1* steady-state transcripts was observed at the 6-hour time point as well but this wasn't statistically significant.

Figure 30. Expression of nascent and steady-state *MECP2E1, MECP2E1* and *BDNF* transcripts in non-serum starved Daoy cells treated with simvastatin. Daoy cells were not serum-starved prior to drug treatment with 2.5 and 5.0 µM simvastatin. Samples were collected at 6 and 24 hours, and gene expression was analyzed by RT-PCR for A) *MECP2E1,* B) *MECP2E2* and C) *BDNF* transcripts. C_T values were normalized to the housekeeping gene *GAPDH* and fold change determined relative to average control. N=3±SEM. Fold change values were analyzed by one-way ANOVA followed by Tukey's multiple comparisons test, *p<0.05, **p<0.01, ***p<0.001.

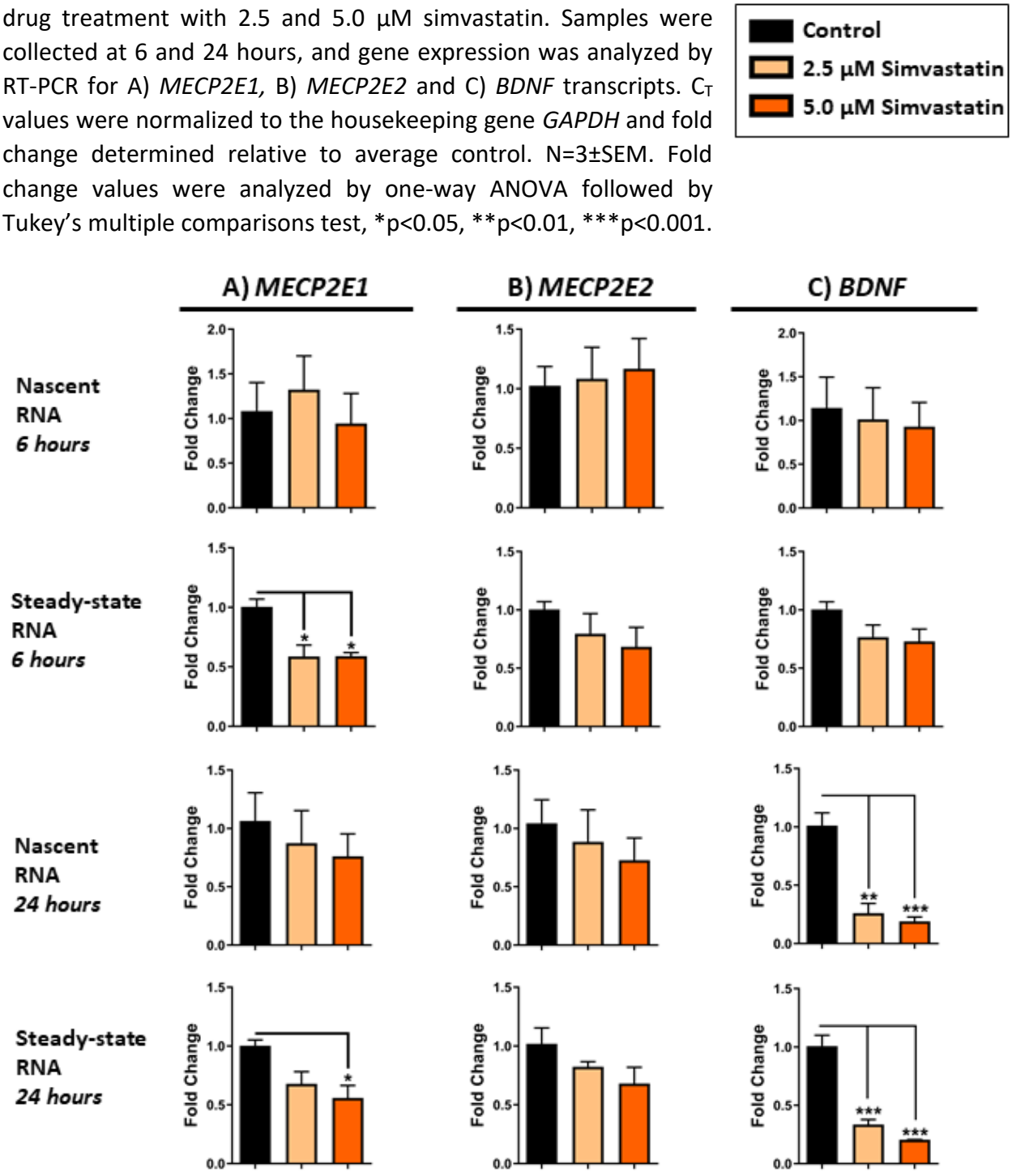

Figure 31. Expression of nascent and steady-state *MECP2E1, MECP2E1* and *BDNF* transcripts in non-serum starved Daoy cells treated with metformin. Daoy cells were not serum-starved prior to drug treatment with 250 and 1000 µM metformin. Samples were collected at 6 and 24 hours, and gene expression was analyzed by RT-PCR for A) *MECP2E1,* B) *MECP2E2* and C) *BDNF* transcripts. C_T values were normalized to the housekeeping gene *GAPDH* and fold change determined relative to average control. N=3±SEM. Fold change values were analyzed by one-way ANOVA followed by Tukey's multiple comparisons test, *p<0.05.

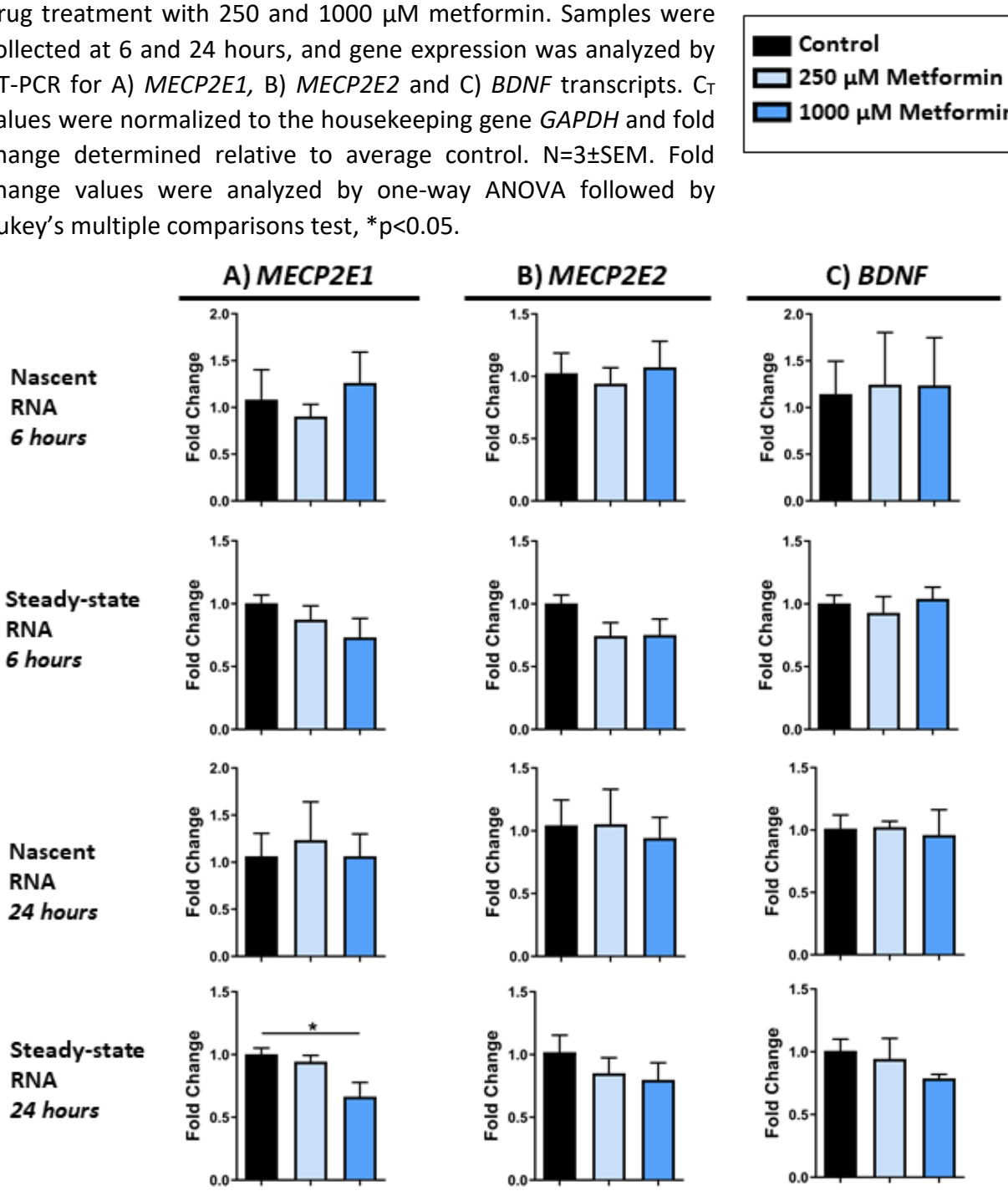

In the combination treatments of metformin and simvastatin in non-serum starved conditions *MECP2E1* steady state transcripts were significantly reduced at both 6 and 24 hours in cells treated with 2.5 µM simvastatin and combination of 2.5 µM simvastatin and 250 µM metformin by approximately 0.5-fold (Figure 32A) ($p<0.5$ and $p<0.01$). *MECP2E2* transcript levels did not show any statistically significant changes in Daoy cells treated with combination of the two drugs, similar to individual treatments, although steady state transcripts were reduced approximately 0.5-fold at 6- and 24- hours, this wasn't statistically significant (Figure 32B). The effect of combination treatment on *BDNF* transcripts was again significant reduction. Nascent and steady state *BDNF* transcripts were not significantly changed at 6 hours (Figure 32C). Nascent *BDNF* transcripts were reduced at 24 hours in cells treated with 2.5 µM simvastatin by approximately 0.3-fold ($p<0.001$) and in cells treated with the combination by approximately 0.2-fold ($p<0.001$). These reductions were also statistically significant compared to 250 µM metformin ($p<0.001$). Steady state *BDNF* transcripts were similarly reduced in cells treated with 2.5 µM simvastatin as well as the combination and these decreases were both statistically significant compared to control ($p<0.01$) and cells treated with 250 µM metformin ($p<0.01$).

Future studies could expand the results to include additional combination treatments of metformin and simvastatin.

Figure 32. Expression of nascent and steady-state *MECP2E1, MECP2E1* and *BDNF* transcripts in non-serum starved Daoy cells treated with a combination of simvastatin and metformin. Daoy cells were not serum-starved prior to drug treatment with 2.5 µM simvastatin (Stat), 250 µM metformin (Met) and a combination of 2.5 µM Stat + 250 µM metformin. Samples were collected at 6 and 24 hours, and gene expression was analyzed by RT-PCR for A) *MECP2E1,* B) *MECP2E2* and C) *BDNF* transcripts. C_T values were normalized to the housekeeping gene *GAPDH* and fold change determined relative to average control. N=3±SEM. Fold change values were analyzed by one-way ANOVA followed by Tukey's multiple comparisons test, *p<0.05, **p<0.01, ***p<0.001.

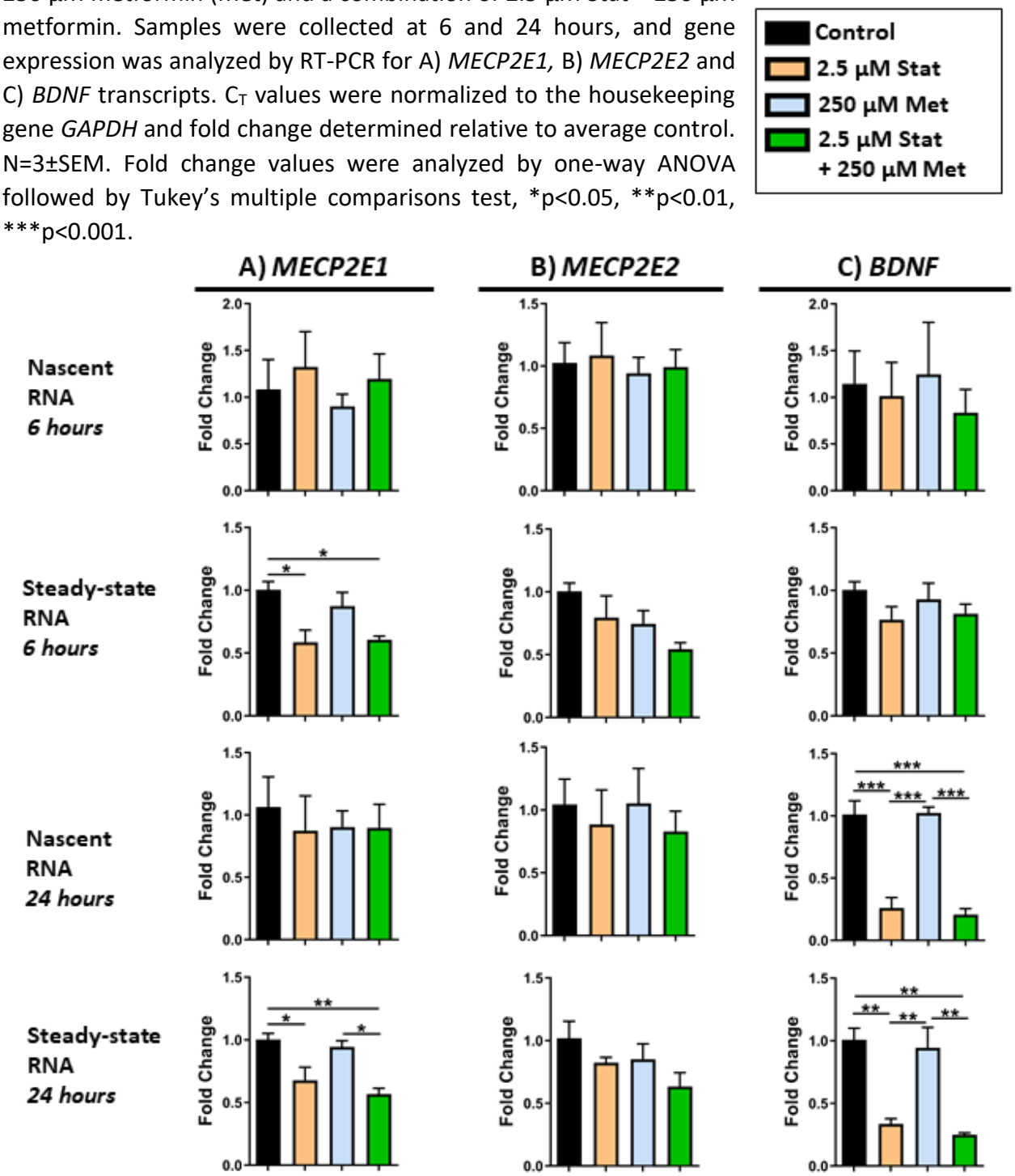

IV.vi. Conclusion

This chapter describes a mechanistic study for the effects of metformin and simvastatin treatment in Daoy cells on nascent transcription of *MECP2E1, MECP2E2,* and *BDNF.* The results indicated that simvastatin reduces transcription of *BDNF,* while metformin increased transcript levels of *E1* and *BDNF* and decreased transcription of *E2.* Nascent transcripts of *E1* and *BDNF* were unchanged by metformin treatment, which indicates that the mechanism by which metformin acts is not directly transcriptional. Future studies could address whether metformin treatment influences the transcript stability of *E1* and *BDNF*, resulting in the increase in steady state transcripts. In connection with Aim 1 of the thesis, the results of metformin treatment also indicate an isoform-specific effect is occurring. This again highlights the importance of investigating the mechanisms of isoform-specific regulation occurring and determining how they may be relevant to the pathology of Rett Syndrome and *MECP2* Duplication Syndrome.

The effects of simvastatin and metformin treatment on MeCP2 and BDNF protein levels is an important step to be evaluated. The true efficacy of these drugs should also be evaluated by *in vivo* studies using Rett Syndrome or MDS, where the systemic effects of aberrant cholesterol and glucose metabolism are present and where the effects on the processes of neurodevelopment can be investigated.

Chapter V: Discussion

The mechanisms of disease for both Rett Syndrome and MDS are very complex with broad effects stemming from mutations in a single protein MeCP2. Studies have shown that inverse changes in gene expression occur in mice overexpressing or loss of MeCP2, but also changes unique to each mutation.[80] While much progress has been made in understanding MeCP2 interactors and targets of expression, an important aspect requiring further studies is understanding the function of the two isoforms of MeCP2E1 and E2. Though E1 is the major isoform expressed in the brain, there is still evidence of E2 being expressed in the brain, and that the isoforms have unique properties and functions.[54,69,262] Within this study, an *in vitro* model overexpressing each isoform was established to test whether gain-of-function in a human brain cell line can yield insights to the different roles of these isoforms in mechanisms of transcriptional gene regulation. Studies on cell signaling pathways will be described as future directions of the model established. The results indicate that E1 and E2 isoforms both activate *BDNF* expression. The effects of two FDA-approved drugs, metformin and simvastatin were evaluated in Daoy cells and the results indicate that metformin increased *BDNF* and *MECP2E1* transcripts but reduced *MECP2E2* transcripts, while simvastatin reduced *BDNF* transcripts.

V.i. Transcriptional effects of MeCP2 isoform-specific overexpression

Lentiviral transduction of Daoy cells proved to be an efficient method to overexpress the MeCP2 isoforms and study changes in nascent RNA expression. Expression of MeCP2 was retained in the nucleus where it is normally endogenously found to function. A benefit of this model is that it can be maintained in culture due to the nature of the cell line and the stable lentiviral transduction which is maintained through cell divisions. Overexpression of each isoform alone was successfully achieved but the combination transduction of both isoforms resulted predominantly in overexpression of *MECP2E2*. In order to achieve a more equal level of the isoforms a different method of transduction could be attempted such as successive transductions, introducing one isoform first and then the other. Transduction of both lentiviral vectors at the same time may have increased the stress on the cells. Additionally, the ratios of E1 and E2 viral titers could be varied to investigate dosage effects of overexpression. In the E1+E2

cells generated in this study, the *MECP2E1* lentiviral vector was incorporated into the genome of E1+E2 levels at a substantial level as seen by genomic DNA analysis, though less by approximately 3-fold than the level of *MECP2E2* incorporation in the genome. Yet the level of *MECP2E1* transcripts and E1 protein were even lower than expected from the significant presence of *MECP2E1* lentivirus incorporation. Therefore, there is a possibility that overexpression of E2 has suppressed expression of E1. This was beyond the scope of this study but presents a future direction of research. In our lab this has already begun by analyzing the stability of MECP2E1 isoform in E1+E2 cells. Future studies could involve assessing the transcript stability of the *MECP2E1* transcripts through actinomycin D treatment.

The effect of MeCP2 overexpression on cell viability by MTT verified that cell viability was not severely impacted by MeCP2 overexpression. Overexpression of either isoform had slight effects on cell viability at an early time point but viability improved over subsequent time points. In previous studies MeCP2E1 overexpression reduced stem cell proliferation[33] and overexpression of MeCP2E2 promoted apoptosis in cerebellar rat granule cells.[193] This may represent an adverse effect present in MDS patient neurons and future studies could address the impact of isoform-specific overexpression on various modes of cell death or growth arrest in cells.

V.i.a. MeCP2 autoregulation and MeCP2, BDNF, *miR-132* homeostasis

The results of this study indicate that overexpression of the E1 isoform did not induce *E2* transcripts or *vice versa* in initial analyses of cells collected at non controlled time points. When nascent expression was analyzed at controlled time points a small but non-significant increase in *E1* transcripts was seen in E2 overexpressing cells.

BDNF belongs to the family of neurotrophins and plays a critical role in neuronal differentiation and growth as well as maintenance and survival.[146] BDNF deregulation has been linked to a number of neurodevelopmental, neurological and neurodegenerative disorders including Rett Syndrome, Alzheimer's disease, Parkinson's disease, depression and drug addiction. Regulation of the *BDNF* human gene is complex with the gene consisting of 11 exons and 9 functional promoters, with the 3' exon containing the coding sequence and alternatively spliced with the various 5' exons to produce a variety of transcripts.[150] This study evaluated changes in total *BDNF*

transcripts in Daoy cells following MeCP2E1 or E2 overexpression, showing that overexpression of either isoform produced increases in the level of nascent *BDNF* transcription (Figure 33). Increased MeCP2 had been linked to increased *BDNF* transcripts previously but has not been shown at the nascent level or isoform-specific level.[80] The changes in nascent transcripts were seen to be slightly more subtle than the increases seen in steady state transcripts. The steady state also includes transcripts that were present in the cells prior to EU labeling was initiated, but could also represent increased *BDNF* transcript stability. Future studies of transcript stabilities in MeCP2 overexpressing cells could characterize this further. Protein BDNF levels weren't yet evaluated and should be included in future studies to evaluate the outcome of MeCP2 overexpression on the functional protein product. However, increases in *BDNF* transcription are significant since *BDNF* transcription is thought to be major contributor to regulation of BDNF expression.[146] The highest fold changes in *BDNF* were seen in MeCP2E2-overexpressing cells, which was at times significantly greater compared to MeCP2E1-overexpressing cells. The differences in *BDNF o*bserved between E1+E2-transduced and E2-transduced cells could be an E2 dosage effect, as *E2* transcripts were about a third lower in E1+E2 cells, but this wasn't confirmed at the E2 protein level. MeCP2 overexpressing cells had increased levels of nascent *BDNF* at the earlier time points compared to controls but this was diminished by 24 hours. This could be an indication of a feedback loop reducing the level of nascent transcription as *BDNF* levels increase. The primers used in this study detect total *BDNF* transcripts. *BDNF* gene has multiple promoters and transcripts which yield the same coding sequence and protein.[150] MeCP2 binding to the *Bdnf* promoter IV has been shown in rodents has been shown in rat cortical neurons[151] and ChIP studies in Daoy cells could investigate whether MeCP2 binds similarly to the analogous promoter in human cells. The results of this study agree with previous findings showing that as MeCP2 protein levels increase in neurons compared to human embryonic stem cells, so does nascent *BDNF* transcription.[33] This regulation has been suggested to follow a methylation dependent mechanism since genes such as *Bdnf* show increased levels of mCH during neuronal maturation.[140] Future studies could investigate global methylation states as well as methylation states of genes of interest in Daoy cells overexpressing MeCP2 compared to control cells.

Figure 33. Schematic of the effect of overexpression of MeCP2 isoforms on selected target genes in Daoy cells. *BDNF* transcripts were elevated by overexpression of either isoform. Changes in *miR-132* transcripts did not appear to be a specific effect of MeCP2 overexpressing cells when compared to EGFP-overexpressing cells. Inhibition of MeCP2 by *miR-132* in these cells requires further investigation by overexpression or knockout of *miR-132* which could clarify whether this network functions in cells of cerebellar origin. Overexpression of the isoforms did not impact *Nucleolin* gene expression. Nucleolin is known to activate ribosomal RNA expression. Results of this study indicate MeCP2 overexpression may repress rRNA expression, but this was not consistently seen at all time points of the study.

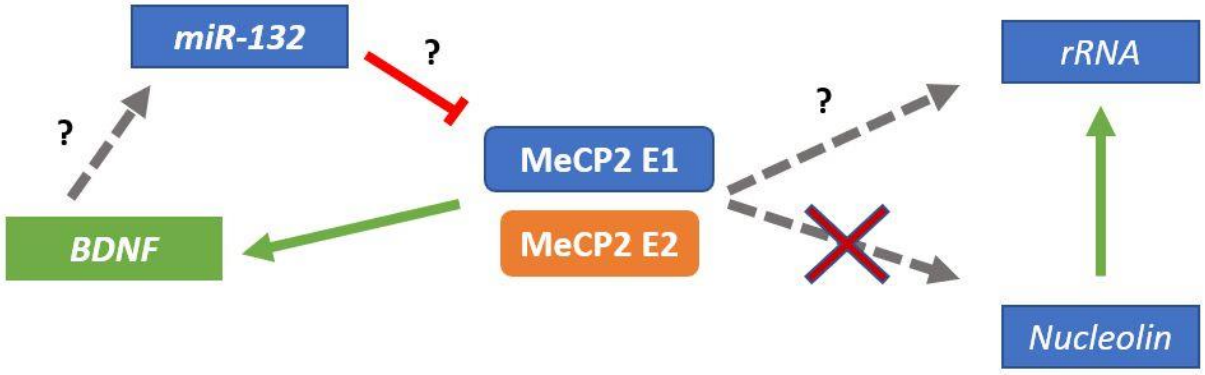

The results of MeCP2 overexpression on *miR-132* was also evaluated in this study as it is proposed to form a homeostatic regulatory network with MeCP2 and BDNF whereby MeCP2 activates BDNF expression, which induces *miR-132* expression, which then inhibits MeCP2. A recent study from our lab on this network in post-mortem human RTT patient brain tissues observed decreased *MECP2* and *BDNF* transcripts in frontal cortex, amygdala, hippocampus, and cerebellum. The frontal cortex, amygdala, and hippocampus also had decreased *miR-132* transcripts but *miR-132* transcripts were unchanged in the cerebellum. The expression of *MECP2* is highest in the cerebellum and perhaps this is due to the fact that *miR-132* expression is kept low there.[56] The *miR-132-3p* strand of the microRNA was observed to be the major strand expressed in the human brain tissues, which was also observed in Daoy cells in this study. In this study Daoy cells overexpressing MeCP2 isoforms had increased *BDNF* transcripts but *miR-132* was unchanged indicating this homeostasis network may not function as suggested by murine studies in the human cerebellum cells. There were changes observed in *miR-132* in this study, but these were seen in EGFP overexpressing control cells as well indicating this wasn't a specific

effect of MeCP2 overexpression. This appears to indicate consistency with what is observed in the human RTT brain context.

V.i.b. Nucleolin and *ribosomal RNAs*

Nucleolin and *ribosomal RNAs* are critical factors in ribosome biogenesis and protein translation in cells which are impaired in RTT. In this study, *Nucleolin* nascent and steady state transcripts were unchanged in Daoy cells overexpressing MeCP2, which is a confirmation along with *GAPDH*, used as the housekeeping gene, that MeCP2 overexpression does not indiscriminately affect gene expression (Figure 33). The changes in Nucleolin in previous studies have been observed primarily at the protein level, which indicates MeCP2 may impact Nucleolin post-translationally, which will require future studies. This could involve investigating whether MeCP2 impacts post-translation modifications, protein stability and localization of the Nucleolin protein.

Ribosomal RNA transcript levels did not appear consistently and significantly changed overall in MeCP2 overexpressing Daoy cells. The only samples which showed a significant change from both polybrene and EGFP-transduced controls was a decrease in *18S rRNA* nascent transcripts in E2- and E1+E2-transduced cells at 1-hour time point. Ribosomal protein and RNA genes were found to be downregulated in *MECP2* knockout hESCs.[84] In mice, *Mecp2* loss- and gain-of-function mutations lead to inverse gene expression changes but can also lead to gene expression changes in the same direction.[140] This may be the case for *ribosomal RNA* genes as well. The primers used in this study for *45S* detect the *45S* transcripts specifically. Since the *45S* transcript contains the *28S* and *18S* transcript sequences prior to its cleavage, the *28S* and *18S* primers detect *45S* transcripts as well. A change in *45S* transcripts alone could indicate a defect in processing of the *45S* transcript but this was not observed here. In addition to *Nucleolin* and *ribosomal RNA* genes, ribosomal protein levels have also been observed to be downregulated in *MECP2* mutant cells, which should be included in future studies using these cells focusing on protein levels.

V.ii. Evaluation of metformin and simvastatin drug treatment on MECP2 and BDNF expression

Since treatment of RTT patients with exogenous BDNF is not feasible due to its low blood brain barrier permeability, small molecule drug treatments which do pass the BBB and stimulate BDNF

expression are of interest. Fingolimod has been used to indirectly stimulate BDNF metabolism, improving locomotion in *Mecp2*-null mice and increasing the volume of the striatum, an important region of BDNF transport and function.[204] Ampakine treatment increased BDNF levels through stimulating neuronal activation and improved breathing patterns in *Mecp2*-null mice.[272] Agonists of the TrkB receptor, the receptor for BDNF, also improve breathing patterns.[273,274] In these studies, treatment had to be initiated before appearance of first symptoms in order to be efficacious but usually RTT is diagnosed long after symptoms begun. Treatment with FK506, a calcineurin inhibitor can be initiated after the symptoms appear and improves the transportation of BDNF between brain regions, improves lifespan, motor strength and coordination, and exploratory behavior, and reduced the frequency of apneas in *Mecp2*-null mice.[205] RTT patients may benefit from a combination treatment, with a drug which induces MeCP2 and/or BDNF expression along with a drug which corrects BDNF transport.

V.ii.a. Metformin

This study is the first to show that metformin induces *MECP2E2* and *BDNF* transcripts while reduced *MECP2E2* transcripts (Figure 34). Perhaps this is part of the mechanism by which metformin enhances neurogenesis in mice.[239] The effects of metformin treatment on transcript levels were time- and concentration- dependent. In Daoy cells, changes in *E1*, *E2,* and *BDNF* transcripts were all seen at 48 hours in cells treated with 2000 μM metformin. There was a slight increase in steady-state *E1* transcripts and approximately 2-fold increase in *BDNF* transcripts, but these were not changed at the nascent RNA level. *E2* transcripts were decreased by metformin treatment at the nascent and steady state levels. Further studies are required to determine how metformin affects transcripts at different levels of regulation, and how it is capable of producing MeCP2 isoform-specific regulation mechanisms. It is still unknown whether these transcript changes are translated to the level of protein as well and this should be analyzed in future studies. *In vivo* studies of metformin in RTT models should evaluate the effects of metformin on glucose metabolism and whether increases in E1 and BDNF are observed *in vivo*. Decreases in *E2,* which were observed in this study have the potential to increase the effect of MeCP2 loss in these mice.

In the case of *MECP2* Duplication Syndrome, metformin may be of interest there if it is capable of somewhat normalizing MeCP2 levels.

Figure 34. Schematic of the effects of metformin and simvastatin treatment on *MECP2E1, MECP2E2* and *BDNF* gene expression in Daoy cells. Metformin treatment elevated *MECP2E1* and *BDNF* transcripts at the steady-state level, indicating a post-transcriptional mechanism, while decreasing *MECP2E2* transcripts at the nascent and steady-state levels, indicating a transcriptional mechanism. Simvastatin treatment reduced *BDNF* transcription in the cells.

V.ii.b. Simvastatin

The results of this study were that 2.5 and 5.0 µM simvastatin treatment significantly inhibited *BDNF* transcription in Daoy cells but did not significantly impact *MECP2* transcripts (Figure 34). The effects of simvastatin on *MECP2* showed some variation between experimental conditions of presence or absence of serum starvation prior to drug treatment. Cells that were not serum starved prior to drug treatment showed some decrease in *E1* and *E2* transcripts, indicating the metabolic state of cells may impact the effect of simvastatin on transcript levels. These results are not the desired effect for RTT Syndrome therapy. Simvastatin treatment of Daoy cells has been tested in applications as a cancer therapeutic. As cancer cells, Daoy cells may respond differently to cholesterol inhibition than perhaps a neuronal *in vitro* model or an *in vivo* model would show. Toxic effects of simvastatin have not been observed previously in other mouse models of neurological disorders, and it may be most ideal to test this drug in the *in vivo* model of RTT.

In addition, the combination of metformin and simvastatin *in vivo* can be tested to target both glucose and cholesterol metabolism abnormalities.

V.iii. Extended future directions

The results of this thesis focus on transcriptional regulation. Initial plans included analyzing the effects of MeCP2 isoform overexpression on selected proteins in the protein translation pathway, mTOR signaling, and components of protein initiation complexes. Further studies are required to clarify how this pathway is impacted by MeCP2 mutations, both in loss- and gain-of-function models, and how it might be therapeutically targeted. Metformin is an mTOR inhibitor and rescues mice with Fragile X Syndrome, which have overactivated mTOR signaling. Knowledge of how the mTOR pathway is affected in RTT and MDS will inform the effectiveness metformin may have as a therapy for these disorders.

V.iv. Conclusion

In conclusion, *BDNF* gene expression was shown to be targeted by both MeCP2 isoforms in a Daoy cell model. Despite their cancerous origin, Daoy cells recapitulate a number of expression patterns seen in human brain tissue. This indicates they are a useful tool to screen for mechanisms of *MECP2* gain- and loss-of-function as well as impacts of small molecules. This would allow a more targeted approach to take into the more complex *in vitro* and *in vivo* models of RTT and MDS. Metformin treatment resulted in significantly increased *BDNF* transcripts in Daoy cells, which along with its previously demonstrated function of enhancing neurogenesis indicate it to be a promising therapeutic for RTT Syndrome.

Chapter VI: References

1. Amir RE, van den Veyver IB, Wan M, Tran CQ, Francke U, Zoghbi HY. Rett syndrome is caused by mutations in X-linked MECP2, encoding methyl-CpG-binding protein 2. *Nat Genet*. 1999;23:185-188. doi:10.1038/13810

2. Van Esch H, Bauters M, Ignatius J, et al. Duplication of the MECP2 region is a frequent cause of severe mental retardation and progressive neurological symptoms in males. *Am J Hum Genet*. 2005;77(3):442-453. doi:10.1086/444549

3. Kishi N, Macklis JD. MECP2 is progressively expressed in post-migratory neurons and is involved in neuronal maturation rather than cell fate decisions. *Mol Cell Neurosci*. 2004;27(3):306-321. doi:10.1016/j.mcn.2004.07.006

4. Kyle SM, Vashi N, Justice MJ. Rett syndrome: A neurological disorder with metabolic components. *Open Biol*. 2018;8(170216). doi:10.1098/rsob.170216

5. Cavalli G, Heard E. Advances in epigenetics link genetics to the environment and disease. *Nature*. 2019;571:489-499. doi:10.1038/s41586-019-1411-0

6. Kuehner JN, Bruggeman EC, Wen Z, Yao B. Epigenetic regulations in neuropsychiatric disorders. *Front Genet*. 2019;10(268). doi:10.3389/fgene.2019.00268

7. Delcuve GP, Rastegar M, Davie JR. Epigenetic control. *J Cell Physiol*. 2009;219:243-250. doi:10.1002/jcp.21678

8. Liyanage VRB, Zachariah RM, Delcuve GP, Davie JR, Rastegar M. New developments in chromatin research: An epigenetic perspective. In: *New Developments in Chromatin Research*. ; 2012.

9. Liyanage V, Zachariah R, Delcuve G, Davie J, Rastegar M. Chromatin Structure and Epigenetics. In: Urbano K, ed. *Advances in Genetics Research*. New York: Nova Science Publishers; 2015:57-88.

10. Luger K, Mäder AW, Richmond RK, Sargent DF, Richmond TJ. Crystal structure of the

nucleosome core particle at 2.8 Å resolution. *Nature*. 1997;389:251-260. doi:10.1038/38444

11. Barber BA, Rastegar M. Epigenetic control of Hox genes during neurogenesis, development, and disease. *Ann Anat*. 2010;192(5):261-274. doi:10.1016/j.aanat.2010.07.009

12. Rastegar M. Epigenetics and Cerebellar Neurodevelopmental Disorders. In: Marzban H, ed. *Development of the Cerebellum from Molecular Aspects to Diseases*. Springer, Cham; 2017:197-218.

13. Dixon JR, Selvaraj S, Yue F, et al. Topological domains in mammalian genomes identified by analysis of chromatin interactions. *Nature*. 2012;485:376-380. doi:10.1038/nature11082

14. Liyanage VRB, Jarmasz JS, Murugeshan N, Bigio MRD, Rastegar M, Davie JR. DNA Modifications: Function and Applications in Normal and Disease States. *Biology (Basel)*. 2014;3(4):670-723. doi:10.3390/biology3040670

15. Lewis JD, Meehan RR, Henzel WJ, et al. Purification, sequence, and cellular localization of a novel chromosomal protein that binds to Methylated DNA. *Cell*. 1992;69(6):905-914. doi:10.1016/0092-8674(92)90610-O

16. Mellén M, Ayata P, Dewell S, Kriaucionis S, Heintz N. MeCP2 binds to 5hmC enriched within active genes and accessible chromatin in the nervous system. *Cell*. 2012;151(7):1417-1430. doi:10.1016/j.cell.2012.11.022

17. Cramer P. Organization and regulation of gene transcription. *Nature*. 2019;573:45-54. doi:10.1038/s41586-019-1517-4

18. Wissink EM, Vihervaara A, Tippens ND, Lis JT. Nascent RNA analyses: tracking transcription and its regulation. *Nat Rev Genet*. 2019;20:705-723. doi:10.1038/s41576-019-0159-6

19. Zabidi MA, Stark A. Regulatory Enhancer–Core-Promoter Communication via

Transcription Factors and Cofactors. *Trends Genet*. 2016;32(12):801-814. doi:10.1016/j.tig.2016.10.003

20. Rastegar M, Kobrossy L, Kovacs EN, Rambaldi I, Featherstone M. Sequential Histone Modifications at Hoxd4 Regulatory Regions Distinguish Anterior from Posterior Embryonic Compartments. *Mol Cell Biol*. 2004;24(18):8090-8103. doi:10.1128/mcb.24.18.8090-8103.2004

21. Nolte C, Rastegar M, Amores A, et al. Stereospecificity and PAX6 function direct Hoxd4 neural enhancer activity along the antero-posterior axis. *Dev Biol*. 2006;299(2):582-593. doi:10.1016/j.ydbio.2006.08.061

22. Kobrossy L, Rastegar M, Featherstone M. Interplay between chromatin and trans-acting factors regulating the Hoxd4 promoter during neural differentiation. *J Biol Chem*. 2006;281(36):25926-25939. doi:10.1074/jbc.M602555200

23. Lahuna O, Rastegar M, Maiter D, Thissen JP, Lemaigre FP, Rousseau GG. Involvement of STAT5 (signal transducer and activator of transcription 5) and HNF-4 (hepatocyte nuclear factor 4) in the transcriptional control of the hnf6 gene by growth hormone. *Mol Endocrinol*. 2000;14(2):285-294. doi:10.1210/mend.14.2.0423

24. Rastegar M, Rousseau GG, Lemaigre FP. CCAAT/enhancer-binding protein-α is a component of the growth hormone-regulated network of liver transcription factors. *Endocrinology*. 2000. doi:10.1210/endo.141.5.7478

25. Will CL, Lührmann R. Spliceosome structure and function. *Cold Spring Harb Perspect Biol*. 2011;3(a003707). doi:10.1101/cshperspect.a003707

26. König J, Zarnack K, Rot G, et al. ICLIP reveals the function of hnRNP particles in splicing at individual nucleotide resolution. *Nat Struct Mol Biol*. 2010;17(7):909-915. doi:10.1038/nsmb.1838

27. Rastegar M, Szpirer C, Rousseau GG, Lemaigre FP. Hepatocyte nuclear factor 6: Organization and chromosomal assignment of the rat gene and characterization of its

promoter. *Biochem J*. 1998;334(3):565-569. doi:10.1042/bj3340565

28. Huang H, Rastegar M, Bodner C, Goh SL, Rambaldi I, Featherstone M. MEIS C termini harbor transcriptional activation domains that respond to cell signaling. *J Biol Chem*. 2005;280(11):10119-10127. doi:10.1074/jbc.M413963200

29. Hirose T, Virnicchi G, Tanigawa A, et al. NEAT1 long noncoding RNA regulates transcription via protein sequestration within subnuclear bodies. *Mol Biol Cell*. 2014;25(1):169-183. doi:10.1091/mbc.E13-09-0558

30. Jao CY, Salic A. Exploring RNA transcription and turnover in vivo by using click chemistry. *Proc Natl Acad Sci U S A*. 2008;105(41):15779-15784. doi:10.1073/pnas.0808480105

31. Akbalik G, Langebeck-Jensen K, Tushev G, et al. Visualization of newly synthesized neuronal RNA in vitro and in vivo using click-chemistry. *RNA Biol*. 2017;14(1):20-28. doi:10.1080/15476286.2016.1251541

32. Tani H, Torimura M, Akimitsu N. The RNA Degradation Pathway Regulates the Function of GAS5 a Non-Coding RNA in Mammalian Cells. *PLoS One*. 2013;8(1):e55684. doi:10.1371/journal.pone.0055684

33. Rodrigues DC, Kim DS, Yang G, et al. MECP2 Is Post-transcriptionally Regulated during Human Neurodevelopment by Combinatorial Action of RNA-Binding Proteins and miRNAs. *Cell Rep*. 2016;17(3):720-734. doi:10.1016/j.celrep.2016.09.049

34. Russo J, Heck AM, Wilusz J, Wilusz CJ. Metabolic labeling and recovery of nascent RNA to accurately quantify mRNA stability. *Methods*. 2017;120:39-48. doi:10.1016/j.ymeth.2017.02.003

35. Du Q, Luu PL, Stirzaker C, Clark SJ. Methyl-CpG-binding domain proteins: Readers of the epigenome. *Epigenomics*. 2015;7(6):1051-1073. doi:10.2217/epi.15.39

36. Amiri S, Davie JR, Rastegar M. Chronic Ethanol Exposure Alters DNA Methylation in Neural Stem Cells: Role of Mouse Strain and Sex. *Mol Neurobiol*. 2020;57:650-667. doi:10.1007/s12035-019-01728-0

37. Xu W, Liyanage VRB, MacAulay A, et al. Genome-Wide Transcriptome Landscape of Embryonic Brain-Derived Neural Stem Cells Exposed to Alcohol with Strain-Specific Cross-Examination in BL6 and CD1 Mice. *Sci Rep*. 2019;9(206). doi:10.1038/s41598-018-36059-y

38. Liyanage VRB, Olson CO, Zachariah RM, Davie JR, Rastegar M. DNA methylation contributes to the differential expression levels of Mecp2 in male mice neurons and astrocytes. *Int J Mol Sci*. 2019;20(8). doi:10.3390/ijms20081845

39. Meehan R, Lewis JD, Bird AP. Characterization of MECP2, a vertebrate DNA binding protein with affinity for methylated DNA. *Nucleic Acids Res*. 1992;20(19):5085-5092. doi:10.1093/nar/20.19.5085

40. Quaderi NA, Meehan RR, Tate PH, et al. Genetic and Physical Mapping of a Gene Encoding a Methyl CpG Binding Protein, Mecp2, to the Mouse X Chromosome. *Genomics*. 1994;22(3):648-651. doi:10.1006/geno.1994.1442

41. Adler DA, Quaderi NA, Brown SDM, et al. The X-linked methylated DNA binding protein, Mecp2, is subject to X inactivation in the mouse. *Mamm Genome*. 1995;6:491-492. doi:10.1007/BF00356163

42. Reichwald K, Thiesen J, Wiehe T, et al. Comparative sequence analysis of the MECP2-locus in human and mouse reveals new transcribed regions. *Mamm Genome*. 2000;11(182-190). doi:10.1007/s003350010035

43. Kriaucionis S, Bird A. The major form of MeCP2 has a novel N-terminus generated by alternative splicing. *Nucleic Acids Res*. 2004;32(5):1818-1823. doi:10.1093/nar/gkh349

44. Mnatzakanian GN, Lohi H, Munteanu I, et al. A previously unidentified MECP2 open reading frame defines a new protein isoform relevant to Rett syndrome. *Nat Genet*. 2004;36(4):339-341. doi:10.1038/ng1327

45. Coy JF, Sedlacek Z, Bächner D, Delius H, Poustka A. A complex pattern of evolutionary conservation and alternative polyadenylation within the long 3'-untranslated region of

the methyl-CpG-binding protein 2 gene (MeCP2) suggests a regulatory role in gene expression. *Hum Mol Genet*. 1999;8(7):1253-1262. doi:10.1093/hmg/8.7.1253

46. Shahbazian MD, Antalffy B, Armstrong DL, Zoghbi HY. Insight into Rett syndrome: MeCP2 levels display tissue- and cell-specific differences and correlate with neuronal maturation. *Hum Mol Genet*. 2002;11(2):115-124. doi:10.1093/hmg/11.2.115

47. Pelka GJ, Watson CM, Christodoulou J, Tam PPL. Distinct expression profiles of Mecp2 transcripts with different lengths of 3'UTR in the brain and visceral organs during mouse development. *Genomics*. 2005;85(4):441-452. doi:10.1016/j.ygeno.2004.12.002

48. Liyanage VRB, Rastegar M. Rett syndrome and MeCP2. *NeuroMolecular Med*. 2014;16(2):231-264. doi:10.1007/s12017-014-8295-9

49. Nan X, Meehan RR, Bird A. Dissection of the methyl-CpG binding domain from the chromosomal protein MeCP2. *Nucleic Acids Res*. 1993;21(21):4886-4892. doi:10.1093/nar/21.21.4886

50. Nan X, Campoy FJ, Bird A. MeCP2 is a transcriptional repressor with abundant binding sites in genomic chromatin. *Cell*. 1997;88(4):471-481. doi:10.1016/S0092-8674(00)81887-5

51. Baker SA, Chen L, Wilkins AD, Yu P, Lichtarge O, Zoghbi HY. An AT-hook domain in MeCP2 determines the clinical course of Rett syndrome and related disorders. *Cell*. 2013;152(5):984-996. doi:10.1016/j.cell.2013.01.038

52. Lyst MJ, Ekiert R, Guy J, et al. Affinity for DNA Contributes to NLS Independent Nuclear Localization of MeCP2. *Cell Rep*. 2018;24(9):2213-2220. doi:10.1016/j.celrep.2018.07.099

53. Zachariah RM, Olson CO, Ezeonwuka C, Rastegar M. Novel MeCP2 Isoform-Specific Antibody Reveals the Endogenous MeCP2E1 Expression in Murine Brain, Primary Neurons and Astrocytes. *PLoS One*. 2012;7(11):24-28. doi:10.1371/journal.pone.0049763

54. Olson CO, Zachariah RM, Ezeonwuka CD, Liyanage VRB, Rastegar M. Brain region-specific expression of MeCP2 isoforms correlates with DNA methylation within Mecp2 regulatory

elements. *PLoS One*. 2014;9(3). doi:10.1371/journal.pone.0090645

55. Liyanage VRB, Zachariah RM, Davie JR, Rastegar M. Ethanol deregulates Mecp2/MeCP2 in differentiating neural stem cells via interplay between 5-methylcytosine and 5-hydroxymethylcytosine at the Mecp2 regulatory elements. *Exp Neurol*. 2015;265(102-117). doi:10.1016/j.expneurol.2015.01.006

56. Pejhan S, Del Bigio MR, Rastegar M. The MeCP2E1/E2-BDNF-miR132 Homeostasis Regulatory Network Is Region-Dependent in the Human Brain and Is Impaired in Rett Syndrome Patients. *Front Cell Dev Biol*. 2020;8(763). doi:10.3389/fcell.2020.00763

57. Ghosh RP, Horowitz-Scherer RA, Nikitina T, Shlyakhtenko LS, Woodcock CL. MeCP2 Binds Cooperatively to Its Substrate and Competes with Histone H1 for Chromatin Binding Sites. *Mol Cell Biol*. 2010;30(19):4656-4670. doi:10.1128/mcb.00379-10

58. Hite KC, Adams VH, Hansen JC. Recent advances in MeCP2 structure and function. *Biochem Cell Biol*. 2009;87(1):219-227. doi:10.1139/O08-115

59. Adams VH, McBryant SJ, Wade PA, Woodcock CL, Hansen JC. Intrinsic disorder and autonomous domain function in the multifunctional nuclear protein, MeCP2. *J Biol Chem*. 2007;282(20):15057-15064. doi:10.1074/jbc.M700855200

60. Skene PJ, Illingworth RS, Webb S, et al. Neuronal MeCP2 Is Expressed at Near Histone-Octamer Levels and Globally Alters the Chromatin State. *Mol Cell*. 2010;37(4):457-468. doi:10.1016/j.molcel.2010.01.030

61. Pejhan S, Siu VM, Ang LC, Del Bigio MR, Rastegar M. Differential brain region-specific expression of MeCP2 and BDNF in Rett Syndrome patients: a distinct grey-white matter variation. *Neuropathol Appl Neurobiol*. 2020;46(7):735-750. doi:10.1111/nan.12619

62. Adachi M, Keefer EW, Jones FS. A segment of the Mecp2 promoter is sufficient to drive expression in neurons. *Hum Mol Genet*. 2005;14(23):3709-3722. doi:10.1093/hmg/ddi402

63. Rastegar M, Hotta A, Pasceri P, et al. MECP2 isoform-specific vectors with regulated

expression for Rett Syndrome gene therapy. *PLoS One*. 2009;4(8). doi:10.1371/journal.pone.0006810

64. Liu JJ, Francke U. Identification of cis-regulatory elements for MECP2 expression. *Hum Mol Genet*. 2006;15(11):1769-1782. doi:10.1093/hmg/ddl099

65. Liyanage VRB, Zachariah RM, Rastegar M. Decitabine alters the expression of Mecp2 isoforms via dynamic DNA methylation at the Mecp2 regulatory elements in neural stem cells. *Mol Autism*. 2013;4(46). doi:10.1186/2040-2392-4-46

66. Singh J, Saxena A, Christodoulou J, Ravine D. MECP2 genomic structure and function: Insights from ENCODE. *Nucleic Acids Res*. 2008;36(19):6035-6047. doi:10.1093/nar/gkn591

67. Han K, Gennarino VA, Lee Y, et al. Human-specific regulation of MeCP2 levels in fetal brains by microRNA miR-483-5p. *Genes Dev*. 2013;27(5):485-490. doi:10.1101/gad.207456.112

68. Klein ME, Lioy DT, Ma L, Impey S, Mandel G, Goodman RH. Homeostatic regulation of MeCP2 expression by a CREB-induced microRNA. *Nat Neurosci*. 2007;10(12):1513-1514. doi:10.1038/nn2010

69. De Paz AM, Khajavi L, Martin H, et al. MeCP2-E1 isoform is a dynamically expressed, weakly DNA-bound protein with different protein and DNA interactions compared to MeCP2-E2. *Epigenetics and Chromatin*. 2019;12(63). doi:10.1186/s13072-019-0298-1

70. Chandler SP, Guschin D, Landsberger N, Wolffe AP. The methyl-CpG binding transcriptional repressor MeCP2 stably associates with nucleosomal DNA. *Biochemistry*. 1999;38(22):7008-7018. doi:10.1021/bi990224y

71. Ishibashi T, Thambirajah AA, Ausió J. MeCP2 preferentially binds to methylated linker DNA in the absence of the terminal tail of histone H3 and independently of histone acetylation. *FEBS Lett*. 2008;582(7):1157-1162. doi:10.1016/j.febslet.2008.03.005

72. Nan X, Tate P, Li E, Bird A. DNA methylation specifies chromosomal localization of

MeCP2. *Mol Cell Biol*. 1996;16(1):414-421. doi:10.1128/mcb.16.1.414

73. Georgel PT, Horowitz-Scherer RA, Adkins N, Woodcock CL, Wade PA, Hansen JC. Chromatin compaction by human MeCP2. Assembly of novel secondary chromatin structures in the absence of DNA methylation. *J Biol Chem*. 2003;278(34):32181-23188. doi:10.1074/jbc.M305308200

74. Nikitina T, Ghosh RP, Horowitz-Scherer RA, Hansen JC, Grigoryev SA, Woodcock CL. MeCP2-chromatin interactions include the formation of chromatosome-like structures and are altered in mutations causing Rett syndrome. *J Biol Chem*. 2007;282(38):28237-28245. doi:10.1074/jbc.M704304200

75. Becker A, Allmann L, Hofstätter M, et al. Direct Homo- and Hetero-Interactions of MeCP2 and MBD2. *PLoS One*. 2013;8(1):e53730. doi:10.1371/journal.pone.0053730

76. Ellis J, Hotta A, Rastegar M. Retrovirus Silencing by an Epigenetic TRIM. *Cell*. 2007;131(1):13-14. doi:10.1016/j.cell.2007.09.029

77. Jones PL, Veenstra GJC, Wade PA, et al. Methylated DNA and MeCP2 recruit histone deacetylase to repress transcription. *Nat Genet*. 1998;19(2):187-191. doi:10.1038/561

78. Nan X, Ng HH, Johnson CA, et al. Transcriptional repression by the methyl-CpG-binding protein MeCP2 involves a histone deacetylase complex. *Nature*. 1998;393:386-389. doi:10.1038/30764

79. Harikrishnan KN, Chow MZ, Baker EK, et al. Brahma links the SWI/SNF chromatin-remodeling complex with MeCP2-dependent transcriptional silencing. *Nat Genet*. 2005;37:254-264. doi:10.1038/ng1516

80. Chahrour M, Sung YJ, Shaw C, et al. MeCP2, a key contributor to neurological disease, activates and represses transcription. *Science (80-)*. 2008;320(5880):1224-1229. doi:10.1126/science.1153252

81. Boxer LD, Renthal W, Greben AW, et al. MeCP2 Represses the Rate of Transcriptional Initiation of Highly Methylated Long Genes. *Mol Cell*. 2020;77(2):294-309.

doi:10.1016/j.molcel.2019.10.032

82. Tate P, Skarnes W, Bird A. The methyl-CpG binding protein MeCP2 is essential for embryonic development in the mouse. *Nat Genet*. 1996;12:205-208. doi:10.1038/ng0296-205

83. Smrt RD, Eaves-Egenes J, Barkho BZ, et al. Mecp2 deficiency leads to delayed maturation and altered gene expression in hippocampal neurons. *Neurobiol Dis*. 2007;27(1):77-89. doi:10.1016/j.nbd.2007.04.005

84. Li Y, Wang H, Muffat J, et al. Global transcriptional and translational repression in human-embryonic- stem-cell-derived rett syndrome neurons. *Cell Stem Cell*. 2013;13(4):446-458. doi:10.1016/j.stem.2013.09.001

85. Chao HT, Zoghbi HY, Rosenmund C. MeCP2 Controls Excitatory Synaptic Strength by Regulating Glutamatergic Synapse Number. *Neuron*. 2007;56(1):58-65. doi:10.1016/j.neuron.2007.08.018

86. Larimore JL, Chapleau CA, Kudo S, Theibert A, Percy AK, Pozzo-Miller L. Bdnf overexpression in hippocampal neurons prevents dendritic atrophy caused by Rett-associated MECP2 mutations. *Neurobiol Dis*. 2009;34(2):199-211. doi:10.1016/j.nbd.2008.12.011

87. Jiang M, Ash RT, Baker SA, et al. Dendritic arborization and spine dynamics are abnormal in the mouse model of MECP2 duplication syndrome. *J Neurosci*. 2013;33(50):19518-19533. doi:10.1523/JNEUROSCI.1745-13.2013

88. Pejhan S, Rastegar M. Role of DNA Methyl-CpG-Binding Protein Mecp2 in Rett Syndrome Pathobiology and Mechanism of Disease. *Biomolecules*. 2021;11(75). doi:10.3390/biom11010075

89. Rett A. On a unusual brain atrophy syndrome in hyperammonemia in childhood [Article in German]. *Wiener medizinische Wochenschrift*. 1966;116(37):723-726.

90. Hagberg B. Rett's Syndrome: Prevalence and Impact on Progressive Severe Mental

Retardation in Girls. *Acta Pædiatrica*. 1985;74(3):405-408. doi:10.1111/j.1651-2227.1985.tb10993.x

91. Mari F, Azimonti S, Bertani I, et al. CDKL5 belongs to the same molecular pathway of MeCP2 and it is responsible for the early-onset seizure variant of Rett syndrome. *Hum Mol Genet*. 2005;14(14):1935-1946. doi:10.1093/hmg/ddi198

92. Ariani F, Hayek G, Rondinella D, et al. FOXG1 Is Responsible for the Congenital Variant of Rett Syndrome. *Am J Hum Genet*. 2008;83(1):89-93. doi:10.1016/j.ajhg.2008.05.015

93. Hagberg B, Aicardi J, Dias K, Ramos O. A progressive syndrome of autism, dementia, ataxia, and loss of purposeful hand use in girls: Rett's syndrome: Report of 35 cases. *Ann Neurol*. 1983;14(4):471-479. doi:10.1002/ana.410140412

94. Hagberg B, Hanefeld F, Percy A, Skjeldal O. An update on clinically applicable diagnostic criteria in Rett syndrome: Comments to Rett syndrome clinical criteria consensus panel satellite to European Paediatric Neurology Society Meeting Baden Baden, Germany, 11 September 2001. *Eur J Paediatr Neurol*. 2002;6(5):293-297. doi:10.1053/ejpn.2002.0612

95. Hagberg B, Witt-Engerstrom I. Rett syndrome: A suggested staging system for describing impairment profile with increasing age towards adolescence. *Am J Med Genet*. 1986;25(S1):47-59. doi:10.1002/ajmg.1320250506

96. Chahrour M, Zoghbi HY. The Story of Rett Syndrome: From Clinic to Neurobiology. *Neuron*. 2007;56(3):422-437. doi:10.1016/j.neuron.2007.10.001

97. Neul JL, Kaufmann WE, Glaze DG, et al. Rett syndrome: Revised diagnostic criteria and nomenclature. *Ann Neurol*. 2010;68(6):944-950. doi:10.1002/ana.22124

98. Freilinger M, Bebbington A, Lanator I, et al. Survival with Rett syndrome: Comparing Rett's original sample with data from the Australian Rett Syndrome Database. *Dev Med Child Neurol*. 2010;52(10):962-965. doi:10.1111/j.1469-8749.2010.03716.x

99. Anderson A, Wong K, Jacoby P, Downs J, Leonard H. Twenty years of surveillance in Rett syndrome: What does this tell us? *Orphanet J Rare Dis*. 2014;9(87). doi:10.1186/1750-

1172-9-87

100. Kerr AM, Armstrong DD, Prescott RJ, Doyle D, Kearney DL. Rett syndrome: Analysis of deaths in the British survey. *Eur Child Adolesc Psychiatry*. 1997;6(S1):71-74.

101. Leonard H, Cobb S, Downs J. Clinical and biological progress over 50 years in Rett syndrome. *Nat Rev Neurol*. 2017;13:37-51. doi:10.1038/nrneurol.2016.186

102. Armstrong D, Dunn JK, Antalffy B, Trivedi R. Selective dendritic alterations in the cortex of rett syndrome. *J Neuropathol Exp Neurol*. 1995;54(2):195-201. doi:10.1097/00005072-199503000-00006

103. Krishnaraj R, Ho G, Christodoulou J. RettBASE: Rett syndrome database update. *Hum Mutat*. 2017;38(8):922-931. doi:10.1002/humu.23263

104. Sung Jae Lee S, Wan M, Francke U. Spectrum of MECP2 mutations in Rett syndrome. *Brain Dev*. 2001;23(S1):138-143. doi:10.1016/S0387-7604(01)00339-4

105. Trappe R, Laccone F, Cobilanschi J, et al. MECP2 mutations in sporadic cases of Rett syndrome are almost exclusively of paternal origin. *Am J Hum Genet*. 2001;68(5):1093-1101. doi:10.1086/320109

106. Goto T, Monk M. Regulation of X-Chromosome Inactivation in Development in Mice and Humans. *Microbiol Mol Biol Rev*. 1998;62(2):362-378. doi:10.1128/mmbr.62.2.362-378.1998

107. Ebert DH, Gabel HW, Robinson ND, et al. Activity-dependent phosphorylation of MeCP2 threonine 308 regulates interaction with NCoR. *Nature*. 2013;499:341-345. doi:10.1038/nature12348

108. Neul JL, Fang P, Barrish J, et al. Specific mutations in Methyl-CpG-Binding Protein 2 confer different severity in Rett syndrome. *Neurology*. 2008;70(16):1313-1321. doi:10.1212/01.wnl.0000291011.54508.aa

109. Cuddapah VA, Pillai RB, Shekar K V., et al. Methyl-CpG-binding protein 2 (MECP2) mutation type is associated with disease severity in rett syndrome. *J Med Genet*.

2014;51:152-158. doi:10.1136/jmedgenet-2013-102113

110. Knudsen GPS, Neilson TCS, Pedersen J, et al. Increased skewing of X chromosome inactivation in Rett syndrome patients and their mothers. *Eur J Hum Genet*. 2006;14:1189-1194. doi:10.1038/sj.ejhg.5201682

111. Hoffbuhr KC, Moses LM, Jerdonek MA, Naidu S, Hoffman EP. Associations between MeCP2 mutations, X-chromosome inactivation, and phenotype. *Ment Retard Dev Disabil Res Rev*. 2002;8(2):99-105. doi:10.1002/mrdd.10026

112. Ramocki MB, Tavyev YJ, Peters SU. The MECP2 duplication syndrome. *Am J Med Genet Part A*. 2010;152(5):1079-1088. doi:10.1002/ajmg.a.33184

113. Peters SU, Fu C, Suter B, et al. Characterizing the phenotypic effect of Xq28 duplication size in MECP2 duplication syndrome. *Clin Genet*. 2019;95(5):575-581. doi:10.1111/cge.13521

114. Guy J, Hendrich B, Holmes M, Martin JE, Bird A. A mouse Mecp2-null mutation causes neurological symptoms that mimic rett syndrome. *Nat Genet*. 2001;27:322-326. doi:10.1038/85899

115. Pelka GJ, Watson CM, Radziewic T, et al. Mecp2 deficiency is associated with learning and cognitive deficits and altered gene activity in the hippocampal region of mice. *Brain*. 2006;129(4):887-898. doi:10.1093/brain/awl022

116. Chen RZ, Akbarian S, Tudor M, Jaenisch R. Deficiency of methyl-CpG binding protein-2 in CNS neurons results in a Rett-like phenotype in mice. *Nat Genet*. 2001;27:327-331. doi:10.1038/85906

117. McGraw CM, Samaco RC, Zoghbi HY. Adult neural function requires MeCP2. *Science (80-)*. 2011;333(6039):186. doi:10.1126/science.1206593

118. Cheval H, Guy J, Merusi C, De Sousa D, Selfridge J, Bird A. Postnatal inactivation reveals enhanced requirement for MeCP2 at distinct age windows. *Hum Mol Genet*. 2012;21(17):3806-3814. doi:10.1093/hmg/dds208

119. Guy J, Gan J, Selfridge J, Cobb S, Bird A. Reversal of neurological defects in a mouse model of Rett syndrome. *Science (80-)*. 2007;315(5818):1143-1147. doi:10.1126/science.1138389

120. Yazdani M, Deogracias R, Guy J, Poot RA, Bird A, Barde YA. Disease modeling using embryonic stem cells: MeCP2 regulates nuclear size and RNA synthesis in neurons. *Stem Cells*. 2012;30(10):2128-2139. doi:10.1002/stem.1180

121. Chao HT, Chen H, Samaco RC, et al. Dysfunction in GABA signalling mediates autism-like stereotypies and Rett syndrome phenotypes. *Nature*. 2010;468:263-269. doi:10.1038/nature09582

122. Ure K, Lu H, Wang W, et al. Restoration of Mecp2 expression in GABAergic neurons is sufficient to rescue multiple disease features in a mouse model of Rett syndrome. *Elife*. 2016;5(e14198). doi:10.7554/eLife.14198

123. Yasui DH, Gonzales ML, Aflatooni JO, et al. Mice with an isoform-ablating Mecp2exon 1 mutation recapitulate the neurologic deficits of Rett syndrome. *Hum Mol Genet*. 2014;23(9):2447-2458. doi:10.1093/hmg/ddt640

124. Itoh M, Tahimic CGT, Ide S, et al. Methyl CpG-binding protein isoform MeCP2-e2 is dispensable for rett syndrome phenotypes but essential for embryo viability and placenta development. *J Biol Chem*. 2012;287(17):13859-13867. doi:10.1074/jbc.M111.309864

125. Schaevitz LR, Gómez NB, Zhen DP, Berger-Sweeney JE. MeCP2 R168X male and female mutant mice exhibit Rett-like behavioral deficits. *Genes, Brain Behav*. 2013;12(7):732-740. doi:10.1111/gbb.12070

126. Lyst MJ, Ekiert R, Ebert DH, et al. Rett syndrome mutations abolish the interaction of MeCP2 with the NCoR/SMRT co-repressor. *Nat Neurosci*. 2013;16:898-902. doi:10.1038/nn.3434

127. Goffin D, Allen M, Zhang L, et al. Rett syndrome mutation MeCP2 T158A disrupts DNA

binding, protein stability and ERP responses. *Nat Neurosci*. 2012;15(2):274-283. doi:10.1038/nn.2997

128. Brown K, Selfridge J, Lagger S, et al. The molecular basis of variable phenotypic severity among common missense mutations causing Rett syndrome. *Hum Mol Genet*. 2016;25(3):558-570. doi:10.1093/hmg/ddv496

129. Collins AL, Levenson JM, Vilaythong AP, et al. Mild overexpression of MeCP2 causes a progressive neurological disorder in mice. *Hum Mol Genet*. 2004;13(21):2679-2689. doi:10.1093/hmg/ddh282

130. Liu Z, Zhou X, Zhu Y, et al. Generation of a monkey with MECP2 mutations by TALEN-based gene targeting. *Neurosci Bull*. 2014;30:381-386. doi:10.1007/s12264-014-1434-8

131. Chen Y, Yu J, Niu Y, et al. Modeling Rett Syndrome Using TALEN-Edited MECP2 Mutant Cynomolgus Monkeys. *Cell*. 2017;169(5):945-955. doi:10.1016/j.cell.2017.04.035

132. Marchetto MCN, Carromeu C, Acab A, et al. A model for neural development and treatment of rett syndrome using human induced pluripotent stem cells. *Cell*. 2010;143(4):527-539. doi:10.1016/j.cell.2010.10.016

133. Kim KY, Hysolli E, Park IH. Neuronal maturation defect in induced pluripotent stem cells from patients with Rett syndrome. *PNAS*. 2011;108(34):14169-14174. doi:10.1073/pnas.1018979108

134. Peddada S, Yasui DH, LaSalle JM. Inhibitors of differentiation (ID1, ID2, ID3 and ID4) genes are neuronal targets of MeCP2 that are elevated in Rett syndrome. *Hum Mol Genet*. 2006;15(12):2003-2014. doi:10.1093/hmg/ddl124

135. Miyake K, Hirasawa T, Soutome M, et al. The protocadherins, PCDHB1 and PCDH7, are regulated by MeCP2 in neuronal cells and brain tissues: Implication for pathogenesis of Rett syndrome. *BMC Neurosci*. 2011;12(81). doi:10.1186/1471-2202-12-81

136. Lombardi LM, Zaghlula M, Sztainberg Y, et al. An RNA interference screen identifies druggable regulators of MeCP2 stability. *Sci Transl Med*. 2017;9(404).

doi:10.1126/scitranslmed.aaf7588

137. Olson CO, Pejhan S, Kroft D, et al. MECP2 Mutation Interrupts Nucleolin–mTOR–P70S6K Signaling in Rett Syndrome Patients. *Front Genet*. 2018;9(635). doi:10.3389/fgene.2018.00635

138. Tudor M, Akbarian S, Chen RZ, Jaenisch R. Transcriptional profiling of a mouse model for Rett syndrome reveals subtle transcriptional changes in the brain. *PNAS*. 2002;99(24):15536-15541. doi:10.1073/pnas.242566899

139. Ben-Shachar S, Chahrour M, Thaller C, Shaw CA, Zoghbi HY. Mouse models of MeCP2 disorders share gene expression changes in the cerebellum and hypothalamus. *Hum Mol Genet*. 2009;18(13):2431-2442. doi:10.1093/hmg/ddp181

140. Chen L, Chen K, Lavery LA, et al. MeCP2 binds to non-CG methylated DNA as neurons mature, influencing transcription and the timing of onset for Rett syndrome. *PNAS*. 2015;112(17):5509-5514. doi:10.1073/pnas.1505909112

141. Yasui DH, Peddada S, Bieda MC, et al. Integrated epigenomic analyses of neuronal MeCP2 reveal a role for long-range interaction with active genes. *PNAS*. 2007;104(49):19416-19421. doi:10.1073/pnas.0707442104

142. Urdinguio RG, Lopez-Serra L, Lopez-Nieva P, et al. Mecp2-null mice provide new neuronal targets for rett syndrome. *PLoS One*. 2008;3(11):e3669. doi:10.1371/journal.pone.0003669

143. Colantuoni C, Jeon OH, Hyder K, et al. Gene expression profiling in postmortem Rett Syndrome brain: Differential gene expression and patient classification. *Neurobiol Dis*. 2001;8(5):847-865. doi:10.1006/nbdi.2001.0428

144. Traynor J, Agarwal P, Lazzeroni L, Francke U. Gene expression patterns vary in clonal cell cultures from Rett syndrome females with eight different MECP2 mutations. *BMC Med Genet*. 2002;3(12). doi:10.1186/1471-2350-3-12

145. Delgado IJ, Kim DS, Thatcher KN, LaSalle JM, Van den Veyver IB. Expression profiling of

clonal lymphocyte cell cultures from Rett syndrome patients. *BMC Med Genet*. 2006;7(61):1-13. doi:10.1186/1471-2350-7-61

146. West AE, Pruunsild P, Timmusk T. Neurotrophins: Transcription and translation. In: Lewin G, Carter B, eds. *Handbook of Experimental Pharmacology*. Berlin, Heidelberg: Springer; 2014:67-100. doi:10.1007/978-3-642-45106-5_4

147. Ghosh A, Carnahan J, Greenberg ME. Requirement for BDNF in activity-dependent survival of cortical neurons. *Science (80-)*. 1994;263(5153):1618-1623. doi:10.1126/science.7907431

148. Huang EJ, Reichardt LF. Trk receptors: Roles in neuronal signal transduction. *Annu Rev Biochem*. 2003;72:609-642. doi:10.1146/annurev.biochem.72.121801.161629

149. Dechant G, Barde YA. The neurotrophin receptor p75NTR: Novel functions and implications for diseases of the nervous system. *Nat Neurosci*. 2002;5:1131-1136. doi:10.1038/nn1102-1131

150. Pruunsild P, Kazantseval A, Aid T, Palm K, Timmusk T. Dissecting the human BDNF locus: Bidirectional transcription, complex splicing, and multiple promoters. *Genomics*. 2007;90(3):397-406. doi:10.1016/j.ygeno.2007.05.004

151. Chen WG, Chang Q, Lin Y, et al. Derepression of BDNF Transcription Involves Calcium-Dependent Phosphorylation of MeCP2. *Science (80-)*. 2003;302(5646):885-889. doi:10.1126/science.1086446

152. Chang Q, Khare G, Dani V, Nelson S, Jaenisch R. The disease progression of Mecp2 mutant mice is affected by the level of BDNF expression. *Neuron*. 2006;49(3):341-348. doi:10.1016/j.neuron.2005.12.027

153. Vanhala R, Korhonen L, Mikelsaar M, Lindholm D, Riikonen R. Neurotrophic factors in cerebrospinal fluid and serum of patients with Rett syndrome. *J Child Neurol*. 1998;13(9):429-433. doi:10.1177/088307389801300903

154. Riikonen R. Neurotrophic factors in the pathogenesis of Rett syndrome. *J Child Neurol*.

2003;18:693-697. doi:10.1177/08830738030180101101

155. Abuhatzira L, Makedonski K, Kaufman Y, Razin A, Shemer R. MeCP2 deficiency in the brain decreases BDNF levels by REST/CoREST-mediated repression and increases TRKB production. *Epigenetics*. 2007;2(4):214-222. doi:10.4161/epi.2.4.5212

156. Deng V, Matagne V, Banine F, et al. FXYD1 is an MeCP2 target gene overexpressed in the brains of Rett syndrome patients and Mecp2-null mice. *Hum Mol Genet*. 2007;16(6):640-650. doi:10.1093/hmg/ddm007

157. Vo N, Klein ME, Varlamova O, et al. A cAMP-response element binding protein-induced microRNA regulates neuronal morphogenesis. *PNAS*. 2005;102(45):16426-16431. doi:10.1073/pnas.0508448102

158. Su M, Hong J, Zhao Y, Liu S, Xue X. MeCP2 controls hippocampal brain-derived neurotrophic factor expression via homeostatic interactions with microRNA-132 in rats with depression. *Mol Med Rep*. 2015;12(4):5399-5406. doi:10.3892/mmr.2015.4104

159. Saxton RA, Sabatini DM. mTOR Signaling in Growth, Metabolism, and Disease. *Cell*. 2017;168(6):960-976. doi:10.1016/j.cell.2017.02.004

160. Song G, Ouyang G, Bao S. The activation of Akt/PKB signaling pathway and cell survival. *J Cell Mol Med*. 2005;9(1):59-71. doi:10.1111/j.1582-4934.2005.tb00337.x

161. Roux PP, Topisirovic I. Signaling Pathways Involved in the Regulation of mRNA Translation. *Mol Cell Biol*. 2018;38(12):e00070-18. doi:10.1128/mcb.00070-18

162. Ricciardi S, Boggio EM, Grosso S, et al. Reduced AKT/mTOR signaling and protein synthesis dysregulation in a Rett syndrome animal model. *Hum Mol Genet*. 2011;20(6):1182-1196. doi:10.1093/hmg/ddq563

163. Slipczuk L, Bekinschtein P, Katche C, Cammarota M, Izquierdo I, Medina JH. BDNF activates mTOR to regulate GluR1 expression required for memory formation. *PLoS One*. 2009;4(6):e6007. doi:10.1371/journal.pone.0006007

164. Sansal I, Sellers WR. The biology and clinical relevance of the PTEN tumor suppressor

pathway. *J Clin Oncol*. 2004;22(14):2954-2963. doi:10.1200/JCO.2004.02.141

165. Mayer C, Zhao J, Yuan X, Grummt I. mTOR-dependent activation of the transcription factor TIF-IA links rRNA synthesis to nutrient availability. *Genes Dev*. 2004;18:423-434. doi:10.1101/gad.285504

166. Jia W, Yao Z, Zhao J, Guan Q, Gao L. New perspectives of physiological and pathological functions of nucleolin (NCL). *Life Sci*. 2017;186:1-10. doi:10.1016/j.lfs.2017.07.025

167. Singleton MK, Gonzales ML, Leung KN, et al. MeCP2 is required for global heterochromatic and nucleolar changes during activity-dependent neuronal maturation. *Neurobiol Dis*. 2011;43(1):190-200. doi:10.1016/j.nbd.2011.03.011

168. Gabel HW, Kinde B, Stroud H, et al. Disruption of DNA-methylation-dependent long gene repression in Rett syndrome. *Nature*. 2015;522:89-93. doi:10.1038/nature14319

169. Zhang J, Liu Q. Cholesterol metabolism and homeostasis in the brain. *Protein Cell*. 2015;6(4):254-264. doi:10.1007/s13238-014-0131-3

170. Mergenthaler P, Lindauer U, Dienel GA, Meisel A. Sugar for the brain: The role of glucose in physiological and pathological brain function. *Trends Neurosci*. 2013;36(10):587-597. doi:10.1016/j.tins.2013.07.001

171. Justice MJ, Buchovecky CM, Kyle SM, Djukic A. A role for metabolism in Rett syndrome pathogenesis. *Rare Dis*. 2013;1:e27265. doi:10.4161/rdis.27265

172. Segatto M, Trapani L, Di Tunno I, et al. Cholesterol metabolism is altered in Rett syndrome: A study on plasma and primary cultured fibroblasts derived from patients. *PLoS One*. 2014;9(8):e104834. doi:10.1371/journal.pone.0104834

173. Freilinger M, Böhm M, Lanator I, et al. Prevalence, clinical investigation, and management of gallbladder disease in Rett syndrome. *Dev Med Child Neurol*. 2014;56(8):756-762. doi:10.1111/dmcn.12358

174. Acampa M, Guideri F, Hayek J, et al. Sympathetic overactivity and plasma leptin levels in Rett syndrome. *Neurosci Lett*. 2008;432(1):69-72. doi:10.1016/j.neulet.2007.12.030

175. Blardi P, De Lalla A, D'Ambrogio T, et al. Long-term plasma levels of leptin and adiponectin in Rett syndrome. *Clin Endocrinol (Oxf)*. 2009;70(5):706-709. doi:10.1111/j.1365-2265.2008.03386.x

176. Buchovecky CM, Turley SD, Brown HM, et al. A suppressor screen in Mecp2 mutant mice implicates cholesterol metabolism in Rett syndrome. *Nat Genet*. 2013;45(9):1013-1020. doi:10.1038/ng.2714

177. Padyana AK, Gross S, Jin L, et al. Structure and inhibition mechanism of the catalytic domain of human squalene epoxidase. *Nat Commun*. 2019;10(97). doi:10.1038/s41467-018-07928-x

178. Kyle SM, Saha PK, Brown HM, Chan LC, Justice MJ. MeCP2 co-ordinates liver lipid metabolism with the NCoR1/HDAC3 corepressor complex. *Hum Mol Genet*. 2016;25(14):3029-3041. doi:10.1093/hmg/ddw156

179. Cooke DW, Naidu S, Plotnick L, Berkovitz GD. Abnormalities of thyroid function and glucose control in subjects with Rett syndrome. *Horm Res*. 1995;43(6). doi:10.1159/000184309

180. Pitcher MR, Ward CS, Arvide EM, et al. Insulinotropic treatments exacerbate metabolic syndrome in mice lacking MeCP2 function. *Hum Mol Genet*. 2013;22(13):2626-2633. doi:10.1093/hmg/ddt111

181. Matsuishi T, Urabe F, Percy AK, et al. Abnormal carbohydrate metabolism in cerebrospinal fluid in Rett syndrome. *J Child Neurol*. 1994;9(1):26-30. doi:10.1177/088307389400900105

182. Villemagne PM, Naidu S, Villemagne VL, et al. Brain glucose metabolism in Rett syndrome. *Pediatr Neurol*. 2002;27(2):117-122. doi:10.1016/S0887-8994(02)00399-5

183. Hanefeld F, Christen HJ, Holzbach U, Kruse B, Frahm J, Hanicke W. Cerebral proton magnetic resonance spectroscopy in Rett syndrome. *Neuropediatrics*. 1995;26(2):126-127. doi:10.1055/s-2007-979742

184. Wakai S, Kameda K, Ishikawa Y, et al. Rett syndrome: findings suggesting axonopathy and mitochondrial abnormalities. *Pediatr Neurol*. 1990;6(5):339-343. doi:10.1016/0887-8994(90)90028-Y

185. Leoncini S, de Felice C, Signorini C, et al. Oxidative stress in Rett syndrome: Natural history, genotype, and variants. *Redox Rep*. 2011;16(4):145-153. doi:10.1179/1351000211Y.0000000004

186. Saxena A, De Lagarde D, Leonard H, et al. Lost in translation: Translational interference from a recurrent mutation in exon 1 of MECP2. *J Med Genet*. 2006;43:470-477. doi:10.1136/jmg.2005.036244

187. Amir RE, Fang P, Yu Z, et al. Mutations in exon 1 of MECP2 are a rare cause of Rett syndrome. *J Med Genet*. 2005;42(e15). doi:10.1136/jmg.2004.026161

188. Quenard A, Yilmaz S, Fontaine H, et al. Deleterious mutations in exon 1 of MECP2 in Rett syndrome. *Eur J Med Genet*. 2006;49(4):313-332. doi:10.1016/j.ejmg.2005.11.002

189. Saunders CJ, Minassian BE, Chow EWC, Zhao W, Vincent JB. Novel exon 1 mutations in MECP2 implicate isoform MeCP2-e1 in classical rett syndrome. *Am J Med Genet Part A*. 2009;149A(5):1019-1023. doi:10.1002/ajmg.a.32776

190. Luikenhuis S, Giacometti E, Beard CF, Jaenisch R. Expression of MeCP2 in postmitotic neurons rescues Rett syndrome in mice. *PNAS*. 2004;101(16):6033-6038. doi:10.1073/pnas.0401626101

191. Giacometti E, Luikenhuis S, Beard C, Jaenisch R. Partial rescue of MeCP2 deficiency by postnatal activation of MeCP2. *PNAS*. 2007;104(6):1931-1936. doi:10.1073/pnas.0610593104

192. Cusack SM, Rohn TT, Medeck RJ, et al. Suppression of MeCP2β expression inhibits neurite extension in PC12 cells. *Exp Cell Res*. 2004;299(2):442-453. doi:10.1016/j.yexcr.2004.05.035

193. Dastidar SG, Bardai FH, Ma C, et al. Isoform-Specific Toxicity of Mecp2 in Postmitotic

Neurons: Suppression of Neurotoxicity by FoxG1. *J Neurosci*. 2012;32(8):2846-2855. doi:10.1523/JNEUROSCI.5841-11.2012

194. Huang HS, Allen JA, Mabb AM, et al. Topoisomerase inhibitors unsilence the dormant allele of Ube3a in neurons. *Nature*. 2012;481:185-189. doi:10.1038/nature10726

195. Gadalla KK, Bailey ME, Spike RC, et al. Improved survival and reduced phenotypic severity following AAV9/MECP2 gene transfer to neonatal and juvenile male Mecp2 knockout mice. *Mol Ther*. 2013;21(1):18-30. doi:10.1038/mt.2012.200

196. Gadalla KKE, Vudhironarit T, Hector RD, et al. Development of a Novel AAV Gene Therapy Cassette with Improved Safety Features and Efficacy in a Mouse Model of Rett Syndrome. *Mol Ther - Methods Clin Dev*. 2017;5:180-190. doi:10.1016/j.omtm.2017.04.007

197. Lamonica JM, Kwon DY, Goffin D, et al. Elevating expression of MeCP2 T158M rescues DNA binding and Rett syndrome-like phenotypes. *J Clin Invest*. 2017;127(5):1889-1904. doi:10.1172/JCI90967

198. Patrizi A, Picard N, Simon AJ, et al. Chronic Administration of the N-Methyl-D-Aspartate Receptor Antagonist Ketamine Improves Rett Syndrome Phenotype. *Biol Psychiatry*. 2016;79(9):755-764. doi:10.1016/j.biopsych.2015.08.018

199. Tropea D, Giacometti E, Wilson NR, et al. Partial reversal of Rett Syndrome-like symptoms in MeCP2 mutant mice. *Proc Natl Acad Sci U S A*. 2009;106(6):2029-2034. doi:10.1073/pnas.0812394106

200. Kline DD, Ogier M, Kunze DL, Katz DM. Exogenous brain-derived neurotrophic factor rescues synaptic dysfunction in Mecp2-null mice. *J Neurosci*. 2010;30(15):5303-5310. doi:10.1523/JNEUROSCI.5503-09.2010

201. Zuccato C, Cattaneo E. Brain-derived neurotrophic factor in neurodegenerative diseases. *Nat Rev Neurol*. 2009;5:311-322. doi:10.1038/nrneurol.2009.54

202. Khwaja OS, Ho E, Barnes K V., et al. Safety, pharmacokinetics, and preliminary

assessment of efficacy of mecasermin (recombinant human IGF-1) for the treatment of Rett syndrome. *Proc Natl Acad Sci U S A*. 2014;111(12):4596-4601. doi:10.1073/pnas.1311141111

203. O'Leary HM, Kaufmann WE, Barnes K V., et al. Placebo-controlled crossover assessment of mecasermin for the treatment of Rett syndrome. *Ann Clin Transl Neurol*. 2018;5(3):323-332. doi:10.1002/acn3.533

204. Deogracias R, Yazdani M, Dekkers MPJ, et al. Fingolimod, a sphingosine-1 phosphate receptor modulator, increases BDNF levels and improves symptoms of a mouse model of Rett syndrome. *PNAS*. 2012;109(35):14230-14235. doi:10.1073/pnas.1206093109

205. Ehinger Y, Bruyère J, Panayotis N, et al. Huntingtin phosphorylation governs BDNF homeostasis and improves the phenotype of Mecp2 knockout mice. *EMBO Mol Med*. 2020;12(2):e10889. doi:10.15252/emmm.201910889

206. Istvan ES, Deisenhofer J. Structural mechanism for statin inhibition of HMG-CoA reductase. *Science (80-)*. 2001;292(5519):1160-1164. doi:10.1126/science.1059344

207. McFarland AJ, Anoopkumar-Dukie S, Arora DS, et al. Molecular mechanisms underlying the effects of statins in the central nervous system. *Int J Mol Sci*. 2014;15(11):20607-20637. doi:10.3390/ijms151120607

208. Orth M, Bellosta S. Cholesterol: Its regulation and role in central nervous system disorders. *Cholesterol*. 2012. doi:10.1155/2012/292598

209. García MJ, Reinoso RF, Sánchez Navarro A, Prous JR. Clinical pharmacokinetics of statins. *Methods Find Exp Clin Pharmacol*. 2003;25(6). doi:10.1358/mf.2003.25.6.769652

210. Kong R, Zhu X, Meteleva ES, et al. Enhanced solubility and bioavailability of simvastatin by mechanochemically obtained complexes. *Int J Pharm*. 2017;534(1-2):108-118. doi:10.1016/j.ijpharm.2017.10.011

211. Yadava SK, Naik JB, Patil JS, Mokale VJ, Singh R. Enhanced solubility and bioavailability of lovastatin using stabilized form of self-emulsifying drug delivery system. *Colloids Surfaces*

A Physicochem Eng Asp. 2015;481:63-71. doi:10.1016/j.colsurfa.2015.04.026

212. DeGorter MK, Tirona RG, Schwarz UI, et al. Clinical and pharmacogenetic predictors of circulating atorvastatin and rosuvastatin concentrations in routine clinical care. *Circ Cardiovasc Genet*. 2013;6(4):400-408. doi:10.1161/CIRCGENETICS.113.000099

213. Neuvonen PJ, Backman JT, Niemi M. Pharmacokinetic comparison of the potential over-the-counter statins simvastatin, lovastatin, fluvastatin and pravastatin. *Clin Pharmacokinet*. 2008;47:463-474. doi:10.2165/00003088-200847070-00003

214. Dietschy JM, Turley SD. Cholesterol metabolism in the brain. *Curr Opin Lipidol*. 2001;12(2):105-112. doi:10.1097/00041433-200104000-00003

215. Nieweg K, Schaller H, Pfrieger FW. Marked differences in cholesterol synthesis between neurons and glial cells from postnatal rats. *J Neurochem*. 2009;109(1):125-134. doi:10.1111/j.1471-4159.2009.05917.x

216. Andersson M, Elmberger PO, Edlund C, Kristensson K, Dallner G. Rates of cholesterol, ubiquinone, dolichol and dolichyl-P biosynthesis in rat brain slices. *FEBS Lett*. 1990;269(1):15-18. doi:10.1016/0014-5793(90)81107-Y

217. Cibičková L. Statins and their influence on brain cholesterol. *J Clin Lipidol*. 2011;5(5):373-379. doi:10.1016/j.jacl.2011.06.007

218. Liao JK, Laufs U. Pleiotropic effects of statins. *Annu Rev Pharmacol Toxicol*. 2005;45:89-118. doi:10.1146/annurev.pharmtox.45.120403.095748

219. Anstey KJ, Lipnicki DM, Low LF. Cholesterol as a risk factor for dementia and cognitive decline: A systematic review of prospective studies with meta-analysis. *Am J Geriatr Psychiatry*. 2008;16(5):343-354. doi:10.1097/01.JGP.0000310778.20870.ae

220. Yaffe K, Barrett-Connor E, Lin F, Grady D. Serum lipoprotein levels, statin use, and cognitive function in older women. *Arch Neurol*. 2002;59(3):378-384. doi:10.1001/archneur.59.3.378

221. Mans RA, McMahon LL, Li L. Simvastatin-mediated enhancement of long-term

potentiation is driven by farnesyl-pyrophosphate depletion and inhibition of farnesylation. *Neuroscience*. 2012;202:1-9. doi:10.1016/j.neuroscience.2011.12.007

222. Robin NC, Agoston Z, Biechele TL, James RG, Berndt JD, Moon RT. Simvastatin promotes adult hippocampal neurogenesis by enhancing Wnt/β-catenin signaling. *Stem Cell Reports*. 2014;2(1):9-17. doi:10.1016/j.stemcr.2013.11.002

223. Lu D, Qu C, Goussev A, et al. Statins increase neurogenesis in the dentate gyrus, reduce delayed neuronal death in the hippocampal CA3 region, and improve spatial learning in rat after traumatic brain injury. *J Neurotrauma*. 2007;24(7):1132-1146. doi:10.1089/neu.2007.0288

224. Wu H, Lu D, Jiang H, et al. Simvastatin-mediated upregulation of VEGF and BDNF, activation of the PI3K/Akt pathway, and increase of neurogenesis are associated with therapeutic improvement after traumatic brain injury. *J Neurotrauma*. 2008;25(2):130-139. doi:10.1089/neu.2007.0369

225. Piermartiri TCB, Vandresen-Filho S, De Araújo Herculano B, et al. Atorvastatin prevents hippocampal cell death due to quinolinic acid-induced seizures in mice by increasing akt phosphorylation and glutamate uptake. *Neurotox Res*. 2009;16:106-115. doi:10.1007/s12640-009-9057-6

226. Zacco A, Togo J, Spence K, et al. 3-Hydroxy-3-Methylglutaryl Coenzyme A Reductase Inhibitors Protect Cortical Neurons from Excitotoxicity. *J Neurosci*. 2003;23(35):11104-11111. doi:10.1523/jneurosci.23-35-11104.2003

227. Ramirez C, Tercero I, Pineda A, Burgos JS. Simvastatin is the statin that most efficiently protects against kainate-induced excitotoxicity and memory impairment. *J Alzheimer's Dis*. 2011;24(1):161-174. doi:10.3233/JAD-2010-101653

228. Gantois I, Khoutorsky A, Popic J, et al. Metformin ameliorates core deficits in a mouse model of fragile X syndrome. *Nat Med*. 2017;23(6):674-677. doi:10.1038/nm.4335

229. Muscas M, Louros SR, Osterweil EK. Lovastatin, not simvastatin, corrects core

phenotypes in the fragile X mouse model. *eNeuro*. 2019;6(3). doi:10.1523/ENEURO.0097-19.2019

230. Osterweil EK, Chuang SC, Chubykin AA, et al. Lovastatin Corrects Excess Protein Synthesis and Prevents Epileptogenesis in a Mouse Model of Fragile X Syndrome. *Neuron*. 2013;77(2):243-250. doi:10.1016/j.neuron.2012.01.034

231. Rena G, Hardie DG, Pearson ER. The mechanisms of action of metformin. *Diabetologia*. 2017;60:1577-1585. doi:10.1007/s00125-017-4342-z

232. Patil SP, Jain PD, Ghumatkar PJ, Tambe R, Sathaye S. Neuroprotective effect of metformin in MPTP-induced Parkinson's disease in mice. *Neuroscience*. 2014;277:747-754. doi:10.1016/j.neuroscience.2014.07.046

233. Wang DS, Jonker JW, Kato Y, Kusuhara H, Schinkel AH, Sugiyama Y. Involvement of organic cation transporter 1 in hepatic and intestinal distribution of metformin. *J Pharmacol Exp Ther*. 2002;302(2):510-515. doi:10.1124/jpet.102.034140

234. Bridges HR, Jones AJY, Pollak MN, Hirst J. Effects of metformin and other biguanides on oxidative phosphorylation in mitochondria. *Biochem J*. 2014;462(3):475-487. doi:10.1042/BJ20140620

235. Zhou G, Myers R, Li Y, et al. Role of AMP-activated protein kinase in mechanism of metformin action. *J Clin Invest*. 2001;108(8):1167-1174. doi:10.1172/JCI13505

236. Zhang CS, Li M, Ma T, et al. Metformin Activates AMPK through the Lysosomal Pathway. *Cell Metab*. 2016;24(4):521-522. doi:10.1016/j.cmet.2016.09.003

237. Łabuzek K, Suchy D, Gabryel B, Bielecka A, Liber S, Okopień B. Quantification of metformin by the HPLC method in brain regions, cerebrospinal fluid and plasma of rats treated with lipopolysaccharide. *Pharmacol Reports*. 2010;62:956-965. doi:10.1016/S1734-1140(10)70357-1

238. Wang J, Weaver ICG, Gauthier-Fisher A, et al. CBP Histone Acetyltransferase Activity Regulates Embryonic Neural Differentiation in the Normal and Rubinstein-Taybi

Syndrome Brain. *Dev Cell*. 2010;18(1):114-125. doi:10.1016/j.devcel.2009.10.023

239. Wang J, Gallagher D, Devito LM, et al. Metformin activates an atypical PKC-CBP pathway to promote neurogenesis and enhance spatial memory formation. *Cell Stem Cell*. 2012;11(1):23-35. doi:10.1016/j.stem.2012.03.016

240. Katila N, Bhurtel S, Shadfar S, et al. Metformin lowers α-synuclein phosphorylation and upregulates neurotrophic factor in the MPTP mouse model of Parkinson's disease. *Neuropharmacology*. 2017;125:396-407. doi:10.1016/j.neuropharm.2017.08.015

241. Fang W, Zhang J, Hong L, et al. Metformin ameliorates stress-induced depression-like behaviors via enhancing the expression of BDNF by activating AMPK/CREB-mediated histone acetylation. *J Affect Disord*. 2020;260:302-313. doi:10.1016/j.jad.2019.09.013

242. Krishnan N, Krishnan K, Connors CR, et al. PTP1B inhibition suggests a therapeutic strategy for Rett syndrome. *J Clin Invest*. 2015;125(8):3163-3177. doi:10.1172/JCI80323

243. Zuliani I, Urbinati C, Valenti D, et al. The Anti-Diabetic Drug Metformin Rescues Aberrant Mitochondrial Activity and Restrains Oxidative Stress in a Female Mouse Model of Rett Syndrome. *J Clin Med*. 2020;9(6). doi:10.3390/jcm9061669

244. Chiarella E, Carrá G, Scicchitano S, et al. Umg lenti: Novel lentiviral vectors for efficient transgene- And reporter gene expression in human early hematopoietic progenitors. *PLoS One*. 2014;9(12):e114795. doi:10.1371/journal.pone.0114795

245. Rafiee MR, Shafaroudi AM, Rohban S, Khayatzadeh H, Kalhor HR, Mowla SJ. Enrichment of A rare subpopulation of miR-302-Expressing glioma cells by serum deprivation. *Cell J*. 2015;16(4):494-505. doi:10.22074/cellj.2015.495

246. Santhana Kumar K, Tripolitsioti D, Ma M, et al. The Ser/Thr kinase MAP4K4 drives c-Met-induced motility and invasiveness in a cell-based model of SHH medulloblastoma. *Springerplus*. 2015;4(19). doi:10.1186/s40064-015-0784-2

247. Gordon J, Wu CH, Rastegar M, Safa AR. β2-microglobulin induces caspase-dependent apoptosis in the CCRF-HSB-2 human leukemia cell line independently of the caspase-3, -8

and -9 pathways but through increased reactive oxygen species. *Int J Cancer*. 2003;103(3):316-327. doi:10.1002/ijc.10828

248. Wu CH, Gordon J, Rastegar M, Ogretmen B, Safa AR. Proteinase-3, a serine protease which mediates doxorubicin-induced apoptosis in the HL-60 leukemia cell line, is downregulated in its doxorubicin-resistant variant. *Oncogene*. 2002;21(33):5160-5174. doi:10.1038/sj.onc.1205639

249. Wu CH, Rastegar M, Gordon J, Safa AR. β2-microglobulin induces apoptosis in HL-60 human leukemia cell line and its multidrug resistant variants overexpressing MRP1 but lacking Bax or overexpressing P-glycoprotein. *Oncogene*. 2001;20(48):7006-7020. doi:10.1038/sj.onc.1204893

250. Sheikholeslami K, Sher AA, Lockman S, et al. Simvastatin induces apoptosis in medulloblastoma brain tumor cells via mevalonate cascade prenylation substrates. *Cancers (Basel)*. 2019;11(7):994. doi:10.3390/cancers11070994

251. Barber BA, Liyanage VRB, Zachariah RM, Olson CO, Bailey MAG, Rastegar M. Dynamic expression of MEIS1 homeoprotein in E14.5 forebrain and differentiated forebrain-derived neural stem cells. *Ann Anat*. 2013;195(5):431-440. doi:10.1016/j.aanat.2013.04.005

252. Ansari N, Müller S, Stelzer EHK, Pampaloni F. Quantitative 3D Cell-Based Assay Performed with Cellular Spheroids and Fluorescence Microscopy. *Methods Cell Biol*. 2013;113:295-309. doi:10.1016/B978-0-12-407239-8.00013-6

253. Zheng SY, Hou JY, Zhao J, Jiang D, Ge JF, Chen S. Clinical outcomes of downregulation of E-cadherin gene expression in non-small cell lung cancer. *Asian Pacific J Cancer Prev*. 2012;13(4):1557-1561. doi:10.7314/APJCP.2012.13.4.1557

254. Sztainberg Y, Chen HM, Swann JW, et al. Reversal of phenotypes in MECP2 duplication mice using genetic rescue or antisense oligonucleotides. *Nature*. 2015;528(7580):123-126. doi:10.1038/nature16159

255. Zuccato C, Marullo M, Vitali B, et al. Brain-derived neurotrophic factor in patients with Huntington's disease. *PLoS One*. 2011;6(8):e22966. doi:10.1371/journal.pone.0022966

256. Stimpson KM, Sullivan LL, Kuo ME, Sullivan BA. Nucleolar Organization, ribosomal DNA array stability, and acrocentric chromosome integrity are linked to telomere function. *PLoS One*. 2014;9(3):e92432. doi:10.1371/journal.pone.0092432

257. Uemura M, Zheng Q, Koh CM, Nelson WG, Yegnasubramanian S, De Marzo AM. Overexpression of ribosomal RNA in prostate cancer is common but not linked to rDNA promoter hypomethylation. *Oncogene*. 2012;31(10):1254-1263. doi:10.1038/onc.2011.319

258. Bailey CJ, Wilcock C, Scarpello JHB. Metformin and the intestine. *Diabetologia*. 2008;51(1552). doi:10.1007/s00125-008-1053-5

259. Graham GG, Punt J, Arora M, et al. Clinical pharmacokinetics of metformin. *Clin Pharmacokinet*. 2011;50:81-98. doi:10.2165/11534750-000000000-00000

260. Blandino G, Valerio M, Cioce M, et al. Metformin elicits anticancer effects through the sequential modulation of DICER and c-MYC. *Nat Commun*. 2012;3(865). doi:10.1038/ncomms1859

261. Björkhem-Bergman L, Lindh JD, Bergman P. What is a relevant statin concentration in cell experiments claiming pleiotropic effects? *Br J Clin Pharmacol*. 2011;72(1):164-165. doi:10.1111/j.1365-2125.2011.03907.x

262. Orlic-Milacic M, Kaufman L, Mikhailov A, et al. Over-expression of either MECP2-e1 or MECP2-e2 in neuronally differentiated cells results in different patterns of gene expression. *PLoS One*. 2014;9(4):e91742. doi:10.1371/journal.pone.0091742

263. Aiken C. Pseudotyping human immunodeficiency virus type 1 (HIV-1) by the glycoprotein of vesicular stomatitis virus targets HIV-1 entry to an endocytic pathway and suppresses both the requirement for Nef and the sensitivity to cyclosporin A. *J Virol*. 1997;71(8):5871-5877. doi:10.1128/jvi.71.8.5871-5877.1997

264. Cockrell AS, Kafri T. Gene delivery by lentivirus vectors. *Mol Biotechnol*. 2007;36:184-204. doi:10.1007/s12033-007-0010-8

265. Buzina A, Lo MYM, Moffett A, et al. β-globin LCR and intron elements cooperate and direct spatial reorganization for gene therapy. *PLoS Genet*. 2008;4(4):e1000051. doi:10.1371/journal.pgen.1000051

266. Yu SF, von Ruden T, Kantoff PW, et al. Self-inactivating retroviral vectors designed for transfer of whole genes into mammalian cells. *Proc Natl Acad Sci U S A*. 1986;83(10):3194-3198. doi:10.1073/pnas.83.10.3194

267. Zufferey R, Dull T, Mandel RJ, et al. Self-Inactivating Lentivirus Vector for Safe and Efficient In Vivo Gene Delivery. *J Virol*. 1998;72(12):9873-9880. doi:10.1128/jvi.72.12.9873-9880.1998

268. Dalle B, Rubin JE, Alkan O, et al. eGFP reporter genes silence LCRβ-globin transgene expression via CpG dinucleotides. *Mol Ther*. 2005;11(4):591-599. doi:10.1016/j.ymthe.2004.11.012

269. Ciapetti G, Cenni E, Pratelli L, Pizzoferrato A. In vitro evaluation of cell/biomaterial interaction by MTT assay. *Biomaterials*. 1993;14(5):359-364. doi:10.1016/0142-9612(93)90055-7

270. Stockert JC, Blázquez-Castro A, Cañete M, Horobin RW, Villanueva Á. MTT assay for cell viability: Intracellular localization of the formazan product is in lipid droplets. *Acta Histochem*. 2012;114(8):785-796. doi:10.1016/j.acthis.2012.01.006

271. Wahlqvist ML, Lee MS, Hsu CC, Chuang SY, Lee JT, Tsai HN. Metformin-inclusive sulfonylurea therapy reduces the risk of Parkinson's disease occurring with Type 2 diabetes in a Taiwanese population cohort. *Park Relat Disord*. 2012;18(6):753-758. doi:10.1016/j.parkreldis.2012.03.010

272. Ogier M, Wang H, Hong E, Wang Q, Greenberg ME, Katz DM. Brain-derived neurotrophic factor expression and respiratory function improve after ampakine treatment in a mouse

model of Rett syndrome. *J Neurosci*. 2007;27(40):10912-10917. doi:10.1523/JNEUROSCI.1869-07.2007

273. Johnson RA, Lam M, Punzo AM, et al. 7,8-Dihydroxyflavone exhibits therapeutic efficacy in a mouse model of Rett syndrome. *J Appl Physiol*. 2012;112(5):704-710. doi:10.1152/japplphysiol.01361.2011

274. Schmid DA, Yang T, Ogier M, et al. A TrkB small molecule partial agonist rescues TrkB phosphorylation deficits and improves respiratory function in a mouse model of rett syndrome. *J Neurosci*. 2012;32(5):1803-1810. doi:10.1523/JNEUROSCI.0865-11.2012